

**THE  $\Delta$ -5 FATTY ACID DESATURASE FADS1 IMPACTS INFLAMMATION  
AND METABOLIC DISEASE BY BALANCING PRO-INFLAMMATORY AND  
PRO-RESOLVING LIPIDS**

**by**

**ANTHONY D. GROMOVSKY**

**Submitted in partial fulfillment of the requirements for the degree of  
Doctor of Philosophy**

**Molecular Medicine PhD Program**

**CASE WESTERN RESERVE UNIVERSITY**

**January, 2018**

**CASE WESTERN RESERVE UNIVERSITY**  
**SCHOOL OF GRADUATE STUDIES**

We hereby approve the dissertation of  
**Anthony D. Gromovsky**

candidate for the degree of **Doctor of Philosophy**.

Committee Chair  
**Jonathan D. Smith, PhD**

Committee Member  
**J. Mark Brown, PhD**

Committee Member  
**Justin D. Lathia, PhD**

Committee Member  
**Bingcheng Wang, PhD**

Date of Defense  
**19 October 2017**

\*We also certify that written approval has been obtained  
for any proprietary material contained therein.

## TABLE OF CONTENTS

LIST OF FIGURES.....	iv
ABSTRACT.....	vi
CHAPTER 1: GENERAL INTRODUCTION.....	1
CHAPTER 2: FADS1 IMPACTS CARDIOMETABOLIC DISEASE BY BALANCING PRO-INFLAMMATORY AND PRO-RESOLVING LIPID MEDIATORS.....	12
2.1 Introduction.....	12
2.2 Materials and Methods.....	14
2.3 Results.....	25
2.4 Discussion.....	52
CHAPTER 3: FADS1 OPPOSES HEPATOCELLULAR CARCINOMA PRPGRESSION BY BALANCING PRO-INFLAMMATORY AND PRO- RESOLVING LIPID MEDIATORS.....	61
3.1 Introduction.....	61
3.2 Materials and Methods.....	65
3.3 Results.....	68
3.4 Discussion.....	79
CHAPTER 4: GENERAL DISCUSSION AND FUTURE DIRECTIONS.....	82
REFERENCES.....	88

## LIST OF FIGURES

(1)	Polyunsaturated Fatty Acid Biosynthesis.....	6
(2)	Fatty Acid Composition of Experimental Diets, Plasma, and Liver.....	27
(3)	<i>Fads1</i> is a Key Determinant of Membrane Phospholipid Composition.....	28
(4)	<i>Fads1</i> is a Key Determinant of Pro-Inflammatory Versus Pro- Resolving Lipid Mediator Balance.....	30
(5)	<i>Fads1</i> Knockdown Diversifies PUFA-Derived Lipid Mediators in a Diet-Specific Manner.....	31
(6)	<i>Fads1</i> is a Critical Regulator of Hepatic Inflammation and Lipogenesis.....	32
(7)	<i>Fads1</i> Knockdown Decreases Adiposity.....	34
(8)	Effects of <i>Fads1</i> Knockdown on Energy Expenditure.....	36
(9)	<i>Fads1</i> Knockdown Improves Glucose Tolerance.....	37
(10)	<i>Fads1</i> Knockdown Promotes Dyslipidemia and Increases Atherosclerosis in a Diet-Specific Manner.....	38
(11)	<i>Fads1</i> Knockdown Reduces Circulating Triglyceride Levels Without Changing Triglyceride Secretion Rate.....	40
(12)	<i>Fads1</i> Knockdown Alters Leukocyte Populations in a Diet-Specific Manner.....	41
(13)	<i>Fads1</i> Knockdown Promotes Classic Activation and Suppresses Alternative Activation Programs in Macrophages.....	43

<b>(14)</b>	<i>Fads1</i> -Driven Alterations in Lipid Mediators Correlate with Cardiometabolic Phenotypes.....	45
<b>(15)</b>	<i>Fads1</i> Knockdown Alters Systemic Inflammation <i>In Vivo</i> .....	47
<b>(16)</b>	<i>Fads1</i> Knockdown Alters Aortic Inflammation <i>In Vivo</i> .....	48
<b>(17)</b>	<i>Fads1</i> Knockdown Impacts LXR-Driven Remodeling of Hepatic Lipids.....	50
<b>(18)</b>	<i>Fads1</i> is an Effector of LXR-Driven Reorganization of Lipid Metabolism.....	51
<b>(19)</b>	Effects of <i>Fads1</i> Knockdown in the Dietary Context of $\omega$ -6 and $\omega$ -3 PUFA Supplementation.....	59
<b>(20)</b>	<i>Fads1</i> Knockdown Prevents Weight Gain and Improves Glucose Tolerance.....	70
<b>(21)</b>	<i>Fads1</i> Knockdown Increases Liver Tumor Burden, Independent of Diet and Adiposity.....	72
<b>(22)</b>	<i>Fads1</i> Regulates Hepatic Inflammation.....	74
<b>(23)</b>	<i>Fads1</i> is a Key Determinant of Pro-Inflammatory Versus Pro- Resolving Lipid Mediator Balance in the Liver.....	76
<b>(24)</b>	<i>Fads1</i> Knockdown Reorganizes Hepatic Lipid Metabolism.....	78

# The $\Delta$ -5 Fatty Acid Desaturase FADS1 Impacts Inflammation and Metabolic Disease by Balancing Pro-Inflammatory and Pro-Resolving Lipids

**Abstract**

**by**

**ANTHONY D. GROMOVSKY**

**Objective** – Human genetic variants near the fatty acid desaturase (FADS) gene cluster (*FADS1-2-3*) are strongly associated with metabolic traits including dyslipidemia, fatty liver, type 2 diabetes, and coronary artery disease. However, mechanisms underlying these genetic associations are unclear.

**Approach and Results** – Here, we specifically investigated the physiologic role of the  $\Delta$ -5 desaturase FADS1 in regulating diet-induced metabolic phenotypes by treating either wild-type or hyperlipidemic low-density lipoprotein receptor-null mice with antisense oligonucleotides (ASO) targeting the selective knockdown of *Fads1*. *Fads1* knockdown resulted in striking reorganization of both  $\omega$ -6 and  $\omega$ -3 polyunsaturated fatty acid (PUFA) levels as well as their associated pro-inflammatory and pro-resolving lipid mediators in a highly diet-specific manner. Loss of *Fads1* activity promoted hepatic inflammation, liver cancer progression, and atherosclerosis, yet was associated with suppression of hepatic lipogenesis. *Fads1* knockdown in isolated macrophages promoted classic pro-inflammatory activation, while suppressing alternative pro-resolving activation programs, and also altered systemic and tissue inflammatory responses *in vivo*. Finally, the

ability of *Fads1* to reciprocally regulate lipogenesis and inflammation may rely in part on its role as an effector of liver X receptor (LXR) signaling.

**Conclusion** – These results position *Fads1* as an underappreciated regulator of inflammation initiation and resolution, and suggest that endogenously synthesized arachidonic acid (AA) and eicosapentaenoic acid (EPA) are key determinates of inflammatory disease progression.

## CHAPTER 1

### GENERAL INTRODUCTION

Dietary fats represent one of the major categories of macronutrients humans rely on for proper nutrition. These nutritional demands go beyond the simplistic provision of caloric fuel, and many physiologic mechanisms are impacted by the composition of the food we eat. Dietary macronutrients are often roughly divided into three main categories: carbohydrate, protein, and fat – although, each represents its own array of diverse molecules. Fats, as a general term, encompass any variety of lipid in the diet. The most basic lipids being fatty acids (FAs), which are aliphatic molecules comprised of an acyl chain of variable length, with a carboxylic acid functional group at one end (when FA is in its free form). Free fatty acids (FFAs) are esterified to glycerol molecules to form complex lipids known as triglycerides (TGs), which are the primary storage form of extra lipid in eukaryotic cells. Dietary TG catabolism takes place primarily in the intestine, and is facilitated by pancreatic lipases and bile acids.<sup>1</sup> This process, known as lipolysis, breaks down TG to its basic components, and liberates monoacylglycerol (MAG) and FFAs for absorption by enterocytes lining the GI tract.<sup>1</sup> Enterocytes subsequently use the absorbed MAGs and FFAs to reassemble TGs and package it together with cholesterol and lipoproteins to generate chylomicrons, which are excreted and ultimately delivered to the bloodstream via the lymphatic system.<sup>1</sup> Circulating TG cannot freely pass through cell membranes, and must be catabolized to FFAs by lipoprotein lipase enzymes on the luminal surface(s) of endothelial cells in the vasculature.<sup>2,3</sup>

Liberated FFAs can then be absorbed by cells via fatty acid transporter-mediated uptake and utilized by host metabolic pathways to satisfy energetic and nutritional demands.

Fats and oils from animal and plant sources have highly variable FA composition, which is an important factor when considering physicochemical properties of dietary lipids.<sup>1,4</sup> FAs are specifically identified by biochemical properties such as carbon chain length, number of double bonds present in the acyl chain, and specific positioning of double bonds relative to specific carbons comprising the fatty acyl chain. The content of double bonds is a major distinction of dietary fats – FA that lack double bonds are termed saturated fatty acids (SFAs), FAs with one double bond are termed monounsaturated fatty acids (MUFAs), and FAs with multiple double bonds are termed polyunsaturated fatty acids (PUFAs). Acyl chains lacking double bonds in SFAs can interact tightly with one another, resulting in stable lipids that are solid at room temperature (such as animal fats). Double bonds present in naturally-derived MUFAs and PUFAs are in *cis* configuration, which disrupt these tight interactions and decrease stability. As a consequence, PUFA-rich substances (such as planted-based oils) are generally liquid at room temperature and are increasingly volatile as double bond content is increased. Saturated and unsaturated FAs are present in variable abundances in foods we eat, and imbalances in the intake of these biochemically distinct lipids can influence metabolic health.<sup>5</sup>

While all FAs have the same caloric value per weight when metabolized for energy, FAs have different physiological effects depending on their structural

identity.<sup>6</sup> In fact, extremely imbalanced relative FA intake can be detrimental to long term health. Studies have shown that diets rich in SFA and MUFA can promote obesity,<sup>7</sup> metabolic syndrome,<sup>8</sup> and cardiovascular disease (CVD),<sup>9</sup> and the American Heart Association states that a healthy diet should prioritize PUFAs and MUFAs over SFAs, specifically recommending inclusion of fatty fish, nuts, seeds, and plant-based oil sources of dietary PUFAs.<sup>5,10,11</sup> Importantly, dietary PUFAs are primarily  $\omega$ -6 or  $\omega$ -3 FAs,<sup>5</sup> which is a nomenclature for identifying double bond positioning relative to the final carbon in the fatty acyl chain. PUFAs containing a double bond at the 6<sup>th</sup> carbon from the methyl end of the acyl chain are termed  $\omega$ -6, while PUFAs containing a double bond at the 3<sup>rd</sup> carbon from the methyl end of the acyl chain are termed  $\omega$ -3. This structural distinction adds another layer of complexity to FA biology because  $\omega$ -6 and  $\omega$ -3 PUFA are utilized in a coordinated manner by numerous pathways in the body to support mechanisms fundamental to life.<sup>12</sup>

Mammals are unable to synthesize essential long chain PUFA *de novo*, and must obtain specific shorter-chain PUFAs from the diet in order to generate the complete repertoire of PUFAs needed by tissues in the body. Mammalian cells use a system of enzymes to successively elongate (add carbons) and desaturate (introduce double bonds) fatty acyl chains in order to make long-chain PUFAs from dietary precursors.<sup>13,14</sup> Humans cells have a restricted PUFA biosynthetic capacity based on the limited types of reactions catalyzed by necessary enzymes. Elongase enzymes catalyze the extension of fatty acyl chains by two carbons at a time, and desaturase enzymes introduce double bonds in a

stereospecific manner.<sup>13,14</sup> Humans only have desaturases capable of adding double bonds at specific acyl chain carbon positions:  $\Delta 4$ ,  $\Delta 5$ ,  $\Delta 6$ , and  $\Delta 9$ . Similar to the methodology behind  $\omega$ -6/ $\omega$ -3 nomenclature,  $\Delta 4$  represents the 4<sup>th</sup> carbon from the carboxylic acid head group of a given FA. Human cells are also incapable of interconverting  $\omega$ -6 and  $\omega$ -3 PUFAs, which necessitates dietary intake of both PUFA varieties. For instance, many plant and seed oils are rich dietary source of  $\alpha$ -linolenic acid (ALA), a shorter-chain  $\omega$ -3 PUFA with 18 carbons and 3 double bonds (18:3  $\Delta 9,12,15$ ). Dietary ALA is metabolized to generate important long-chain  $\omega$ -3 fatty acids, particularly eicosapentaenoic acid (EPA, 20:5  $\Delta 5,8,11,14,17$ ) and docosahexaenoic acid (DHA, 22:6  $\Delta 4,7,10,13,16,19$ ). Analogously, many plant and animal fats are rich dietary sources of linoleic acid (LA), the shortest-chained  $\omega$ -6 PUFA (18:2  $\Delta 9,12$ ). Dietary LA is elongated and desaturated to produce downstream long-chain  $\omega$ -6 fatty acids, most importantly arachidonic acid (AA, 20:4  $\Delta 5,8,11,14$ ). Dietary PUFA act as competing substrates for the same enzymes during long chain  $\omega$ -3 and  $\omega$ -6 PUFA synthesis, which highlights the importance of the proportion of  $\omega$ -3 to  $\omega$ -6 fatty acids in the diet.<sup>13,14</sup> Consider a very simplified scenario as an example: dietary enrichment in ALA will result in higher levels of EPA in comparison to AA, simply as a result of substrate availability being skewed in favor of  $\omega$ -3 PUFA precursors.

Long-chain  $\omega$ -6 and  $\omega$ -3 PUFAs are fundamental to proper growth and development because they play pivotal signaling roles throughout every tissue in the body.<sup>15,16</sup> Structurally, PUFA contribute to the proper regulation of

phospholipid (PL) membrane fluidity and specialized tissue function.<sup>16</sup> Lipid profiling of the human body reveals that different organ systems have distinct PUFA compositions.<sup>17-19</sup> Of note, the human brain is known to be very rich in DHA, and cognitive development is stunted without sufficient  $\omega$ -3 PUFA in the diet.<sup>19-22</sup> However, the physiologic requirement of long-chain PUFA is not satisfied by diet alone. Humans rely on the function of two enzymes that play indispensable roles in essential PUFA synthesis: the  $\Delta$ 5 desaturase Fatty Acid Desaturase 1 (FADS1, encoded by the *FADS1* gene in humans), and the  $\Delta$ 6 desaturase Fatty Acid Desaturase 2 (FADS2, encoded by the *FADS2* gene in humans).<sup>23-25</sup> *FADS1* and *FADS2* share a bidirectional promoter region on chromosome 11 (11q12-13.1).<sup>25</sup> This region also harbors *FADS3*, a gene encoding Fatty Acid Desaturase 3 (FADS3), a protein with predicted desaturase ability, but no known function to date.<sup>25</sup> FADS2 has 4 main substrates: LA (18:2), ALA (18:3), tetracosatetraenoic acid (24:4,  $\omega$ -6) and tetracosapentaenoic acid (24:5,  $\omega$ -3), which it converts into  $\gamma$ -linolenic acid (18:3), stearidonic acid (18:4), tetracosapentaenoic acid (24:5,  $\omega$ -6), and tetracosahexaenoic acid (24:6,  $\omega$ -3), respectively (Figure 1). FADS1 catalyzes the conversion of dihomo- $\gamma$ -linolenic acid (DGLA, 20:3) and eicosatetraenoic acid (ETA, 20:4) into AA (20:4) and EPA (20:5), respectively (Figure 1). FADS1 is the only human enzyme known to have  $\Delta$ 5 desaturase activity, making it the sole source of endogenously-derived AA and EPA, and essential for life. Although *FADS1* is expressed in all tissues throughout the body, highest protein expression is found in the liver, heart muscle, skeletal muscle, gastrointestinal tract, and male reproductive organs.<sup>26,27</sup>

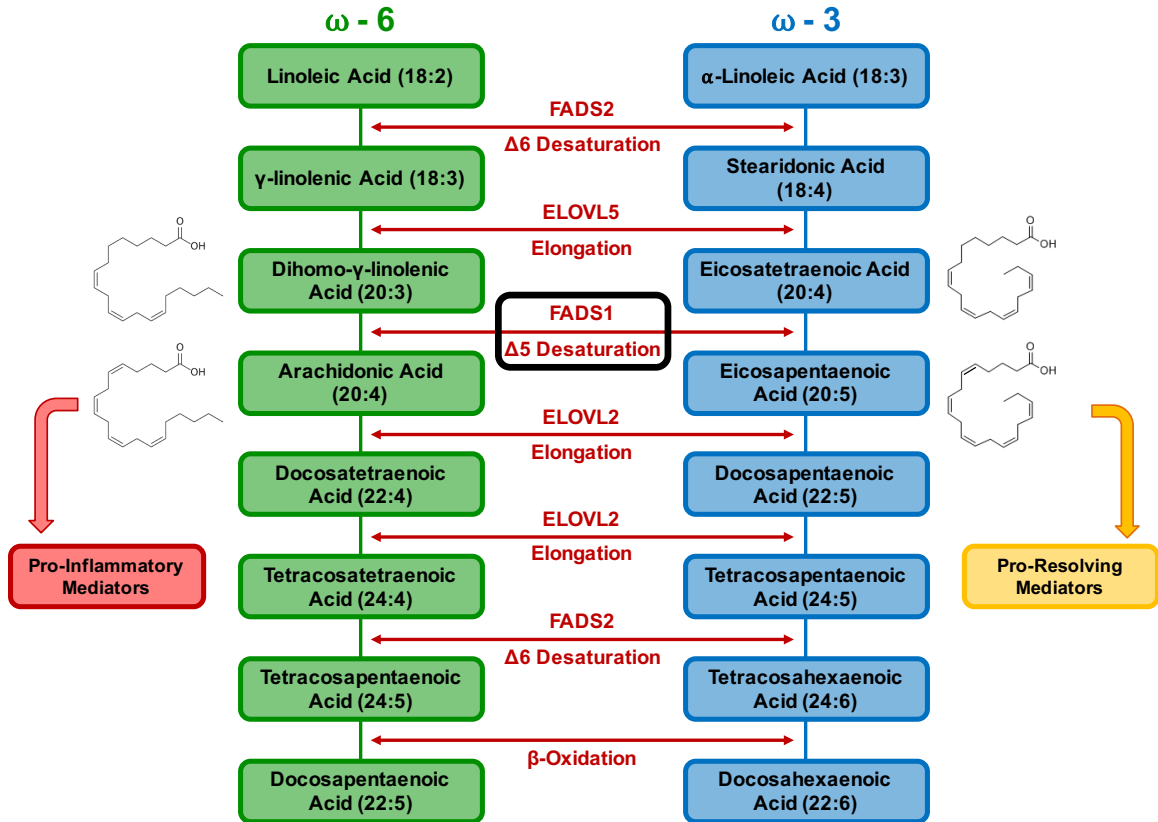


**Figure 1. Polyunsaturated Fatty Acid Biosynthesis.** Schematic representation of endogenous  $\omega$ -6 and  $\omega$ -3 polyunsaturated fatty acid metabolism.

Genetic deletion of *Fads1* in mice causes death within 8-12 weeks after birth in the absence of exogenous AA and EPA supplementation,<sup>28,29</sup> demonstrating that the importance of  $\Delta 5$  desaturase function is conserved across species.

Proper PUFA balance is achieved through a combination of exogenous (dietary) and endogenous (enzymatic) contributions, and genome-wide association (GWA) studies have recently highlighted the significance of this nutritional interplay by revealing that human genetics may have evolved to adapt to human dietary regimens. In particular, genetic data from Greenlandic Inuit populations demonstrate high frequency single nucleotide polymorphisms (SNPs) in the *FADS1-2-3* gene locus.<sup>30</sup> These SNPs translate to reduced levels of AA and EPA, and concomitantly increased levels of DGLA and ETA – a shift in substrate and product levels indicative of reduced FADS1 function.<sup>30</sup> It is thought that the Greenlandic Inuit population has a high incidence of reduced function *FADS* gene variants due to their unique diet, which is traditionally rich in fatty/oily fish.<sup>30</sup> Oily fish are bountiful sources of  $\omega$ -3 PUFA,<sup>5,11</sup> especially EPA, which is a FADS1 product. With so much EPA being supplied exogenously, the Greenlandic Inuit people evolved with a relatively reduced dependence on FADS1-derived PUFA, and genetic variants that better suited their physiological demands presumptively developed and persisted in the population over time. These observations suggest that regulation and balance of PUFA levels are of paramount importance, so much so that human genetics can change in order to account for dietary patterns.

In all tissues of the body, PUFA metabolism can dramatically affect the regulation of inflammation state by dictating the identity of locally active lipid signaling mediators.<sup>31</sup> Lipid mediator biology became a topic of interest following early studies which discovered that ovine tissues could enzymatically convert AA into prostaglandin E2 (PGE2), a physiologically active lipid agent which promotes inflammation and the sensation of pain during the early phase tissue responses to trauma and/or infection.<sup>32</sup> In the following years, numerous classes of distinct lipid mediators – prostacyclins, thromboxanes, and leukotrienes – were characterized and broadly classified as eicosanoids. Produced from 20-carbon essential PUFA in response to growth and/or stress signals, eicosanoids are short-lived lipid signaling molecules that function in autocrine and paracrine fashion(s) to coordinate the body's metabolic and inflammatory state.<sup>33,34</sup> Cellular stress signals, such as pro-inflammatory cytokines and damage associated molecular patterns, promote the activation of phospholipase enzymes, which catalyze the removal of PUFA from PL membranes in cells to facilitate lipid mediator synthesis.<sup>35,36</sup> Enzymes with oxidoreductive capacity such as cyclooxygenases, lipoxygenases, and certain cytochrome P450s subsequently catalyze stereospecific modifications of the PUFA being drawn from PL reserves.<sup>37-39</sup> Structural diversity of PUFA substrates and positional selectivity of enzyme catalysis contribute to a cell's ability to synthesize a vast array of oxidized PUFA metabolites. Broadly, eicosanoids synthesized from  $\omega$ -6 PUFA (mainly AA) are more potently pro-inflammatory than those synthesized from  $\omega$ -3 PUFA (mainly EPA). Importantly, cells also generate distinct non-eicosanoid

varieties of immunomodulatory lipid mediators during inflammatory responses to stress stimuli.

Different phases of inflammation are coordinated in part by lipid mediator signaling, requiring temporal regulation of PUFA metabolites in order to properly manage local inflammation.<sup>40</sup> Immune cells must work in concert with proximal parenchymal and stromal cells to properly resolve inflammatory responses.

Timely and complete resolution of inflammation is critical for maintaining tissue health and function, and unresolved inflammation can be pathogenic.<sup>40</sup>

Resolution is an active process orchestrated, in part, by specialized pro-resolving mediators (SPM) that signal through distinct receptors to both dampen local inflammation and promote resolution.<sup>41,42</sup> SPM are a class of PUFA metabolites that encompass lipoxins, resolvins, maresins, and protectins that function to actively modulate the duration and intensity of inflammatory responses.<sup>41,42</sup>

Lipoxins are bioactive autacoid metabolites of AA during inflammatory responses, and are the only subset of biologically relevant SPM derived mainly from  $\omega$ -6 PUFA. Resolvins are dihydroxy or trihydroxy metabolites of  $\omega$ -3 PUFA, primarily EPA and DHA, while maresins and protectins are derived from DHA.<sup>41,42</sup> Common enzymes catalyze the synthesis of all pro-inflammatory lipid mediators and SPM – the oxygenase enzymes that are primarily responsible for metabolizing PUFA to lipid mediators are: 15-lipoxygenase-1 (encoded by the *ALOX15* gene in humans), 12-lipoxygenase (encoded by the *ALOX12* gene in humans), 5-lipoxygenase (encoded by the *ALOX5* gene in humans), cyclooxygenase-2 (encoded by the *PTGS2* gene in humans), and certain

cytochrome P450 monooxygenases.<sup>35-39</sup> It is important to note that human ALOX12 and ALOX15, as well as murine leukocyte-type *Alox12* and *Alox15*, are commonly referred to as 12/15-lipoxygenases based on their shared ability to metabolize AA to both 15-hydroperoxyeicosatetraenoic acid (15-HpETE) and 12-hydroperoxyeicosatetraenoic acid (12-HpETE).<sup>43</sup> Enzyme expression is cell specific, which influences the repertoire of PUFA metabolites generated by different cells in a given microenvironment. Differential synthetic capacities promote the local exchange of oxidized PUFA metabolites among cells that cannot produce critical hydroperoxy intermediates on their own, allowing for transcellular biosynthetic potential.<sup>44</sup> For example, platelets synthesize lipoxin A4 (LXA4) to aid in the contractile homeostasis of vascular smooth muscle cells, but lack expression of ALOX5, which is required to catalyze the production of a 5,6-epoxide intermediate, leukotriene A4 (LTA4). Platelets circumvent this limitation by sourcing LTA4 from proximal neutrophils and other cells with 5-lipoxygenase activity, and further metabolizing it through ALOX12 to ultimately generate the 15-hydroxy product, LXA4.<sup>44</sup> Metabolite exchange also contributes to lipid mediator regulation because it can necessitate the interplay of resident cells and recruited leukocytes, thus restricting synthesis to separate phases of inflammation that involve different cell types.

The local microenvironment is dynamic and busy with signaling factors during acute inflammation, and temporal orchestration of lipid mediator synthesis is critical to both the induction and resolution of inflammatory responses.<sup>41,42</sup> At the onset of inflammation, AA-derived pro-inflammatory lipid mediators dominate the

microenvironment and drive immune cell recruitment to sites of developing inflammation.<sup>41,42</sup> As tissue injury endures, inflammatory cytokines and eicosanoids instruct cells to synthesize SPM in order to resolve injurious signaling and induce healing mechanisms.<sup>41,42</sup> Overall, AA-derived mediators are present early in inflammatory responses, and decrease in abundance at the relative expense of EPA- and DHA-derived SPM as the body works to reestablish local tissue homeostasis. Because distinct phases of inflammation are characterized by lipid mediators of different PUFA origin, immune responses are significantly influenced by PUFA metabolism and the overall ratio of  $\omega$ -6 PUFA to  $\omega$ -3 PUFA ( $\omega$ -6/ $\omega$ -3 ratio) in tissues. FADS1 is the sole endogenous source of AA and EPA, which uniquely positions this enzyme to potentially modulate the onset and resolution of inflammation by determining the amount of long-chain  $\omega$ -6 and  $\omega$ -3 PUFA available for lipid mediator biosynthesis. The work here investigates how FADS1-dependent PUFA metabolism impacts inflammatory processes that contribute to overall health and, in some cases, pathogenesis.

## CHAPTER 2

### FADS1 IMPACTS CARDIOMETABOLIC DISEASE BY BALANCING PRO-INFLAMMATORY AND PRO-RESOLVING LIPID MEDIATORS

#### 2.1 Introduction

Human genetic studies have transformed cardiometabolic drug discovery, providing an unparalleled prediction tool for identification of new drug targets. This is exemplified by the recent success story of large-scale genetic studies leading to rapid development of monoclonal antibodies targeting proprotein convertase subtilisin/kexin type 9 for hyperlipidemia and cardiovascular disease.<sup>45</sup> Given the target prediction power of human genetics, large consortium genome-wide association study efforts have identified hundreds of genomic loci linked to cardiometabolic disease traits, providing a refined list of new drug targets. However, many genome-wide association studies have identified loci containing genes of unknown function. Single nucleotide polymorphisms in the *FADS1-2-3* gene cluster have been repeatedly identified in genome-wide association studies across the cardiometabolic disease spectrum, including strong associations with obesity, type 2 diabetes, dyslipidemia, non-alcoholic fatty liver disease, liver enzyme elevation, coronary artery disease, and heart rate.<sup>46-56</sup> However, mechanisms by which *FADS1-2-3* polymorphisms link to these comorbid disease phenotypes are unclear. Given that expression quantitative trait loci studies have revealed altered expression of *FADS1* in several of these human genetic studies, we set out to investigate the specific role

of *FADS1* in regulating diet-induced cardiometabolic phenotypes in hyperlipidemic mice.

FADS1 is the only mammalian  $\Delta$ -5 fatty acid desaturase enzyme capable of producing the important polyunsaturated fatty acids (PUFAs) arachidonic acid (AA) and eicosapentaenoic acid (EPA) from substrates dihomo- $\gamma$ -linolenic acid (DGLA) and eicosatetraenoic acid (ETA), respectively.<sup>57,58</sup> Downstream enzymatic and non-enzymatic oxidation of FADS1 product PUFAs (AA and EPA) generates diverse lipid signaling mediators that coordinate both the initiation and resolution phases of inflammatory processes.<sup>36,40-42</sup> In general, AA-derived eicosanoids are thought to initiate and potentiate pro-inflammatory responses,<sup>36,40</sup> while EPA- and docosohexaenoic acid (DHA)-derived mediators function in direct opposition to resolve inflammation and initiate wound healing and tissue regenerative responses.<sup>41,42</sup> In particular, lipoxins, resolvins, and protectins are important lipid autacoids with varying structures and functions that are collectively defined as specialized pro-resolving lipid mediators (SPMs) for their ability to actively resolve inflammation.<sup>41,42</sup> Given FADS1's unique position as the sole enzymatic source of endogenous AA and EPA, we hypothesized that *Fads1* loss of function would dramatically alter both pro-inflammatory and pro-resolving lipid mediators to impact diseases of unresolved inflammation such as atherosclerosis, obesity, insulin resistance, and steatohepatitis. Metabolic phenotyping of global *Fads1*<sup>-/-</sup> mice has been limited due to the fact that these mice are only viable for approximately 8-12 weeks without supraphysiological supplementation of AA and EPA in the diet.<sup>28,29</sup> To overcome this barrier, here

we used second-generation antisense oligonucleotides (ASOs),<sup>59</sup> which predominately target liver, adipose tissue, and cells within the reticuloendothelial system to selectively knock down *Fads1* in adult hyperlipidemic mice, thereby circumventing postnatal lethality of global *Fads1* deletion. We hypothesized that the underlying mechanism by which *FADS1* polymorphisms alter cardiometabolic disease phenotypes is by determining the balance of endogenous AA and EPA substrates available for the production of SPMs, thereby impacting the proper resolution of inflammation. To specifically address whether endogenous EPA production by *Fads1* is necessary for SPM generation and inflammation resolution, we provided a subset of mice a diet enriched in  $\omega$ -3 precursor fatty acids.

## **2.2 Materials and Methods**

### **Animal Studies**

To study the specific role of the *Fads1* in cardiometabolic disease without the associated postnatal lethality of genetic *Fads1* deletion,<sup>28,29</sup> we employed an *in vivo* antisense oligonucleotide (ASO)-mediated knockdown approach in male low-density lipoprotein receptor-knockout mice on a pure C57BL/6J background as previously described.<sup>59</sup> Starting at 8 weeks of age, ASOs were injected intraperitoneally (50mg/kg BW per week) for the duration of the 16-week study period. To carefully alter the fatty acids present in the diet, *Fads1* loss of function was studied under two dietary contexts. One set of mice were fed a saturated and monounsaturated fatty acid-enriched synthetic diet (SFA-rich diet) with an oil

base originating from palm oil. The palm oil used for diet synthesis was purchased from Shay and Co. (Portland, OR). To specifically alter the  $\omega$ -3 *Fads1* substrate fatty acid eicosatetraenoic acid, another subset of mice received a diet designed to provide elevated amounts of precursor fatty acid ( $\alpha$ -linolenic acid = 18:3 -  $\omega$ -3 and stearidonic acid = 18:4 -  $\omega$ -3) that can be easily converted into eicosatetraenoic acid. The seed oil used for this  $\omega$ -3 substrate diet originates from *Echium plantagineum*, and was a generous gift from Croda Europe Ltd. (Leek, Staffordshire, UK). Synthesis of these diets has been described in detail in previous publications.<sup>60,61</sup> All oils and synthetic diets were authenticated by the Wake Forest University Center for Botanical Lipids and Inflammatory Disease Prevention, and a certificate of analysis can be provided upon request. All mice studies were approved by the Institutional Animal Care and Use Committee of the Cleveland Clinic.

### **Plasma Lipid, Lipoprotein, and Fatty Acid Composition Analyses**

Total plasma triacylglycerol levels (L-Type TG M, Wako Diagnostics) and total plasma cholesterol levels were quantified enzymatically (Infinity Cholesterol Reagent, Thermo/Fisher). The distribution of cholesterol across lipoprotein classes was performed by fast-protein liquid chromatography using tandem superose-6 HR columns for coupled with an online enzymatic cholesterol quantification as previously described.<sup>62-65</sup> To quantify to total plasma fatty acid composition, alkaline hydrolysis of plasma was performed and fatty acid species were quantified by LC-MS/MS. Briefly, chemical standards of palmitic acid,

palmitoleic acid, stearic acid, oleic acid, linoleic acid,  $\gamma$ -linolenic acid,  $\alpha$ -linolenic acid, stearidonic acid, dihomo- $\gamma$ -linoleic acid, arachidonic acid, eicosapentaenoic acid and docosahexaenoic acid were purchased from Sigma-Aldrich (Vienna, Austria). In parallel, isotope labeled standards of palmitic acid-d<sub>2</sub>, linoleic acid-d<sub>4</sub>, arachidonic acid-d<sub>8</sub> and docosahexaenoic acid-d<sub>5</sub> were purchased from Avanti Polar Lipids, Inc. (700 Industrial Park Drive, Alabaster, Alabama 35007, USA). A 100  $\mu$ l aliquot of plasma was mixed with 10  $\mu$ l of mixed internal standards at the concentration of 10  $\mu$ g/ml and the lipids were extracted into the hexane using the Liquid/Liquid extraction method.<sup>66</sup> The hexane layer is dried under nitrogen flow and the pellet was resuspended with 200  $\mu$ l 85% methanol. Following centrifugation at 12000 rcf for 10 minutes, 100  $\mu$ l of supernatant was transferred into a vial for FA analysis by LC-MS/MS. A volume at 20  $\mu$ l was injected on a C18 column (Gemini, 3  $\mu$ m, 2 x 150mm, Phenomenex) for the separation of FA species. Mobile phases were A (water containing 0.2% acetic acid) and B (methanol containing 0.2% acetic acid) and the pH was adjusted with ammonium hydroxide solution to 8.0 respectively. Mobile phase B at 85% was used at 0-2 min, a linear gradient was used starting from 85% B to 100% B at 2-6 min, kept at 100% at 6-22 min at the flow rate of 0.2 ml/min. The HPLC system is Waters 2690. The HPLC eluent was directly injected into a triple quadrupole mass spectrometer (Quattro Ultima, Micromass) and the FA species were ionized at ESI negative mode. Analytes were quantified using Selected Reaction Monitoring (SRM) and the SRM transitions (m/z) were precursor to precursor ions (m/z) at 255 > 255 for palmitic acid, 253 > 253 for palmitoleic acid, 283 > 283 for stearic

acid, 281 > 281 for oleic acid, 279 > 279 for linoleic acid, 277 > 277 for  $\gamma$ -linolenic acid, 277 > 277 for  $\alpha$ -linolenic acid, 275 > 275 for stearidonic acid, 305 > 305 for dihomogamma-linoleic acid, 303 > 303 for arachidonic acid, 301 > 301 for eicosapentaenoic acid, 327 > 327 for docosahexaenoic acid, 257 > 257 for palmitic acid-d2, 283 > 283 for linoleic acid-d4, 311 > 311 for arachidonic acid-d8 and 332 > 332 for docosahexaenoic acid-d5. Internal standard calibration curves were used for quantitation of FA species. Resulting data were analyzed using Masslynx Software.

## **Hepatic Phospholipid Fatty Acid Composition and Molecular Species**

### **Analyses**

To measure total hepatic phospholipid fatty acid composition, a total lipid extract was made using the method of Folch and colleagues.<sup>67</sup> Total lipid extracts were separated into cholesteryl ester, triglyceride, and phospholipid fractions by thin layer chromatography using a hexane/diethyl ether/acetic acid (70/30/1) solvent system. Alkaline hydrolysis was conducted on phospholipids recovered from the thin layer chromatography origin, and percentage fatty acid composition was quantified by the LC-MS/MS method described above for plasma fatty acid composition analysis using a C18 column-based HPLC separation followed by triple quadrupole mass spectrometry (Quattro Ultima, Micromass). To more broadly examine the molecular lipid species in *Fads1* knockdown livers we developed a shotgun lipidomics method for semi-quantitation of multiple lipid species as previously described<sup>68</sup> with minor modifications. All the internal

standards were purchased from Avanti Polar Lipids, Inc. (700 Industrial Park Drive, Alabaster, Alabama 35007, USA). Ten internal standards (12:0 diacylglycerol, 14:1 monoacylglycerol, 17:0 lysophosphatidylcholine, 17:0 phosphatidylcholine, 17:0 phosphatidic acid; 17:0 phosphatidylethanolamine, 17:0 phosphatidylglycerol, 17:0 sphingomyelin, 17:1 lysosphingomyelin, and 17:0 ceramide) were mixed together with the final concentration of 100  $\mu$ M each. Total hepatic lipids were extracted using the method of Bligh and Dyer<sup>69</sup> with minor modifications. In brief, 50  $\mu$ L of 100  $\mu$ M internal standards were added to tissue homogenates and lipids were extracted by adding by adding MeOH/CHCl<sub>3</sub> (v/v, 2/1) in the presence of dibutylhydroxytoluene (BHT) to limit oxidation. The CHCl<sub>3</sub> layer was collected and dried under N<sub>2</sub> flow. The dried lipid extract was dissolved in 1 ml the MeOH/CHCl<sub>3</sub> (v/v, 2/1) containing 5mM ammonium acetate for injection. The solution containing the lipid extract was pumped into the TripleTOF 5600 mass spectrometer (AB Sciex LLC, 500 Old Connecticut Path, Framingham, MA 01701, USA) at a flow rate of 40  $\mu$ L/min for 2 minutes for each ionization mode. Lipid extracts were analyzed in both positive and negative ion modes for complete lipidome coverage using the TripleTOF 5600 System. Infusion MS/MSALL workflow experiments consisted of a TOF MS scan from m/z 200-1200 followed by a sequential acquisition of 1001 MS/MS spectra acquired from m/z 200 to 1200.<sup>68</sup> The total time required to obtain a comprehensive profile of the lipidome was approximately 10 minutes per sample. The data was acquired with high resolution (>30000) and high mass accuracy (~5 ppm RMS). Data processing using LipidView Software identified 150-300 lipid species,

covering diverse lipids classes including major glycerophospholipids and sphingolipids. The peak intensities for each identified lipid, across all samples were normalized against an internal standard from same lipid class for the semi-quantitation purpose.

### **Quantification of Pro-Inflammatory and Pro-Resolving Lipid Mediators by LC-MS/MS**

Livers collected from low-density lipoprotein receptor-null mice exposed to control or *Fads1* ASO treatment and diets for 16 weeks were minced in ice-cold methanol containing internal deuterium-labeled standards and stored at -80°C. These standards, which included d<sub>5</sub>-RvD2, d<sub>4</sub>-LTB<sub>4</sub>, d<sub>8</sub>-5-HETE, d<sub>4</sub>-PGE<sub>2</sub> and d<sub>5</sub>-LXA<sub>4</sub>, were used to assess extraction recovery. The tissue samples were then centrifuged (3,000 rpm) and the supernatants were subjected to solid phase extraction and LC-MS/MS analysis, essentially as described by English et al.<sup>70</sup> Briefly, lipid mediators were extracted by C18 column chromatography and were eluted in methyl formate fractions. The solvent was then evaporated under N<sub>2</sub> gas and lipid mediators were resuspended in methanol:water (50:50). For analysis, a high performance liquid chromatograph (HPLC, Shimadzu) coupled to a QTrap5500 mass spectrometer (AB Sciex) was used and operated in negative ionization mode. Identification and quantification of lipid mediators was achieved using multiple reaction monitoring transitions, information-dependent acquisition and enhanced product ion scanning.<sup>70</sup> The levels of individual lipid mediators were normalized to extraction recovery of internal deuterium-labeled standards

and quantified based on calibration curves using external standards for each mediator. The levels of each compound were then imported into MetaboAnalyst where further statistical analyses could be performed. For this, missing value imputation was performed in which half the minimum positive value was used for compounds that were not detected in all samples. Next, the data were subjected to a log transformation and autoscaling so that all metabolites carried equal importance. We then conducted partial least squares-discriminant analysis and volcano plot analysis. The relative levels of each detected compound was also compared and displayed in a heatmap format to more easily appreciate the differences between individual samples, as well as experimental groups.

### **Atherosclerosis Quantification**

Atherosclerosis burden was quantified in the aortic root after 16 weeks of diet and ASO treatment as previously described.<sup>71</sup> Briefly, hearts were formalin fixed and sectioned, and slides were stained with Oil Red O and hematoxylin. Aortic root lesion area was quantified by ImageJ software taking the mean value from six sections, as described previously.<sup>71</sup> Additionally, all aortae were subjected to biochemical analyses to determine free and esterified cholesterol mass as previously described.<sup>72-74</sup> Hematoxylin & eosin staining of aortic root cross sections were utilized to measure necrotic core area, as described previously.<sup>75</sup>

## **Primary Macrophage Studies**

Elicited peritoneal macrophages were collected 4 days after injection of 1ml of 10% thioglycolate into the peritoneal cavities of mice that had been treated with control or *Fads1* ASOs and fed the SFA-rich diet for 8 weeks as previously described.<sup>61,65,76</sup> Following 2 hours of culture, non-adherent cells were removed by washing three times with PBS, and remaining adherent macrophages were stimulated with lipopolysaccharide (50 ng/ml) or recombinant interleukin 4 (10 ng/ml) to promote classic/pro-inflammatory) or alternative/pro-resolving skewing, respectively. Six hours after stimulus addition RNA and conditioned media were collected for subsequent analysis.

## ***In vivo* Immune Stimulation Studies**

Animals were fed diets and treated with ASOs for a period of 8 weeks before receiving intraperitoneal injections of vehicle (0.9% saline), lipopolysaccharide (LPS) (*Escherichia coli* 0111:B4), or IL-4 (2 µg, Peprotech) that was complexed with anti-IL4 mAb (10 µg, clone 11B11) as previously described.<sup>77,78</sup> Following injection, plasma was collected at 1 h via tail snip (for acute phase cytokine measurements), and exactly 6 h after injection mice were sacrificed. Thereafter, a midline laparotomy was performed, and blood was collected by heart puncture (for terminal cytokine measurements). After blood collection, a whole-body perfusion was conducted by puncturing the inferior vena cava and slowly delivering 10 mL sterile 0.9% saline into the left ventricle of the heart to remove residual blood. Aortic arches and livers were harvested and snap-frozen for

subsequent analyses. Plasma cytokine concentrations were determined using the MSD V-PLEX Proinflammatory Panel I, a highly sensitive multiplex enzyme-linked immunosorbent assay (ELISA) designed to quantitatively measure 10 cytokines including interferon  $\gamma$  (IFN- $\gamma$ ), interleukin (IL)-1 $\beta$ , IL-2, IL-4, IL-6, IL-8, IL-10, IL-12p70, IL-13, and tumor necrosis factor  $\alpha$  (TNF $\alpha$ ) from a single specimen using an electrochemiluminescent detection method (MesoScale Discovery, Gaithersburg, MD, USA).

### **Oxymax/CLAMS Energy Expenditure Studies**

For indirect calorimetry studies, mice ( $n=6$ ) were treated with ASOs and fed diets for 6 weeks prior to study. Animals were allowed to equilibrate to metabolic cage environments at room temperature (22°C) for ~72 hours before 24 hours of continuous data collection. Oxygen consumption ( $VO_2$ ), heat, and respiratory exchange ratio (RER), and activity were constantly monitored using the Oxymax Comprehensive Laboratory Animal Monitoring System (CLAMS) home cage system (Columbus Instruments).

### **Glucose Tolerance Testing**

Glucose tolerance tests were performed after a 4-6 hour fast by injecting 1 g/kg body weight of glucose into the peritoneal cavity. Tail vein plasma glucose levels were measured using a commercial glucometer (ACCU-CHEK Performa, Roche). Glucose tolerance tests were performed on mice that had been treated with diet and ASO for 14 weeks.

## **Liver Histological Analysis**

Hematoxylin and eosin staining of paraffin-embedded liver sections was performed as previously described.<sup>62</sup> Histopathologic evaluations were scored in a blinded fashion by a board certified pathologist (Daniela S. Allende – Cleveland Clinic).

## **Total Hepatic Triglyceride, Free Cholesterol, and Phosphatidylcholine Analyses**

Extraction of liver lipids and quantification of total hepatic triglyceride, free cholesterol, and phosphatidylcholine was conducted using enzymatic assays as described previously.<sup>64,65</sup>

## **Hepatic Triglyceride Secretion Assay**

Mice were fasted for ~18h on fresh bedding with free access to drinking water. Blood was collected via tail snip prior to (0 h) and 1, 2, and 3 h after intraperitoneal injection of tyloxapol (500 mg/kg Triton WR-1339). Serum triglyceride levels were measured at each time point enzymatically (L-Type TG M, Wako Diagnostics).

## **Fecal Neutral Sterol Quantification**

Animals were housed in wire-bottomed cages for 3 days to isolate feces, and feces were subsequently dried and ground into a fine powder. A measured

amount of powdered feces (~100 mg) was extracted as described previously.<sup>79</sup> Mass fecal neutral sterol analysis was performed by gas liquid chromatography as previously described.<sup>64,80</sup>

### **Flow Cytometric Quantification of Circulating Leukocyte Populations**

Peripheral blood was obtained following 10 weeks of diet and ASO treatment by submandibular vein puncture for circulating leukocyte analysis. Red blood cells were removed from flow cytometry preparations by treatment with ammonium, chloride, potassium (ACK) lysing buffer (BioWhittaker, Lonza, Walkersville, MD). The remaining white blood cells were incubated with the following monoclonal antibodies: CD3e-APC-Cy7 clone: 145-2C11 (BD Pharmingen, BD Biosciences, Becton, Dickinson and Company, Franklin Lakes, NJ); CD4-Alexa Fluor 700 clone: RM4-5 (BD Pharmingen, BD Biosciences, Becton, Dickinson and Company, Franklin Lakes, NJ); CD8a-PE-Cyanine7 clone: 53-6.7 (eBioscience, San Diego, CA); CD115-PE clone: AFS98 (eBioscience, San Diego, CA); Ly-6G-APC clone: 1A8 (eBioscience, San Diego, CA); Ly-6C-FITC clone: AL-21 (BD Pharmingen, BD Biosciences, Becton, Dickinson and Company, Franklin Lakes, NJ). Data were acquired on a BD LSRFortessa (BD Biosciences, Becton, Dickinson and Company, Franklin Lakes, NJ) and analyzed using FlowJo Data Analysis Software v.10.0.8 (FlowJo, LLC, Ashland, Oregon).

### **Real-Time PCR Analysis of Gene Expression**

Cells or tissue RNA extraction was performed as previously described for all

mRNA analyses.<sup>62,64,65,77</sup> Quantitative real time PCR (qPCR) analyses were conducted as previously described.<sup>62,64,65,77</sup> Cyclophilin A was used as a housekeeping gene for all qPCR analyses and mRNA expression levels were calculated based on the  $\Delta\Delta$ -CT method. qPCR was conducted using the Applied Biosystems 7500 Real-Time PCR System. Primers used for qPCR are available on request.

### **Statistical Analysis**

All data were analyzed using either *t*-test, one-way, or two-way analysis of variance (ANOVA) where appropriate, followed by Tukey-HSD post hoc analysis. Only lipid mediator data required transformation (subjected to a log transformation and autoscaling so that all metabolites carried equal importance). Differences were considered significant at  $p < 0.05$ . Statistical analyses were performed using JMP Pro 10 (SAS Institute; Cary, NC), Graphpad Prism 6 (La Jolla, CA) and Metaboanalyst 3.0 (<http://www.metaboanalyst.ca/>) software.

## **2.3 Results**

### ***Fads1* is a Key Determinant of Membrane Phospholipid Composition and Pro-Inflammatory Versus Pro-Resolving Lipid Mediator Balance**

To understand the role of *Fads1* in maintaining membrane lipid composition and lipid mediator balance in the context of cardiometabolic disease, we utilized an *in vivo* ASO-mediated knockdown approach<sup>59</sup> in hyperlipidemic low-density lipoprotein receptor-null mice. To selectively alter pro-inflammatory versus pro-

resolving lipid mediator balance in the context of *Fads1* loss of function, mice were also fed synthetic diets specifically designed to provide low or high levels of the  $\omega$ -3 FADS1 substrate fatty acid ETA (Figure 2A) as previously described by Shewale and colleagues.<sup>60</sup> *Fads1* ASO treatment resulted in selective knockdown of hepatic *Fads1* mRNA, without altering *Fads2* or *Fads3* mRNA expression (Figure 3A). In agreement with selective *Fads1* knockdown, *Fads1* ASO treatment resulted in plasma accumulation of the FADS1  $\omega$ -6 substrate DGLA and  $\omega$ -3 substrate ETA in a diet-specific manner (Figures 2B, and 3B, 3C). Reciprocally, FADS1 product fatty acids (AA and EPA) were significantly diminished in the plasma of *Fads1* ASO-treated mice (Figures 2B, and 3B, 3C). Similar diet-specific changes in FADS1 substrate (DGLA and ETA) and product (AA and EPA) fatty acids were seen in the liver of *Fads1* ASO-treated mice, where PUFA biosynthesis is known to be most active (Figure 3D, 3E). Strikingly, when mice were fed a diet enriched in  $\omega$ -3 PUFA precursors for ETA biosynthesis, *Fads1* knockdown resulted in greater than 80% of the total phospholipid fatty acid pool containing ETA (Figure 3D). This was associated with reciprocal reductions in the  $\omega$ -3 FADS1 product EPA in total hepatic phospholipids (Figure 3D). This FADS1 substrate/product shift was also seen in several phospholipid classes including phosphatidylethanolamines and phosphatidylcholines (Figures 2C and 3E). These results suggest that *Fads1* is a major contributor to membrane phospholipid remodeling under certain dietary conditions. Given the fundamental roles that AA and EPA play in lipid mediator production, we next quantified a wide array of pro-inflammatory and pro-resolving

**A**

Fatty Acid	SFA-Rich Diet	$\omega$ -3 Substrate Diet
	% of total FA	% of total FA
Palmitic acid (16:0)	43.05	25.2
Palmitoleic acid (16:1)	0.4	0.3
Stearic acid (18:0)	4.4	4.05
Oleic acid (18:1)	37.9	27.75
Linoleic acid (18:2 $\omega$ -6)	11	14
$\alpha$ -Linolenic acid (18:3 $\omega$ -3)	0.3	15.2
$\gamma$ -Linolenic acid (18:3 $\omega$ -6)	0	4.6
Stearidonic acid (18:4 $\omega$ -3)	0	6.25
Euric acid (22:1 $\omega$ -9)	0	0.15
Eicosapentaenoic acid (20:5 $\omega$ -3)	0.31	0.29
Docosahexaenoic acid (22:6 $\omega$ -3)	0.3	0.33

**B**

Plasma Fatty Acids ( $\mu$ g/ml)	SFA-Rich Diet		$\omega$ -3 Substrate Diet	
	Control ASO	Fads1 ASO	Control ASO	Fads1 ASO
Palmitic acid (16:0)	602.3 $\pm$ 22.3	765.9 $\pm$ 51.2*	506.5 $\pm$ 24.9*	*503.3 $\pm$ 13.0
Palmitoleic acid (16:1)	85.8 $\pm$ 5.2	99.5 $\pm$ 15.2	64.7 $\pm$ 7.4*	40.2 $\pm$ 2.8*#
Stearic acid (18:0)	188.7 $\pm$ 34.8	93.7 $\pm$ 13.4*	48.4 $\pm$ 8.6*	99.3 $\pm$ 20.3*#
Oleic acid (18:1)	482.4 $\pm$ 16.3	683.4 $\pm$ 39.1*	289.0 $\pm$ 24.1*	275.2 $\pm$ 28.6*
Linoleic acid (18:2 $\omega$ -6)	635.8 $\pm$ 46.3	655.1 $\pm$ 81.7	546.5 $\pm$ 36.7	426.2 $\pm$ 12.6*#
$\alpha$ -Linolenic acid (18:3 $\omega$ -3)	2.7 $\pm$ 0.3	2.4 $\pm$ 0.4	73.0 $\pm$ 4.1*	46.2 $\pm$ 2.9*#
$\gamma$ -Linolenic acid (18:3 $\omega$ -6)	8.6 $\pm$ 0.8	18.5 $\pm$ 1.7*	62.8 $\pm$ 6.5*	43.0 $\pm$ 2.1*#
Stearidonic acid (18:4 $\omega$ -3)	0.5 $\pm$ 0.08	0.7 $\pm$ 0.1	14.0 $\pm$ 2.3*	12.8 $\pm$ 1.6*
Dihomo- $\gamma$ -Linolenic acid (20:3 $\omega$ -6)	63.8 $\pm$ 5.6	258.9 $\pm$ 16.9*	97.1 $\pm$ 6.6*	178.1 $\pm$ 14.1*#
Arachidonic acid (20:4 $\omega$ -6)	304.1 $\pm$ 15.7	177.6 $\pm$ 21.7*	184.1 $\pm$ 6.9*	81.1 $\pm$ 6.5*#
Eicosatetraenoic acid (20:4 $\omega$ -3)	1.6 $\pm$ 0.1	9.1 $\pm$ 1.6*	53.3 $\pm$ 6.3*	136.4 $\pm$ 8.3*#
Eicosapentaenoic acid (20:5 $\omega$ -3)	40.4 $\pm$ 3.9	23.1 $\pm$ 3.5*	173.0 $\pm$ 16.2*	40.5 $\pm$ 1.6#
Docosahexaenoic acid (22:6 $\omega$ -3)	303.2 $\pm$ 25.1	345.4 $\pm$ 9.9	309.5 $\pm$ 13.6	317.6 $\pm$ 20.1

**C**

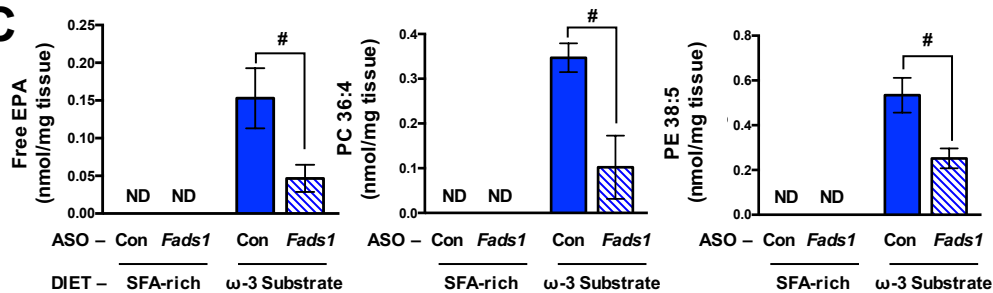


**Figure 2. Fatty Acid Composition of Experimental Diets, Plasma, and Liver. (A)** Fatty acid composition of individual fatty acids in experimental diets. **(B)** Total fatty acid composition of plasma (displayed as  $\mu$ g/ml) from mice treated with diet and ASOs for 16 weeks;  $n=6$  per group. Table displays mean  $\pm$  SEM. Statistical significance is determined by 2-way ANOVA, \* = significantly different from the control ASO – SFA-rich diet group (\* $p<0.05$ ); # = significantly different from control ASO group within the  $\omega$ -3 substrate diet group (# $p<0.05$ ). **(C)** Hepatic levels of eicosapentaenoic acid (EPA), phosphatidylcholine (PC) 36:4, and phosphatidylethanolamine (PE) 38:5 from mice treated with diet and ASOs for 16 weeks;  $n=5$  per group. Graphs display mean  $\pm$  SEM. Statistical significance determined by  $t$ -test (# $p<0.05$ ).

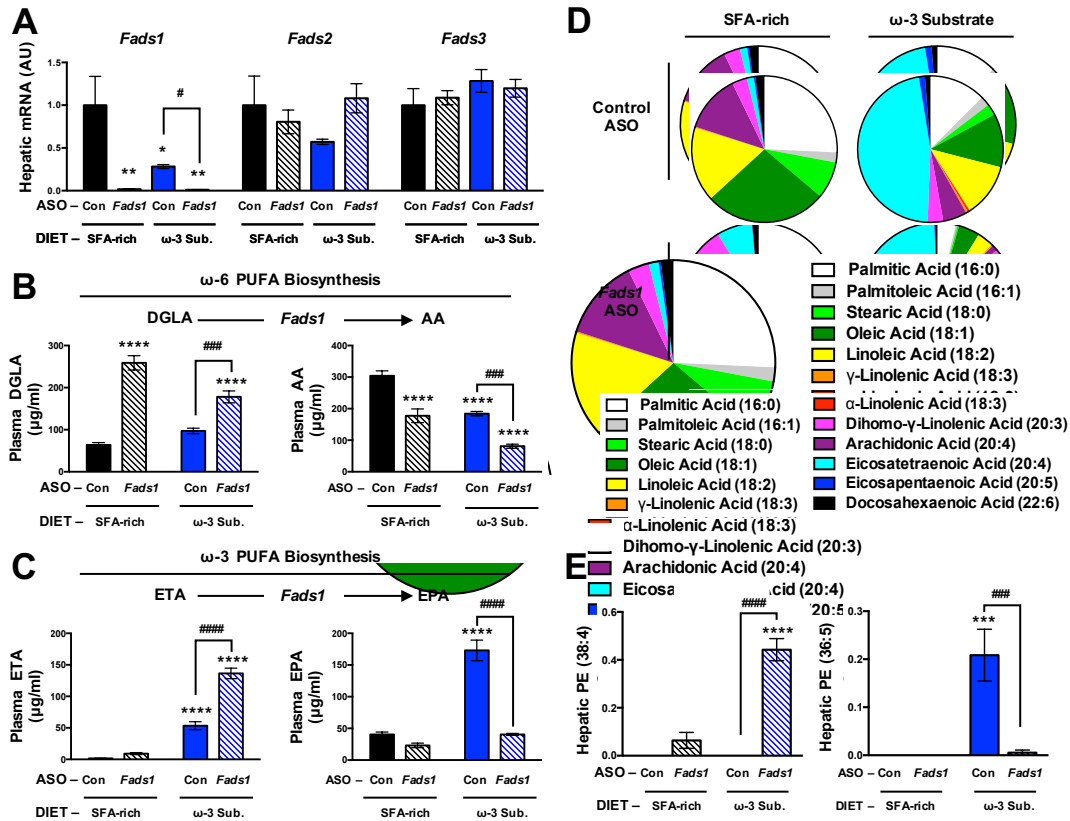


**Figure 3. *Fads1* is a Key Determinant of Membrane Phospholipid Composition.** (A) qPCR quantification of hepatic *Fads1*, *Fads2*, and *Fads3* mRNA;  $n=5$  per group. (B-C) FADS1 substrate ( $\omega$ -6 dihomo- $\gamma$ -linolenic acid, DGLA and  $\omega$ -3 eicosatetraenoic acid, ETA) and product ( $\omega$ -6 arachidonic acid, AA and  $\omega$ -3 eicosapentaenoic acid, EPA) fatty acid concentrations in plasma;  $n=6$  per group. (D) Total hepatic phospholipid fatty acid composition,  $n=5$  per group. (E) Hepatic phosphatidylethanolamine (PE) species 38:4 and 36:5,  $n=5$  per group. Graphs display mean  $\pm$  S.E.M. Statistical significance is determined by 2-way ANOVA. \* = significantly different from the control ASO – saturated and monounsaturated fatty acid (SFA)-rich diet group (\* $p<0.05$ , \*\* $p<0.01$ , \*\*\* $p<0.001$ , \*\*\*\* $p<0.0001$ ); # = significantly different from control ASO group within the  $\omega$ -3 substrate diet group (# $p<0.05$ , ## $p<0.01$ , ### $p<0.001$ , #### $p<0.0001$ ).

lipid mediators in the liver (Figure 4A-4E). Global lipid mediator product profiles were clearly distinct for both dietary and genetic (*Fads1*) interventions. In mice fed the diet enriched  $\omega$ -3 PUFA precursors, a clear shift in the production of SPMs was observed (Figure 4A-4E). In the presence of the  $\omega$ -3 PUFA substrate diet, *Fads1* knockdown resulted in a clear imbalance between pro-inflammatory and pro-resolving lipid mediators that would be predicted to oppose proper inflammation resolution. When broadly comparing the ratio of 5-lipoxygenase-derived SPMs to the pro-inflammatory mediator leukotriene B<sub>4</sub>, *Fads1* knockdown skews towards a more pro-inflammatory and less pro-resolving mediator profile (Figures 4E, and 5). In fact, *Fads1* knockdown resulted in significantly diminished levels of many of the major bioactive pro-resolving lipid mediators originating from enzymatic conversion of AA (lipoxin A<sub>4</sub>, lipoxin B<sub>4</sub>), EPA (15-hydroxyeicosapentaenoic acid, lipoxin A<sub>5</sub>), and DHA (17*R*-resolvin D1, resolvin D1; protectin D1) (Figures 4A-4E, and 5). Collectively, these results suggest that *Fads1* is a major contributor to diet-induced PUFA remodeling of hepatic membrane lipids, thereby dictating the balance of pro-inflammatory and pro-resolving lipid mediators.

### ***Fads1* Reciprocally Regulates Hepatic Inflammation and Lipogenesis**

In parallel to the observed imbalance between pro-inflammatory and pro-resolving lipid mediators, mice treated with *Fads1* ASO develop pathological histology and gene expression signatures that are characteristic of chronic hepatic inflammation (Figure 6A-6E). *Fads1* ASO-treated mice exhibited

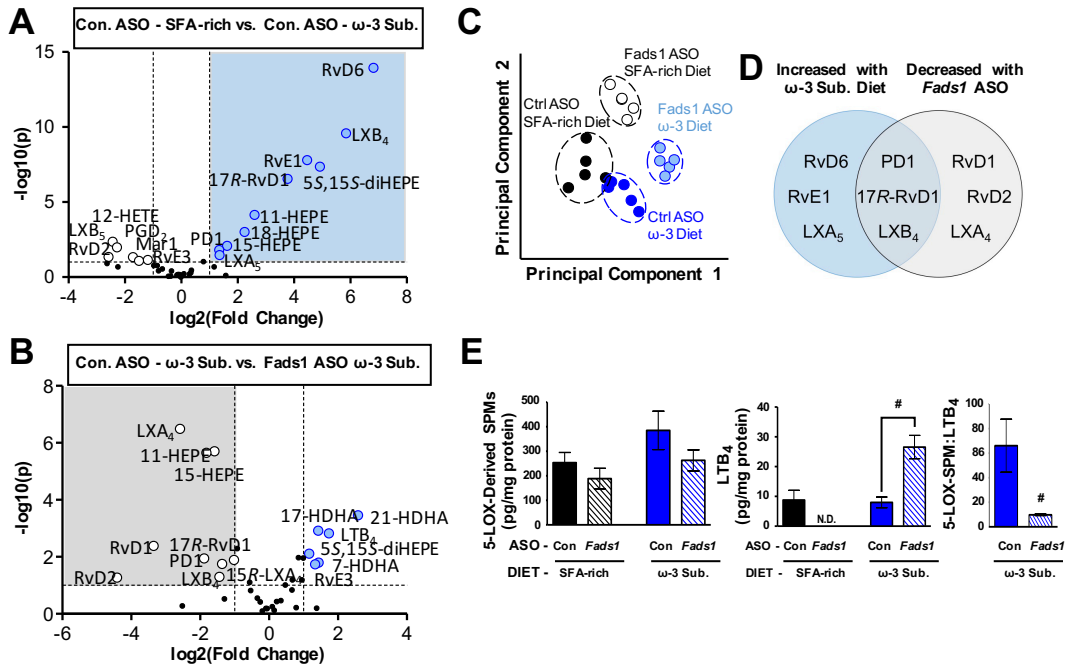


**Figure 4. *Fads1* is a Key Determinant of Pro-Inflammatory Versus Pro-Resolving Lipid Mediator Balance.** (A) Volcano plot of all metabolites detected with the larger circles that are labeled representing metabolites that exceeded the minimum thresholds for significance ( $p < 0.05$ ) and fold change ( $>$  or  $<$  2). Lipid mediators that were significantly increased in  $\omega$ -3 diet-fed animals are blue and appear in the shaded region while those that were significantly decreased are white;  $n = 5$  per group. (B) Volcano plot of all metabolites detected with the larger circles that are labeled representing metabolites that exceeded the minimum threshold for significance ( $p < 0.05$ ) and fold change ( $>$  or  $<$  2). Lipid mediators that were significantly decreased by *Fads1* ASO are white and appear in the shaded region while those that significantly increased are blue;  $n = 5$  per group. (C) Partial least squares-discriminant analysis two-dimensional scores plot demonstrated clustering of samples into distinct and separate groups based on both diet and ASO. (D) Venn diagram displaying the lipid mediators that were significantly increased by  $\omega$ -3 diet with control ASO in the blue circle and those that were significantly decreased by *Fads1* ASO while on  $\omega$ -3 diet in the gray circle. Those metabolites in the overlapping region both increased on  $\omega$ -3 diet and were decreased by *Fads1* ASO;  $n = 5$  per group. (E) (Left) Combined levels of 5-lipoxygenase (5-LOX)-derived specialized pro-resolving lipid mediators (SPM) are shown for each diet and treatment group. SPM included in this index are resolvin (Rv) D1, 17R-RvD1, RvD2, 17R-RvD3, RvD4, RvD6, RvE1, RvE2, lipoxin (LX) A<sub>4</sub>, 15R-LXA<sub>4</sub>, LXA<sub>5</sub>, LXB<sub>4</sub> and LXB<sub>5</sub>;  $n = 5$  per group. Graph displays mean  $\pm$  S.E.M. (Middle) Levels of leukotriene B<sub>4</sub> (LTB<sub>4</sub>). Only one of the five samples in the group fed a control diet and treated with *Fads1* ASO contained LTB<sub>4</sub> above the limit of detection (0.1 pg) and thus the entire group was omitted;  $n = 3-5$  per group. Graph displays mean  $\pm$  S.E.M. Statistical significance is determined by *t*-test. #  $p < 0.05$  control ASO vs *Fads1* ASO. (Right) The ratio of 5-LOX-derived SPM to LTB<sub>4</sub> is shown for mice on  $\omega$ -3 rich diet exposed to control or *Fads1* ASO;  $n = 5$  per group. Graph displays mean  $\pm$  S.E.M. Statistical significance is determined by *t*-test. #  $p < 0.05$  control ASO vs *Fads1* ASO).

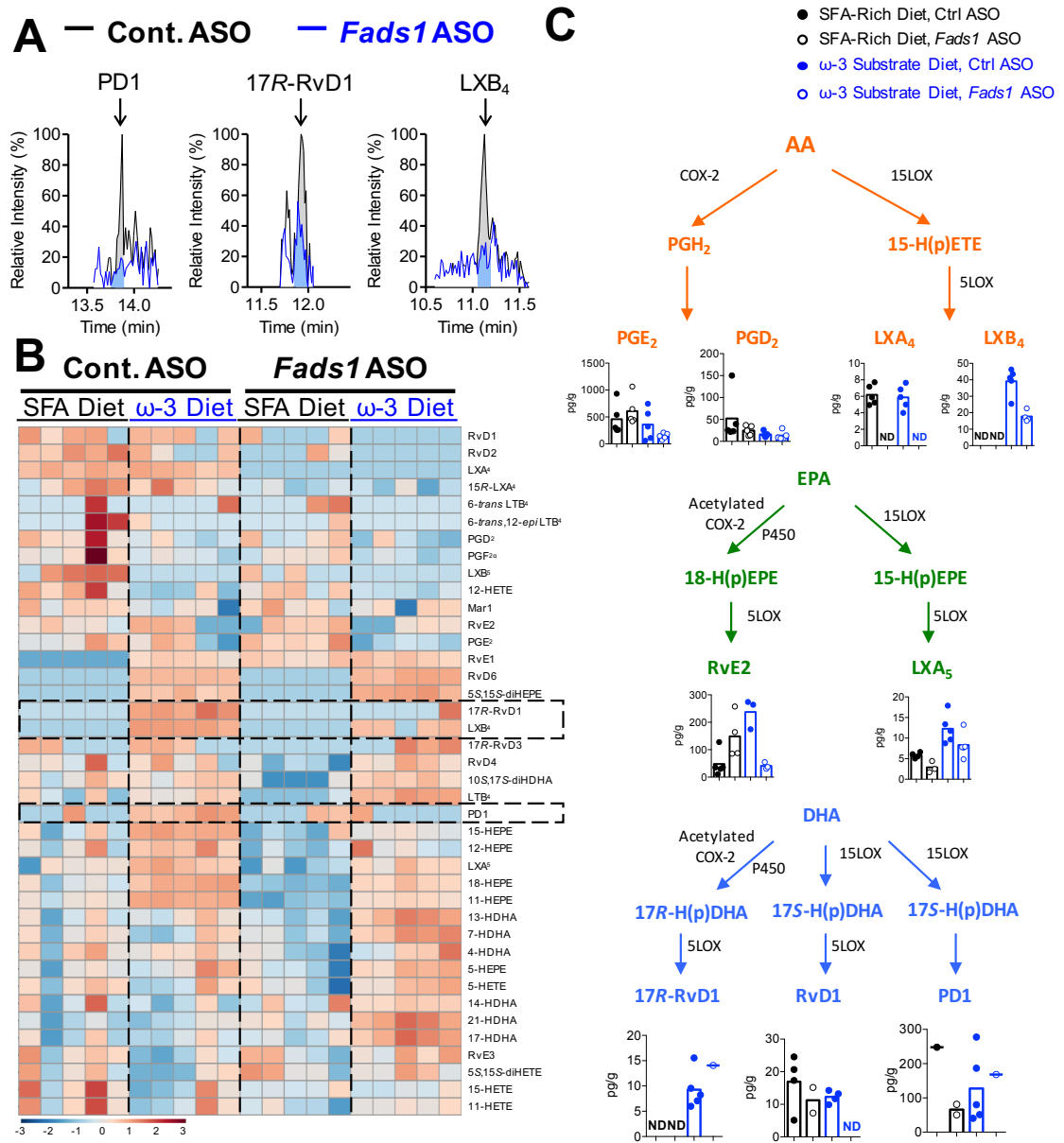


**Figure 5. *Fads1* Knockdown Diversifies PUFA-Derived Lipid Mediators in a Diet-Specific Manner.** (A) Representative multiple reaction monitoring (MRM) chromatograms used for identification of protectin D1 (PD1), 17*R*-resolvin D1 (17*R*-RvD1) and lipoxin B4 (LXB<sub>4</sub>). (B) A heatmap delineates the relative levels of all metabolites measured in each sample. (C) Data representing selected arachidonic acid (AA)-, eicosapentaenoic acid (EPA)-, and docosahexaenoic acid (DHA)-derived lipid mediators that were altered by *Fads1* knockdown in a diet-specific manner.

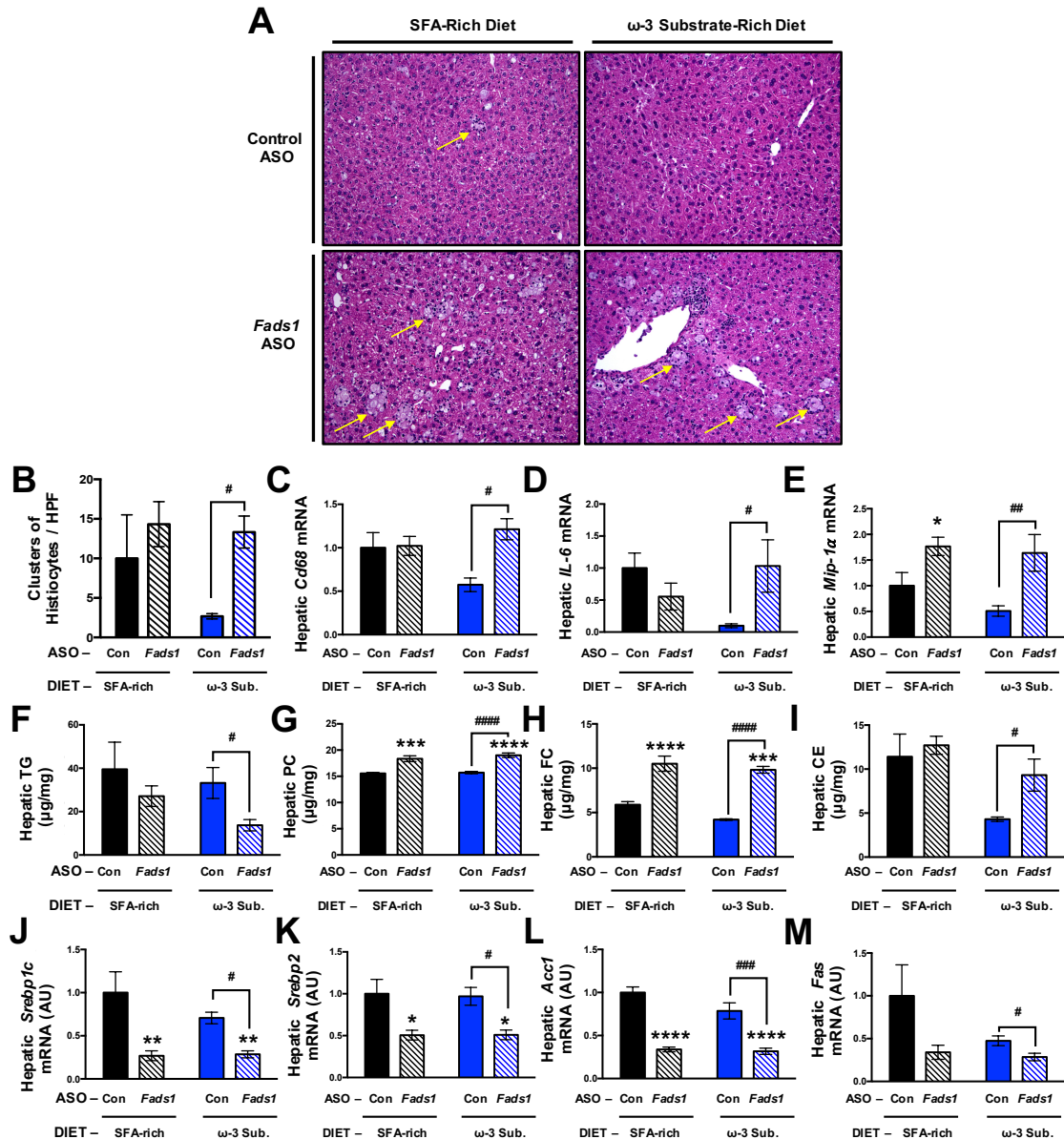


**Figure 6. *Fads1* is a Critical Regulator of Hepatic Inflammation and Lipogenesis.** (A) H&E-stained liver sections show enhanced immune cell invasion characterized mainly by foamy histiocytes in the context of *Fads1* knockdown (shown at 200x magnification); Arrows indicate areas of foamy histiocytes. (B) Pathologist quantified foamy histiocyte clusters per 40x field,  $n=3$  per group. (C-E) Hepatic expression of macrophage genes including cluster of differentiation 68 (*Cd68*), interleukin 6 (*IL-6*), and macrophage inflammatory protein 1 $\alpha$  (*Mip-1 $\alpha$* );  $n=5$  per group. (F-I) Total hepatic triglycerides (TG), phosphatidylcholine (PC), free cholesterol (FC), and cholesteryl ester (CE);  $n=6$  per group. (J-M) Hepatic expression of lipogenic genes including sterol regulatory element-binding proteins 1c (*Srebp1c*) and 2 (*Srebp2*), acetyl-CoA carboxylase 1 (*Acc1*), and fatty acid synthase (*Fas*);  $n=5$  per group. All graphs display mean  $\pm$  S.E.M. Statistical significance is determined by 2-way ANOVA. \* = significantly different from the control ASO – saturated and monounsaturated fatty acid (SFA)-rich diet group (\* $p<0.05$ , \*\* $p<0.01$ , \*\*\* $p<0.001$ , \*\*\*\* $p<0.0001$ ); # = significantly different from control ASO group within the  $\omega$ -3 substrate diet group (# $p<0.05$ , ## $p<0.01$ , ### $p<0.001$ , #### $p<0.0001$ ).

abnormal appearance of foamy histiocyte clusters that were significantly increased in mice fed the  $\omega$ -3 PUFA substrate diet (Figure 6A, 6B). *Fads1* knockdown was also associated with increased expression of macrophage-selective genes including cluster of differentiation 68 (*Cd68*), interleukin-6 (*IL-6*), and macrophage inflammatory protein 1  $\alpha$  (*Mip-1 $\alpha$* ) (Figure 6C-6E). It is important to note that *Fads1* ASO-driven hepatic inflammation was most apparent in mice fed the  $\omega$ -3 PUFA substrate diet (Figure 6A-6E), a condition where the ratio of 5-lipoxygenase-derived SPMs to leukotriene B<sub>4</sub> is dramatically decreased (Figure 4E). In addition to effects on hepatic inflammation, *Fads1* knockdown was also associated with reorganization of hepatic lipid metabolism that extends beyond the scope of direct effects on PUFA biosynthesis. *Fads1* knockdown resulted in reduced hepatic triglycerides in mice fed the  $\omega$ -3 PUFA substrate diet (Figure 6F), while increasing phosphatidylcholine, free cholesterol and cholesteryl ester levels (Figure 6G-6I). In conjunction with these alterations in major hepatic lipid species, *Fads1* knockdown was associated with reorganization of lipid metabolic gene expression. *Fads1* knockdown significantly reduced the expression of the master lipogenic transcription factors sterol regulatory element-binding proteins 1c (*Srebp1c*) and 2 (*Srebp2*), and their downstream target genes including acetyl-CoA carboxylase 1 (*Acc1*), and fatty acid synthase (*Fas*) in the liver (Figure 6J-6M). In agreement with suppression of hepatic *de novo* lipogenesis, *Fads1* ASO-treated mice also exhibited reduced body weight and white adipose tissue mass (Figure 7), despite eating the same amount of food (data not shown). Although *Fads1* ASO treatment produced very

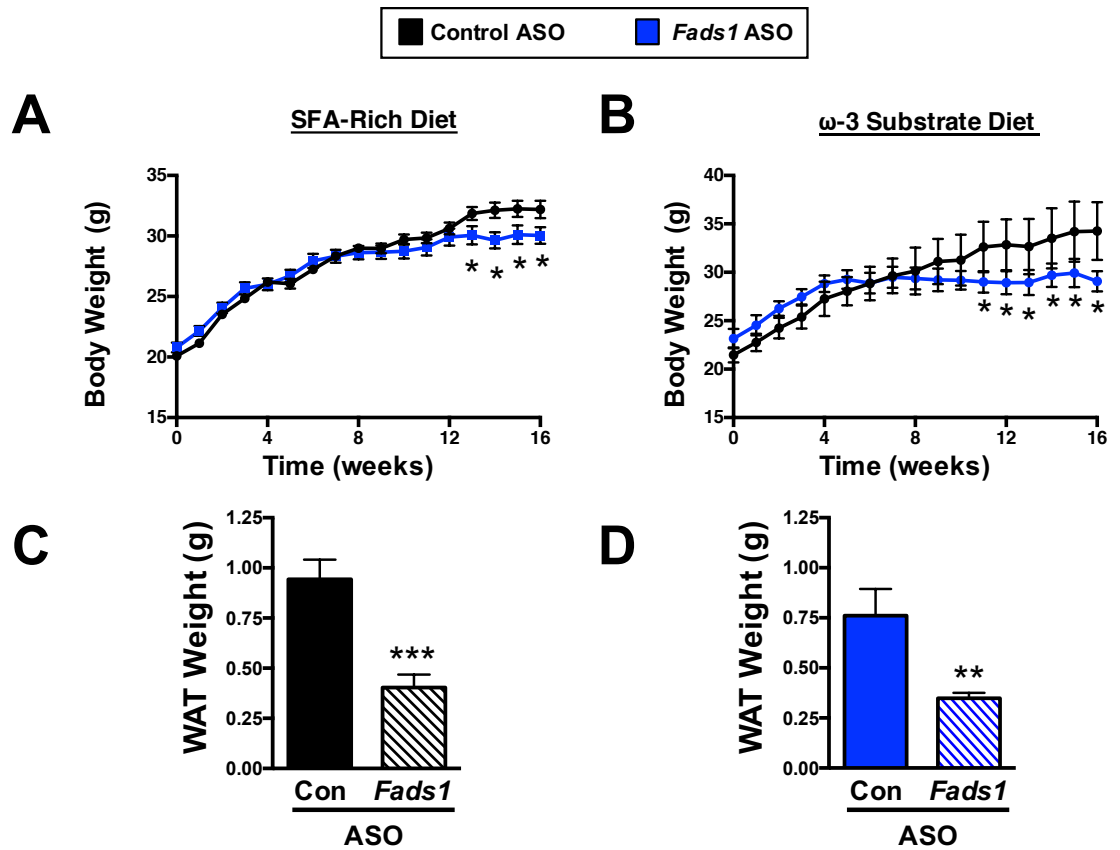


**Figure 7. *Fads1* Knockdown Decreases Adiposity.** (A-B) Body weight curves over the study period;  $n=9-12$  per group. (C-D) Gonadal white adipose tissue weight from mice fed diets and treated with ASOs for 16 weeks;  $n=9-12$  per group. Graphs display mean  $\pm$  SEM. Statistical significance determined by  $t$ -test ( $*p<0.05$ ).

minor alterations in oxygen consumption ( $VO_2$ ) and carbon dioxide production ( $VCO_2$ ), *Fads1* knockdown did significantly increase the respiratory exchange ratio (RER) in the SFA-fed group (Figure 8F). In line with alterations in adiposity, *Fads1* ASO-treated mice had improvements in glucose tolerance and modest reductions in fasting plasma insulin levels (Figure 9). Collectively, these data suggest that *Fads1* knockdown limits hepatic fatty acid synthesis, adipose tissue expansion, and glucose intolerance, while promoting hepatic inflammation under dietary conditions that favor an imbalance of pro-inflammatory and pro-resolving lipid mediators.

### ***Fads1* Knockdown Promotes Dyslipidemia and Atherosclerosis in a Diet-Specific Manner**

Polymorphisms in the *FADS1-2-3* gene cluster have been repeatedly associated with plasma lipids and other cardiovascular disease risk factors,<sup>46-56</sup> yet whether *FADS1*-driven  $\Delta$ -5 desaturation underlies these genetic associations has remained elusive. Selective ASO-mediated knockdown of *Fads1* trended ( $p=0.06$ ) towards promoting aortic root atherosclerosis in saturated fat-fed mice, and significantly increased aortic root lesion size in mice fed the  $\omega$ -3 PUFA substrate diet (Figure 10A, 10B). In agreement with effects in the aortic root, *Fads1* knockdown increased cholesteryl ester levels in whole aortae of mice fed the  $\omega$ -3 PUFA substrate diet, and also trended towards elevating aortic free cholesterol levels (Figure 10C, 10D). In contrast, *Fads1* knockdown did not significantly alter the total necrotic core area on either dietary background (Figure

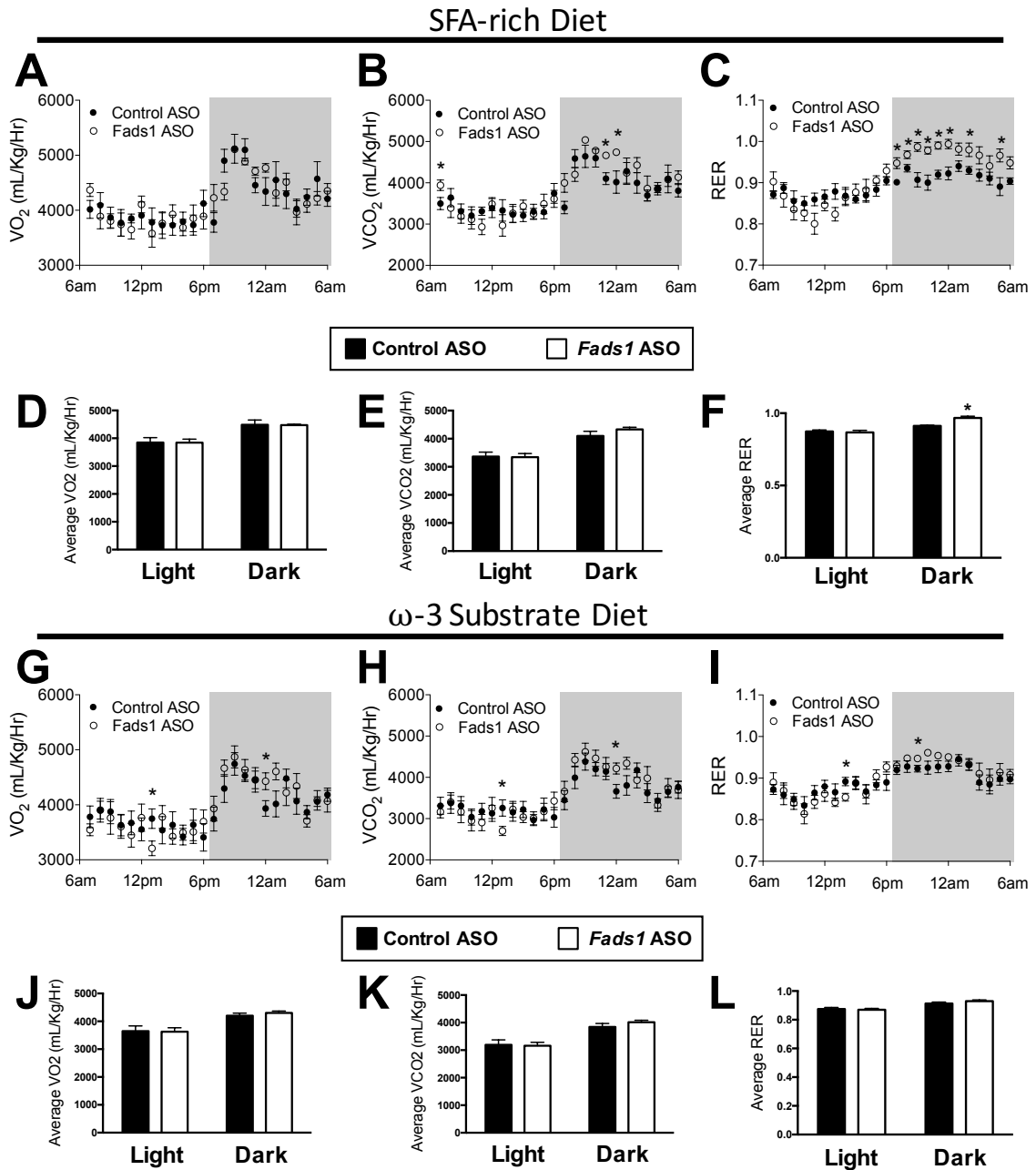


**Figure 8. Effects of *Fads1* Knockdown on Energy Expenditure.** (A-F) Oxymax/CLAMS data from mice fed SFA-rich diet and treated with ASOs for 6 weeks;  $n=6$  per group. (G-L) Oxymax/CLAMS data from mice fed  $\omega$ -3 substrate diet and treated with ASOs for 6 weeks;  $n=6$  per group. Graphs display mean  $\pm$  SEM. Statistical significance is determined by  $t$ -test (\* $p<0.05$ ).

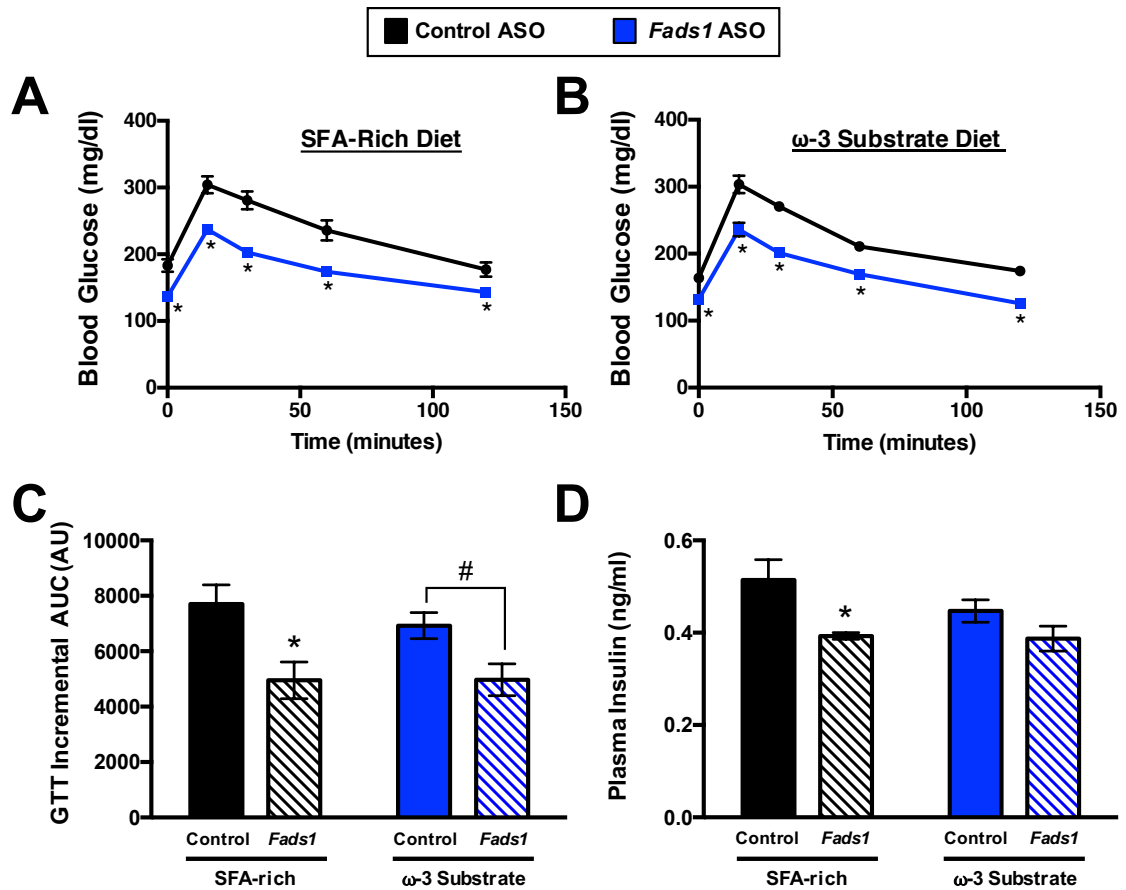
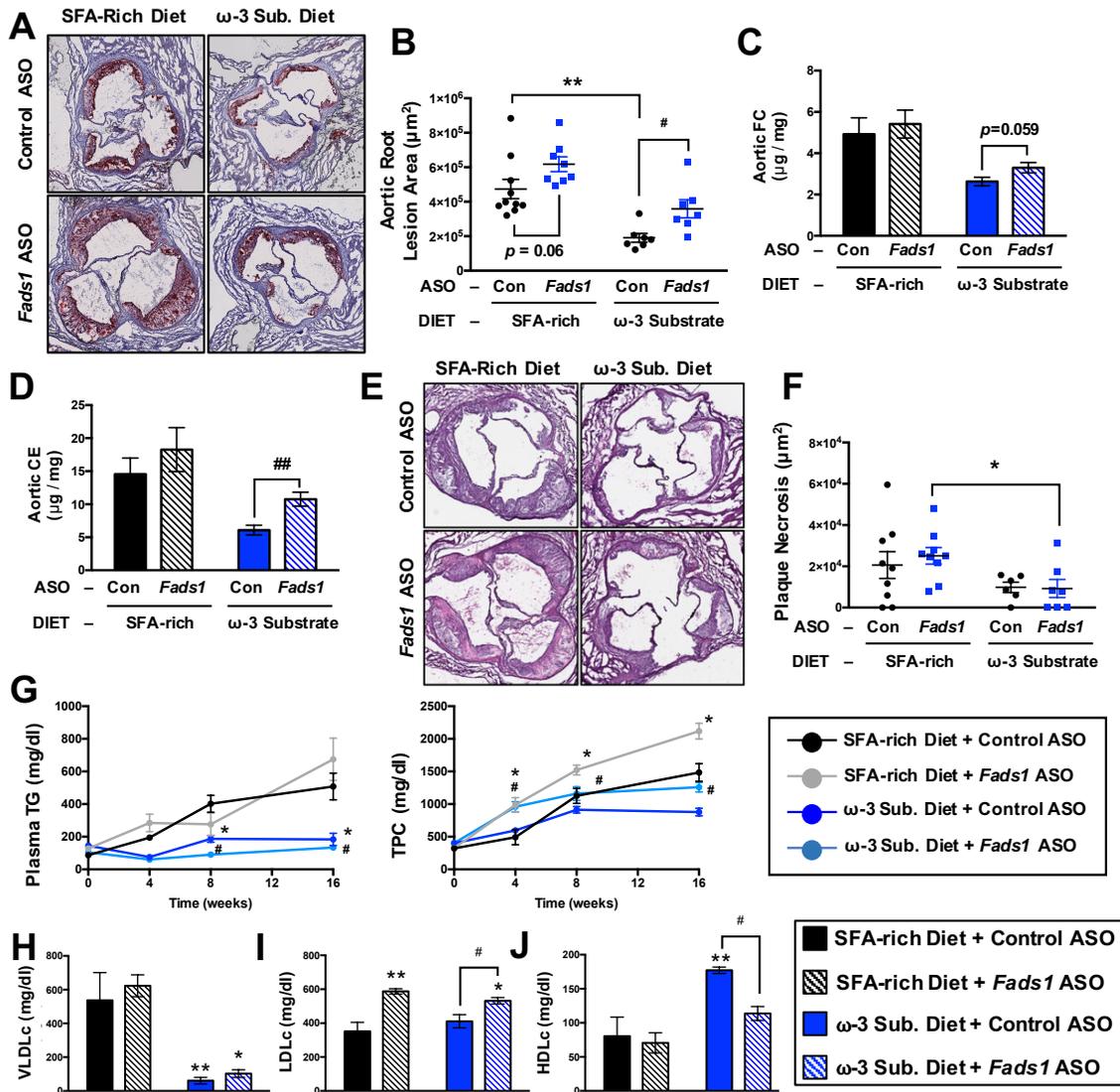


**Figure 9. *Fads1* Knockdown Improves Glucose Tolerance.** (A-B) Glucose tolerance tests in mice fed diets and treated with ASOs for 14 weeks;  $n=8-10$  per group. (C) Incremental AUCs corresponding to glucose tolerance tests:  $n=8-10$  per group. (D) Plasma insulin in mice fed diets and treated with ASOs for 16 weeks;  $n=6$  per group. Graphs display mean  $\pm$  SEM. Statistical significance is determined by 2-way ANOVA, \* = significantly different from the control ASO – SFA-rich diet group ( $*p<0.05$ ); # = significantly different from control ASO group within the  $\omega$ -3 substrate diet group ( $\#p<0.05$ ).



10E, 10F). Unlike the significant effects on hepatic triglyceride levels (Figure 6F, 6J-6M), *Fads1* knockdown resulted in very minor alterations in plasma triglycerides, producing a transient triglyceride lowering effect that was only apparent at 8 weeks of dietary induction (Figure 10G). Given that very low-density lipoprotein triglyceride secretion rates were not significantly altered by *Fads1* knockdown (Figure 11), the alterations in plasma triglyceride and cholesterol levels observed in *Fads1* ASO-treated mice likely arise from altered intravascular metabolism and turnover of apoB-containing lipoproteins. Interesting, the hepatic expression of lipoprotein lipase (*Lpl*) was increased in *Fads1* ASO treatment (Figure 18L), which may contribute to the dyslipidemia seen in *Fads1* knockdown mice. However, *Fads1* ASO treatment promoted hypercholesterolemia under both dietary settings, characterized by significant increases in low-density lipoprotein cholesterol levels (Figure 10I) without altering very low-density lipoprotein cholesterol levels (Figure 10H). The previously reported ability of the  $\omega$ -3 PUFA substrate diet to increase high-density lipoprotein cholesterol levels<sup>60</sup> was abolished by *Fads1* knockdown (Figure 10J), indicating that endogenous EPA biosynthesis is necessary for this phenotype. In addition to alterations in plasma lipid levels, *Fads1* knockdown resulted in diet-specific reorganization of circulating leukocyte populations. In saturated fat-fed mice, *Fads1* knockdown reduced Ly6C<sup>High</sup> monocytes, and similarly reduced both CD4<sup>+</sup> and CD8<sup>+</sup> T cell populations (Figure 12A-12F). When challenged with the  $\omega$ -3 PUFA substrate diet *Fads1* ASO-treated mice exhibited elevations in Ly6C<sup>High</sup> and Ly6C<sup>Low</sup> monocytes and neutrophils, without significant alterations

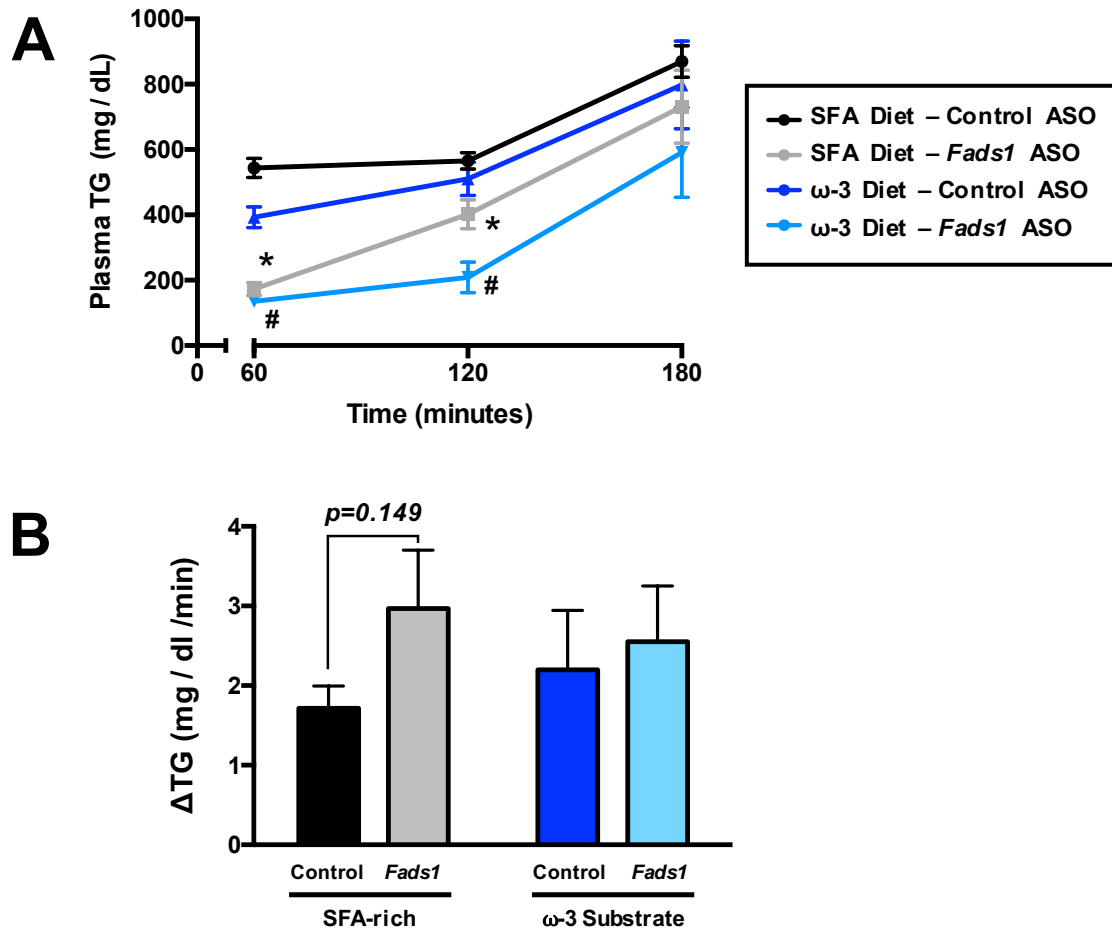


**Figure 11. *Fads1* Knockdown Reduces Circulating Triglyceride Levels Without Changing Triglyceride Secretion Rate.** (A) Triglyceride accumulation in plasma following Tyloxapol administration in mice fed diets and treated with ASOs for 10 weeks;  $n=5$  per group. Graph displays mean  $\pm$  SEM. Statistical significance is determined  $t$ -test at each time point. \* = significantly different from the control ASO – SFA-rich diet group ( $*p<0.05$ ); # = significantly different from control ASO group within the  $\omega$ -3 substrate diet group ( $#p<0.05$ ). (B) Calculated rates of triglyceride accumulation in plasma following Tyloxapol administration in mice fed diets and treated with ASOs for 10 weeks;  $n=5$  per group. Graph displays mean  $\pm$  SEM. Statistical significance is determined by 2-way ANOVA, \* = significantly different from the control ASO – SFA-rich diet group ( $*p<0.05$ ); # = significantly different from control ASO group within the  $\omega$ -3 substrate diet group ( $#p<0.05$ ).

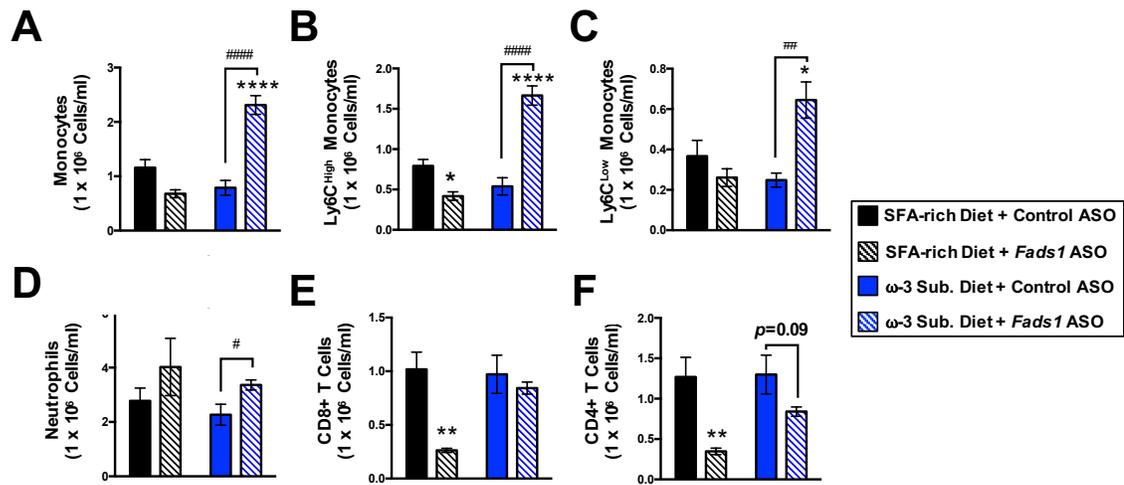


**Figure 12. *Fads1* Knockdown Alters Leukocyte Populations in a Diet-Specific Manner. (A-F)** Flow cytometric detection of circulating leukocyte populations;  $n=6$  per group. All graphs display mean  $\pm$  S.E.M. Statistical significance is determined by 2-way ANOVA. \* = significantly different from the control ASO – saturated and monounsaturated fatty acid (SFA)-rich diet group (\* $p<0.05$ , \*\* $p<0.01$ , \*\*\* $p<0.001$ , \*\*\*\* $p<0.0001$ ); # = significantly different from control ASO group within the  $\omega$ -3 substrate diet group (# $p<0.05$ , ## $p<0.01$ , ### $p<0.001$ , #### $p<0.0001$ ).

in T cell populations (Figure 12A-12F). Collectively, these data suggest that *Fads1*-driven  $\Delta$ -5 desaturation balances pro-atherogenic dyslipidemia and monocytes in a diet-specific manner (Figures 10 and 12).

### ***Fads1* Impacts Macrophage-Driven Inflammation and Resolution Programs Both *In Vitro* and *In Vivo***

Macrophages are requisite players in the pathogenesis of atherosclerosis, playing important roles in both the initiation and resolution phases of the disease progression.<sup>81</sup> Whereas classically activated macrophages are generally pro-inflammatory in nature, alternatively activated macrophages are thought to be involved in the resolution of inflammation during plaque regression and stabilization.<sup>82</sup> To address the role of *Fads1* in macrophage phenotype switching, we elicited peritoneal macrophages from ASO-treated mice, and acutely induced polarization programs with pro-inflammatory (lipopolysaccharide, LPS) or pro-resolving (interleukin 4, IL-4) stimuli (Figure 13). It is important to note that *Fads1* mRNA expression was suppressed by lipopolysaccharide treatment (Figure 13A), yet was increased by IL-4 treatment (Figure 13F). *Fads1* knockdown in macrophages was associated with skewing towards pro-inflammatory and away from pro-resolving polarization (Figure 13). In support of this, *Fads1* knockdown resulted in augmented lipopolysaccharide-driven pro-inflammatory gene expression (Figure 13A-13E), yet was associated with diminished IL-4-driven alternative activation gene signatures (Figure 13F-13J). The expression of AA and EPA oxidizing enzymes cyclooxygenases 1 (*Cox-1*)

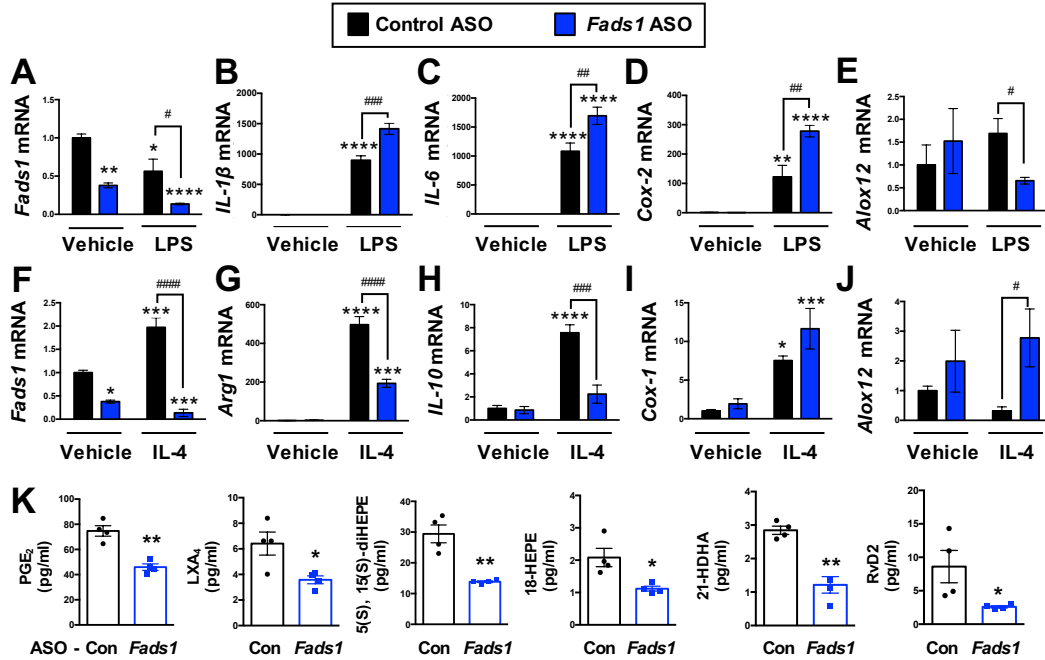


**Figure 13. *Fads1* Knockdown Promotes Classic Activation and Suppresses Alternative Activation Programs in Macrophages.** Low-density lipoprotein receptor-knockout mice were treated with ASOs and the saturated and monounsaturated fatty acid (SFA)-rich diet for 8 weeks, and then primary macrophages were elicited from the peritoneal cavity for functional characterization. **(A-E)** Macrophages isolated from control and *Fads1* ASO-treated mice were stimulated with 50 ng/ml lipopolysaccharide (LPS). 6 hours later gene expression was quantified by qPCR;  $n=4$  per group. **(F-J)** Macrophages isolated from control and *Fads1* ASO-treated mice were stimulated with 10 ng/ml interleukin 4 (IL-4). 6 hours later gene expression was quantified by qPCR;  $n=4$  per group. **(K)** Conditioned media was collected from non-stimulated macrophages for LC-MS/MS detection of lipid mediators;  $n=4$  per group. All graphs display mean  $\pm$  S.E.M. For panels A-J, statistical significance is determined by 2-way ANOVA. \* = significantly different from the control ASO – vehicle stimulus group (\* $p<0.05$ , \*\* $p<0.01$ , \*\*\* $p<0.001$ , \*\*\*\* $p<0.0001$ ); # = significantly different from control ASO group within the LPS or IL-4 treatment group (# $p<0.05$ , ## $p<0.01$ , ### $p<0.001$ , #### $p<0.0001$ ). For panel K, statistical significance is determined by *t*-test. \* = significantly different from control ASO group (\* $p<0.05$ , \*\* $p<0.01$ ).

and 2 (*Cox-2*) and 12-lipoxygenase (*Alox12*) were differentially expressed with *Fads1* knockdown under certain stimulated conditions (Figure 13D, 13E, 13I, 13J). *Fads1* knockdown in macrophages was also associated with generally lower levels of lipid mediators originating from oxidation of AA, EPA, and DHA (Figure 13K). Given that *Fads1* knockdown was associated with such striking diversification of lipid mediators both in isolated macrophages (Figure 13K) and in the liver (Figures 2 and 4A-4E), we performed linear regression analysis to correlate lipid mediator concentrations in the liver to the major *in vivo* phenotypes under study. The EPA-derived lipid mediator lipoxin A<sub>5</sub> was negatively associated ( $R^2=0.5299$ ,  $p=0.0003$ ) with atherosclerotic lesion area (Figure 14C), while the AA-derived mediator 5(S),15(S)-dihydroxyeicosatetraenoic acid was positively associated ( $R^2=0.2467$ ,  $p=0.026$ ) with atherosclerosis (Figure 14D). Circulating monocyte numbers were positively correlated with the AA-derived mediator leukotriene B<sub>4</sub> ( $R^2=0.6743$ ,  $p<0.0001$ ) and the poorly studied DHA-derived lipid mediator 21-hydroxydocosahexaenoic acid ( $R^2=0.612$ ,  $p=0.0003$ ) (Figure 14E, 14F). Also, blood glucose levels were negatively associated with the DHA-derived lipid mediators 17-hydroxydocosahexaenoic acid ( $R^2=0.5001$ ,  $p=0.0005$ ) and 21-hydroxydocosahexaenoic acid ( $R^2=0.3468$ ,  $p=0.006$ ) (Figure 14G, 14H). Collectively, these data suggest that *Fads1* plays an underappreciated role in macrophage polarization and lipid mediator production, and provide initial clues into potential *Fads1*-regulated lipid mediators driving diverse cardiometabolic phenotypes.

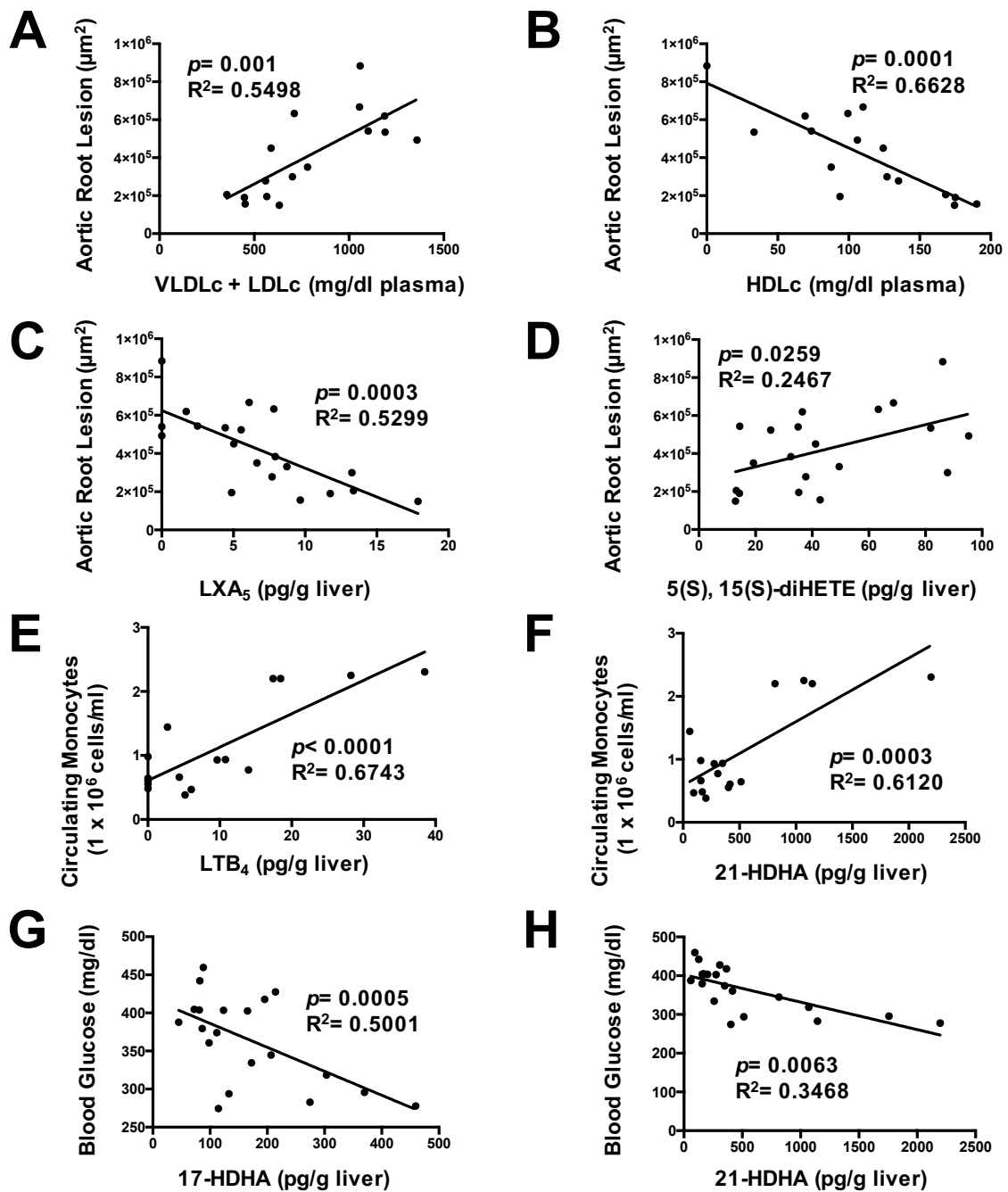


**Figure 14. *Fads1*-Driven Alterations in Lipid Mediators Correlate with Cardiometabolic Phenotypes.** Linear regression analysis of cardiometabolic phenotypes vs. lipid mediators. Each point represents an individual animal. Regression coefficient is shown for entire data set. **(A-B)** Lipoprotein-associated cholesterol (LDL+VLDL, and HDL) levels associate with atherosclerosis burden. **(C-D)** Lipoxin A<sub>5</sub> (LXA<sub>5</sub>) and 5(S), 15(S)-dihydroxyeicosatetraenoic acid (5(S), 15(S)-diHETE) levels associate with atherosclerosis burden. **(E-F)** Leukotriene B<sub>4</sub> (LTB<sub>4</sub>) and 21-hydroxydocohexaenoic acid (21-HDHA) levels associate with circulating monocyte levels. **(G-H)** 17-hydroxydocohexaenoic acid (17-HDHA) and 21-hydroxydocohexaenoic acid (21-HDHA) levels associate with blood glucose levels.

To further investigate the role of *Fads1* in orchestrating pro-inflammatory and pro-resolving macrophage programs *in vivo*, we treated diet-fed control and *Fads1* knockdown mice with pro-inflammatory (LPS) or pro-resolving (IL-4) skewing stimuli and followed acute inflammatory responses in the circulation (Figure 15), liver (Figure 15), and aortic arch (Figure 16). *Fads1* knockdown did not appreciably alter plasma cytokine levels under IL-4-stimulated conditions (data not shown), but did significantly alter LPS-stimulated plasma cytokine responses. Although *Fads1* knockdown did not alter the early LPS-induced burst of circulating tumor necrosis factor  $\alpha$  (TNF $\alpha$ ), *Fads1* ASO treatment was associated with significantly elevated LPS-stimulated levels of several interleukins (IL-1 $\beta$ , IL-12p70, and IL-10) after six hours (Figure 15A-15D). In the liver, *Fads1* knockdown was associated with increased expression of the macrophage marker genes *F4/80* and *Cd68*, and this effect was particularly apparent in mice fed the  $\omega$ -3 substrate diet (Figure 15F, 15G). *Fads1* knockdown in the liver was associated with reduced expression of the alternative/pro-resolving macrophage marker gene arginase 1 under all conditions (Figure 15H). In contrast, *Fads1* knockdown enhanced LPS-stimulated expression of macrophage-derived cytokines including MCP-1, MIP-1 $\alpha$ , and TNF $\alpha$  (Figure 15I-15K), yet modestly blunted expression of the acute phase protein serum amyloid A (SAA) in  $\omega$ -3 substrate diet-fed mice (Figure 15L). In the aortic arch, there was a roughly 50% knockdown of *Fads1* with *Fads1* ASO treatment, and much like what was seen in elicited macrophages (Figure 13A), LPS alone suppressed *Fads1* expression by 50% when compared

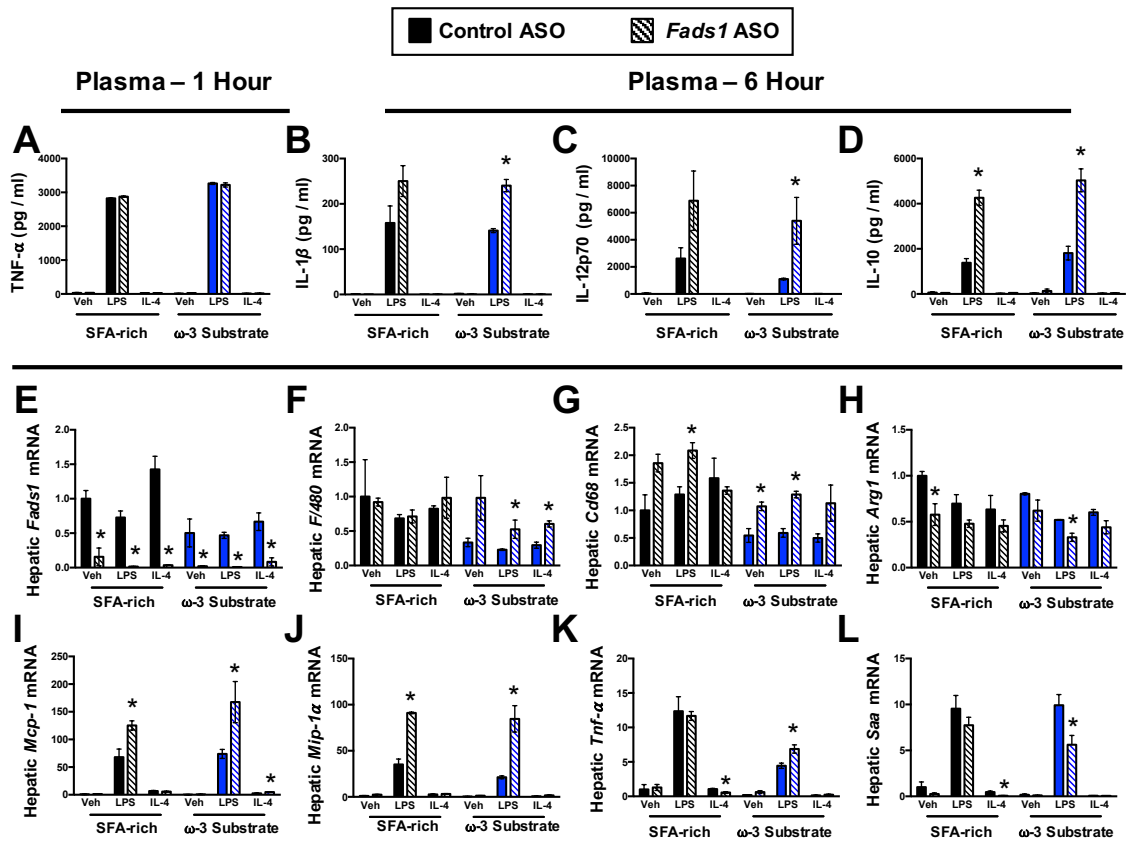


**Figure 15. *Fads1* Knockdown Alters Systemic Inflammation *In Vivo*.** (A) Acute phase TNF- $\alpha$  levels in plasma 1 hour after Veh/LPS/IL-4 stimulation in mice fed diet and treated with ASOs for 8 weeks;  $n=3$  per group. (B-D) Terminal cytokine levels in plasma 6 hours after Veh/LPS/IL-4 stimulation;  $n=3$  per group. (E-L) qPCR quantification of hepatic gene expression;  $n=3$  per group. All graphs display mean  $\pm$  S.E.M. Statistical significance is determined by *t*-test. \* = significantly different from control ASO group within the same diet group (\* $p<0.05$ ).

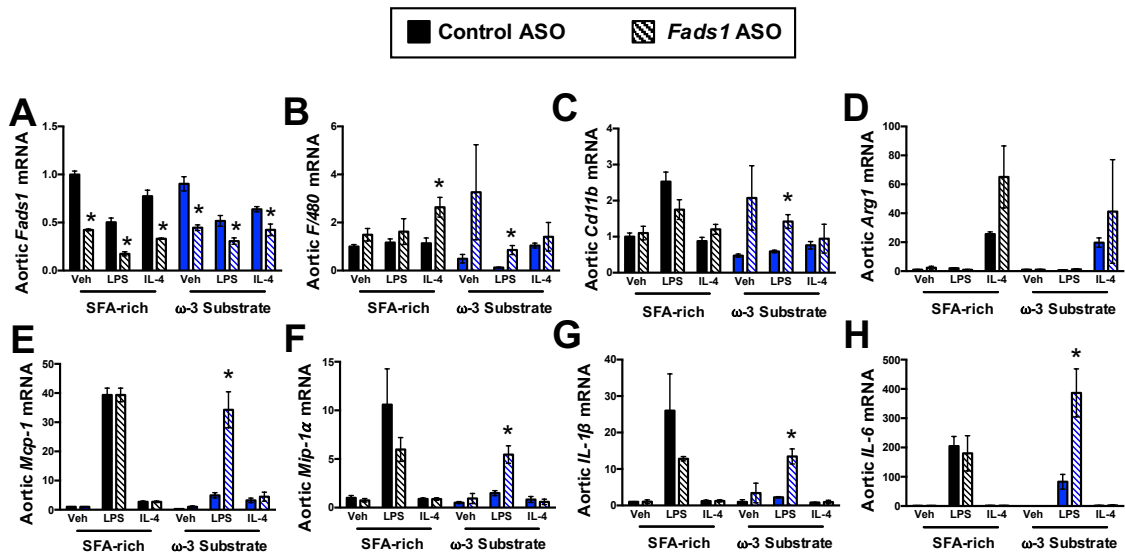


**Figure 16. *Fads1* Knockdown Alters Aortic Inflammation *In Vivo*.** (A-H) qPCR quantification of aortic arch gene expression;  $n=3$  per group. All graphs display mean  $\pm$  S.E.M. Statistical significance is determined by *t*-test. \* = significantly different from control ASO group within the same diet group ( $*p < 0.05$ ).

to saline injected mice (Figure 15A). *Fads1* knockdown in the aortic arch was associated with increased expression genes encoding macrophage markers such as *F4/80* and *Cd11b*, particularly in the  $\omega$ -3 substrate diet groups (Figure 16B, 16C). Furthermore, *Fads1* knockdown was associated with diet-specific effects on both LPS- and IL-4-stimulated cytokine expression in the aortic arch (Figure 16D-16H). Collectively, these results suggest that *Fads1* regulates systemic inflammation, tissue macrophage abundance, and macrophage polarization *in vivo* in a highly gene- and tissue-specific manner.

### ***Fads1* Determines the Reciprocal Regulation of Inflammation and Lipogenesis Driven by Liver X Receptor (LXR).**

The nuclear hormone receptor LXR is a well-known regulator of tissue inflammation, atherosclerosis, cholesterol balance, *de novo* lipogenesis, and membrane PUFA-diversification.<sup>83-88</sup> Given that our results here link *Fads1* to these same phenotypes we hypothesized that *Fads1* may be an important effector of LXR signaling. To test this, we examined LXR agonist-induced metabolic reprogramming in control and *Fads1* knockdown mice maintained on a chow diet (Figures 17 and 18). *Fads1* knockdown was associated with enhanced basal and LXR-stimulated fecal neutral sterol loss, yet was associated with blunted basal and LXR-stimulated liver triglyceride levels (Figure 17A, 17B). In contrast to these LXR-associated lipid phenotypes, the ability of *Fads1* knockdown to alter hepatic cholesterol levels was largely independent of LXR activation state (Figure 17C-17E). However, *Fads1* knockdown significantly

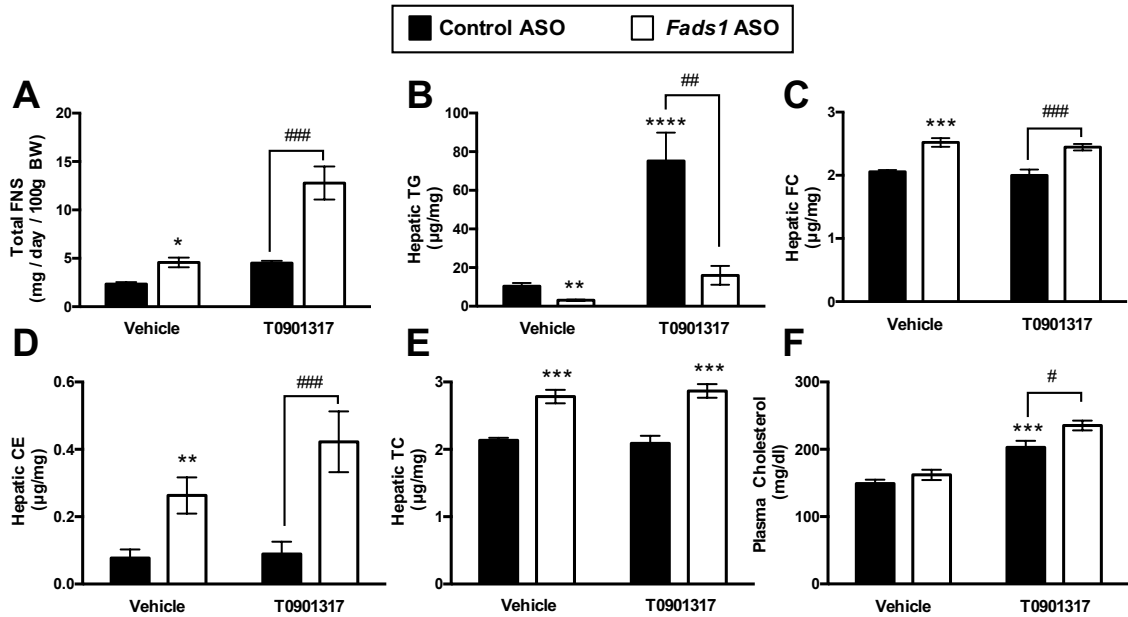


**Figure 17. *Fads1* Knockdown Impacts LXR-Driven Remodeling of Hepatic Lipids.** Chow-fed C57BL/6J mice were treated with control or *Fads1* ASO for 10 consecutive weeks, and then were also gavaged daily with Vehicle or T0901317 (25 mg/kg/day) during the tenth week; *n*=6 per group. **(A)** Total fecal neutral sterol loss from mice fed chow and treated with ASOs for 10 weeks. **(B)** Total hepatic triglycerides (TG); *n*=6 per group. **(C)** Hepatic free cholesterol (FC); *n*=6 per group. **(D)** Hepatic cholesteryl ester (CE); *n*=6 per group. **(E)** Hepatic total cholesterol (TC); *n*=6 per group. **(F)** Total plasma cholesterol in mice fed chow and treated with ASOs for 10 weeks; *n*=6 per group. All graphs display mean ± S.E.M. Statistical significance is determined by 2-way ANOVA. \* = significantly different from the control ASO – vehicle gavage group (\**p*<0.05, \*\**p*<0.01, \*\*\**p*<0.001, \*\*\*\**p*<0.0001); # = significantly different from control ASO group within the T0901317 gavage group (#*p*<0.05, ##*p*<0.01, ###*p*<0.001, ####*p*<0.0001).

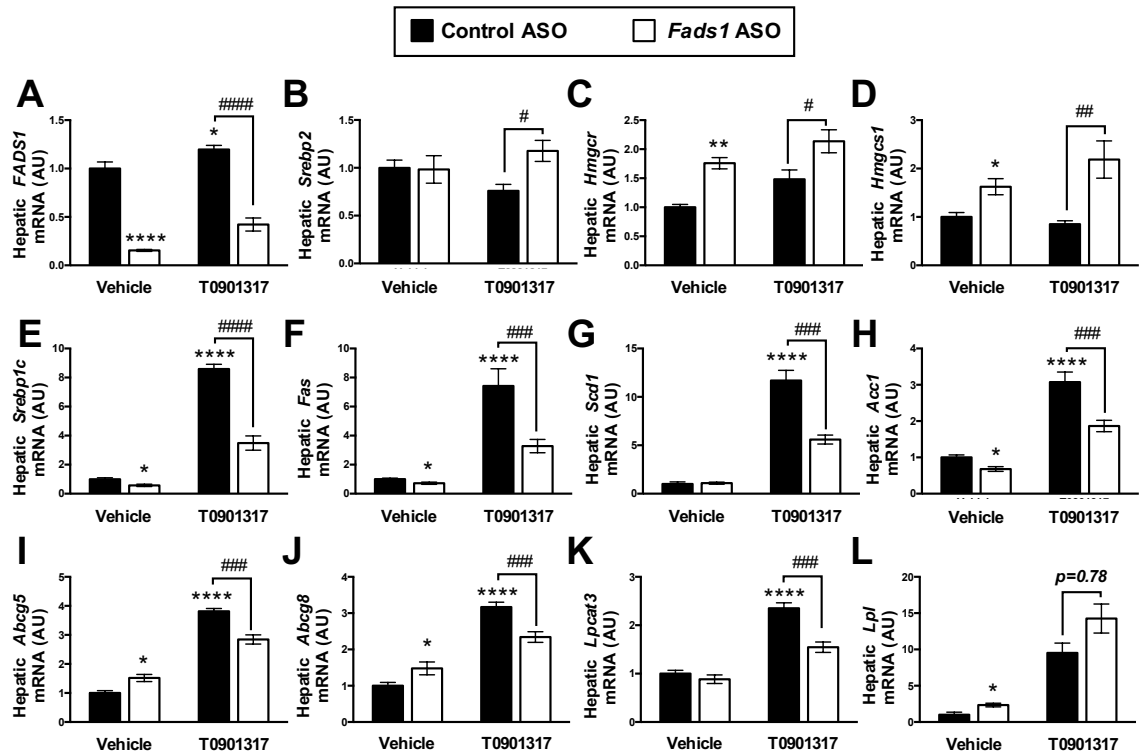


**Figure 18. *Fads1* is an Effector of LXR-Driven Reorganization of Lipid Metabolism.** Chow-fed C57BL/6J mice were treated with control or *Fads1* ASO for 10 consecutive weeks, and then were also gavaged daily with Vehicle or T0901317 (25 mg/kg/day) during the tenth week;  $n=6$  per group. (A-L) qPCR quantification of hepatic gene expression,  $n=6$  per group. All graphs display mean  $\pm$  S.E.M. Statistical significance is determined by 2-way ANOVA. \* = significantly different from the control ASO – vehicle gavage group (\* $p<0.05$ , \*\* $p<0.01$ , \*\*\* $p<0.001$ , \*\*\*\* $p<0.0001$ ); # = significantly different from control ASO group within the T0901317 gavage group (# $p<0.05$ , ## $p<0.01$ , ### $p<0.001$ , #### $p<0.0001$ ).

increased plasma cholesterol only in animals treated with pharmacological LXR agonist (Figure 17F). Knockdown of *Fads1* did not significantly alter the hepatic expression of *LXRα* itself (data not shown), but did result in selective alterations in LXR-stimulated gene expression (Figure 18A-18L). For instance, the ability of the LXR agonist T0901317 to increase the expression of *Srebp1c* and its target genes (*Fas*, *Scd1*, and *Acc1*) was blunted in *Fads1* knockdown mice (Figure 18E-18H). In parallel, LXR-stimulated expression of genes involved in cholesterol efflux (ATP-binding cassette transporters G5 and G8) and phosphatidylcholine remodeling (lysphosphatidylcholine acyltransferase) were also blunted in *Fads1* knockdown mice (Figure 18I-18K). However, not all LXR-stimulated gene expression was blunted in *Fads1* knockdown mice, as was the case for lipoprotein lipase (*Lpl*) (Figure 18L). The hepatic expression of HMG-CoA reductase (*Hmgcr*) and HMG-CoA synthase (*Hmgcs1*) were increased in both the basal and LXR-stimulated state (Figure 18C, 18D). However, *Fads1* knockdown only increased hepatic expression of *Srebp2* in the T0901317-treated mice (Figure 18B). These results suggest that *Fads1* is an effector of LXR agonist-driven transcriptional control of fatty acid and cholesterol metabolic programs in the liver.

## 2.4 Discussion

Cardiometabolic diseases including obesity, insulin resistance, atherosclerosis, and steatohepatitis all share tissue-specific features of chronic unresolved inflammation.<sup>89-92</sup> Although often underappreciated, membrane

PUFA-derived lipid mediators play requisite roles in both the initiation and resolution phase of inflammation. There is a wealth of evidence showing beneficial effects of dietary PUFA supplementation on cardiometabolic diseases,<sup>93-95</sup> yet the specific contribution of endogenous PUFA synthesis driven by FADS1 (i.e. AA and EPA generation) has been elusive. Here we provide new evidence that *Fads1*-driven PUFA biosynthesis plays a role in cardiometabolic diseases associated with chronic unresolved inflammation (obesity, insulin resistance, atherosclerosis, and steatohepatitis). The main findings of the current study are: (1) *Fads1* is a major contributor to diet-driven enrichment of PUFAs in membrane phospholipids; (2) *Fads1* loss of function results in diminished levels of AA-, EPA-, and DHA-derived pro-resolving lipid mediators; (3) *Fads1* knockdown promotes hepatic inflammation in a diet-specific manner; (4) *Fads1* knockdown promotes atherosclerosis in a diet-specific manner; (5) *Fads1* knockdown results in the suppression of hepatic *de novo* lipogenesis; (6) *Fads1* knockdown is associated with reduced adiposity and improved glucose tolerance; (7) *Fads1* knockdown results in atherogenic dyslipidemia; (8) *Fads1* activity impacts circulating monocyte and T cell levels in a diet-specific manner; (9) *Fads1* reciprocally regulates pro-inflammatory and pro-resolving polarization programs in macrophages; (10) *Fads1* is a tissue-specific effector of LPS- and IL-4-driven reprogramming of systemic inflammatory responses *in vivo*; and (11) *Fads1* reciprocally regulates fatty acid and cholesterol reprogramming driven by the liver X receptor (LXR). Collectively, these data support a model in which *Fads1*-driven AA and EPA production diversifies both pro-inflammatory and pro-

resolving lipid mediator production to dictate proper inflammation initiation and resolution in cardiometabolic disease.

The *FADS1-2-3* genetic locus is unique in that it shares genome-wide significant associations with almost all cardiometabolic phenotypes across the metabolic syndrome spectrum.<sup>46-56</sup> However, the relative roles of the three separate enzymes (*FADS1*, *FADS2*, and *FADS3*) encoded at this locus in driving cardiometabolic disease has been elusive. This study provides the first evidence that specific loss of the  $\Delta$ -5 desaturase *FADS1* can dynamically alter many of the cardiometabolic phenotypes originally identified in human genome-wide association studies. However, it is important to compare and contrast our findings to a recent manuscript describing cardiometabolic phenotypes in a gene trap *Fads1* loss of function mouse model.<sup>96</sup> The work by Powell and colleagues reported similar improvements in body weight and glucose tolerance with *Fads1* loss of function, but also reported modest reductions in atherosclerotic burden in *Fads1* loss of function mice on an apolipoprotein E-null background.<sup>96</sup> Given these discrepant results, it is essential to note that hepatic expression levels of *Fads1* were not reported in the work by Powell and colleagues,<sup>96</sup> and AA and EPA levels were very modestly reduced in their *Fads1* targeted mice. In fact, the authors speculate that this model produced a hypomorphic allele rather than a complete loss of function allele.<sup>96</sup> Furthermore, the work by Powell and colleagues is complicated by the fact that mice were studied on diets containing supplemental AA, thereby potentially masking the phenotypes driven by lack of endogenous AA production. Notably, a major difference between the current

studies and the work by Powell and colleagues<sup>96</sup> is the use of different hyperlipidemic mouse models. Whereas atherosclerosis in the *Ldlr*<sup>-/-</sup> model used here is mainly driven by VLDL and LDL accumulation, the more rapid atherosclerosis progression in apoE<sup>-/-</sup> mice is driven largely by the accumulation of intestinally-derived apoB-containing lipoproteins. Given early postnatal lethality of global *Fads1* knockout mice,<sup>28,29</sup> and obvious limitations of genetic hypomorphs and ASO-mediated knockdown, additional tissue-specific genetic approaches will ultimately be necessary to fully understand the cell autonomous roles of *Fads1* in cardiometabolic disease. It is important to note that the ASO knockdown approach used here does not accurately reflect the anticipated effect of common *FADS1* polymorphisms. In fact, ASOs typically only achieve appreciable knockdown in the liver, adipose, kidney, and some cells with the reticuloendothelial cell system, whereas the human *FADS1* variants likely affect expression across all tissues. Moving forward it will be important to study each individual *FADS1* SNP using non-ASO genetic approaches to fully understand the functional consequences of the cardiometabolic disease-associated variants.

Given the fact that *Fads1* knockdown dramatically reorganizes membrane phospholipids as well as diversifies downstream oxidation products of AA, EPA, and DHA (Figures 2-5), it is challenging to define a single unifying mechanistic link between  $\Delta$ -5 desaturation and cardiometabolic disease phenotypes. In fact, it is most likely that certain lipid mediator alterations seen in *Fads1* knockdown mice may drive specific aspects of the phenotype. For instance, recent work has shown that vulnerable regions within human atherosclerotic plaques exhibit a

lower SPM to leukotriene ratio similar to what is seen with *Fads1* knockdown (Figure 4E).<sup>89,97</sup> Moreover, direct administration of resolvin D1 (which is reduced in *Fads1* ASO-treated mice, Figure 4A-4E) promotes features of atherosclerotic plaque stability (e.g. increased fibrous cap thickness) in mice.<sup>89</sup> Furthermore, the AA-derived lipid mediator lipoxin A<sub>4</sub>, which is severely reduced in *Fads1* ASO-treated mice (Figures 4A-4E and 5C), has been shown to limit chronic inflammation in adipose tissue and liver.<sup>98-100</sup> Importantly, *Fads1*'s ability to alter lipid mediator balance is very dependent on dietary provision of substrate fatty acids (Figures 4A-4E and 5). In support of this concept, *Fads1* knockdown has minimal effects on phospholipid acyl chain composition when a primary saturated fat source is provided, yet when a diet enriched in 18 carbon length  $\omega$ -3 fatty acid precursors is fed, *Fads1* knockdown is associated with striking alterations in membrane phospholipids (Figures 2C and 3D, 3E) and downstream lipid mediators (Figures 4A-4E and 5). These results suggest that FADS1 activity becomes particularly important in lipid mediator balance under dietary conditions where precursor essential fatty acid substrates for long-chain PUFA biosynthesis are provided.

Another important finding of this work is that *Fads1* is novel effector of LXR signaling *in vivo*, reciprocally balancing LXR-driven increases in fecal cholesterol disposal and *de novo* lipogenesis (Figures 17 and 18). Additional work is needed to understand how *Fads1*-driven AA- and EPA-derived lipid mediators impact reverse cholesterol transport and fatty acid biosynthesis, but in line with our observations a recent report linked the AA-derived metabolome to reverse

cholesterol transport in mice and humans.<sup>101</sup> Furthermore, AA has also been shown to inhibit LXR-driven transactivation of the SREBP1c promoter, thereby impacting a number of downstream lipid signaling pathways in cells.<sup>102</sup> Based on these collective observations it is tempting to speculate that AA itself, or more likely some downstream oxidative metabolite of AA, allows for coordinated regulation of LXR, SREBP1c, and PPAR $\alpha$  signaling to balance lipid metabolic and inflammatory transcriptional programs. However, when considering the ability of *Fads1* to alter LXR signaling in our studies it is important to note that we studied LXR activation in different dietary cholesterol levels and genetic backgrounds. For instance, all studies examining effects of *Fads1* knockdown on atherosclerosis and hepatic inflammation (Figures 2-16) were done in *Ldlr*<sup>-/-</sup> mice fed synthetic diets supplemented with 0.2% cholesterol, whereas the exogenous LXR agonist studies (Figures 17 and 18) were done in chow-fed C57BL/6 mice. It has previously been demonstrated that dietary cholesterol levels can dramatically alter LXR target gene expression, with high dietary cholesterol providing substrate for endogenous oxysterol ligand production<sup>84,103,104</sup>. Therefore, the ability of *Fads1* to alter LXR signaling is likely determined in part by dietary cholesterol levels. It is also important to note that the ability of *Fads1* to alter hepatic cholesterol levels does not solely rely on its ability to alter LXR-driven transcriptional programs. In support of this, *Fads1* ASO-driven increases in hepatic free cholesterol levels are apparent in both basal (vehicle) and LXR-stimulated (T0901317-treated) conditions (Figure 17). Therefore, *Fads1* likely impacts cholesterol homeostasis by LXR-dependent and independent

mechanisms. One potential way that *Fads1* could impact hepatic free cholesterol levels is by altering membrane phospholipid fatty acid composition to secondarily alter the stability of cholesterol-rich lipid rafts. It is well known that PUFA-enrichment in membrane phospholipids can have profound effects on lipid raft formation and stability.<sup>105,106</sup> Our data suggest that under certain dietary conditions *Fads1* can be a major determinant of phospholipid fatty acid composition (Figure 3D). Therefore, we hypothesize that one plausible way *Fads1* could alter hepatic FC levels in a LXR-independent manner may be by altering the stability of cholesterol-rich lipid raft domains.

Since FADS1 is the sole endogenous source of AA, it is important to note that these studies were also conducted in the setting of  $\omega$ -6 FADS1 substrate dietary supplementation (Figure 19A). As observed in the control and  $\omega$ -3 substrate diet cohorts, *Fads1* knockdown increased circulating FADS1 substrate concentrations and decreased circulating FADS1 product concentrations (Figure 19B). Both *Fads1* knockdown and  $\omega$ -6 PUFA diet changed hepatic lipid mediator concentrations (Figure 19C), especially altering the AA metabolome. Analogous to the observations in the dietary context of  $\omega$ -3 PUFA supplementation, *Fads1* knockdown increased hepatic total cholesterol levels and reduced hepatic triglyceride levels independent of diet. *Fads1* knockdown increased LDL and decreased HDL similarly in the  $\omega$ -6 and  $\omega$ -3 PUFA supplemented cohorts (Figure 19F, 19G), yet did not significantly increase atherosclerosis in the  $\omega$ -6 diet (Figure 19H). These results suggest that PUFA supplementation in general may have atheroprotective effects, but the benefits of  $\omega$ -3 PUFA supplementation are

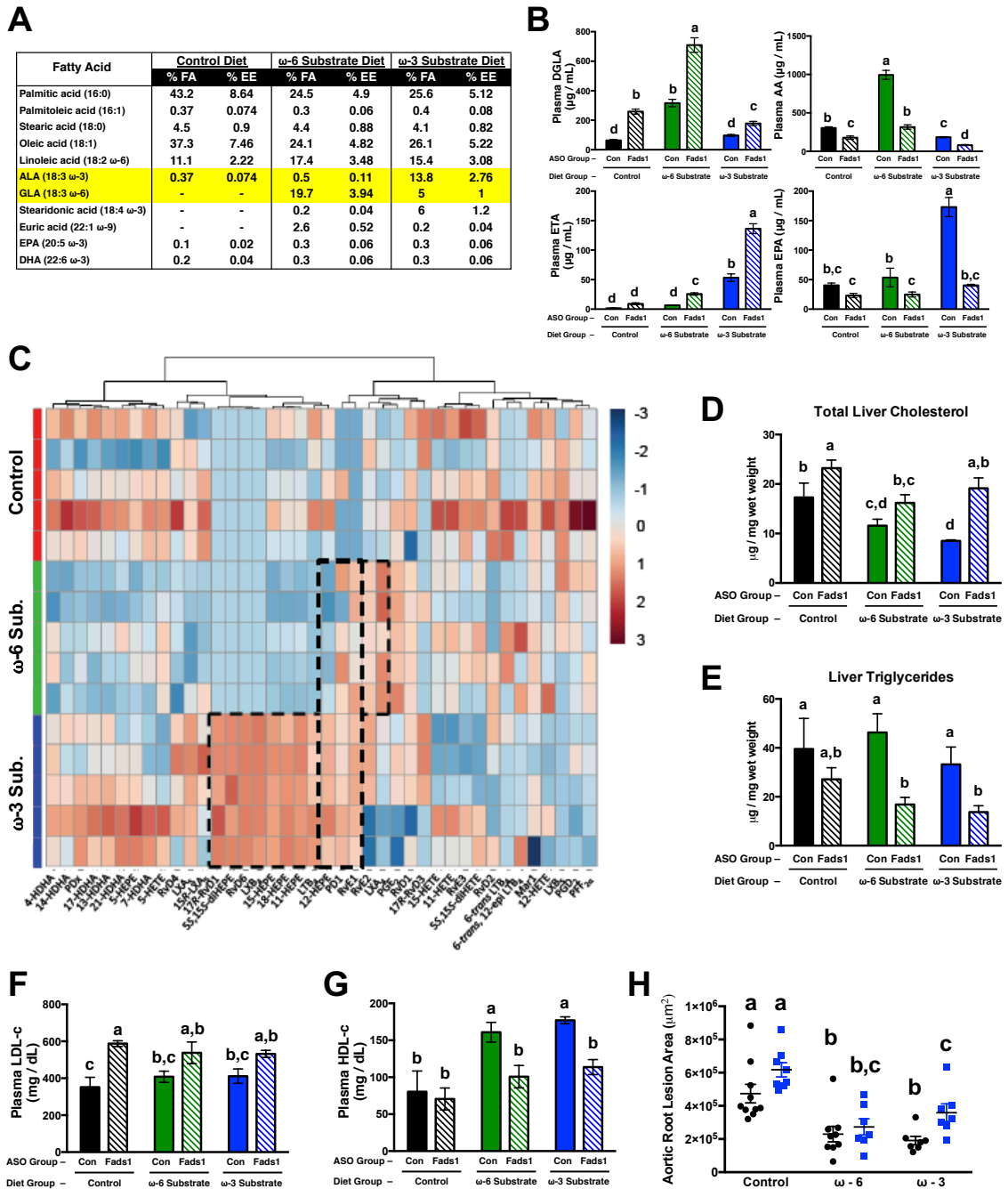


**Figure 19. Effects of *Fads1* Knockdown in the Dietary Context of  $\omega$ -6 and  $\omega$ -3 PUFA Supplementation.** (A) Fatty acid composition of individual fatty acids in experimental diets. (B) FADS1 substrate ( $\omega$ -6 dihomo-g-linolenic acid, DGLA and  $\omega$ -3 eicosatetraenoic acid, ETA) and product ( $\omega$ -6 arachidonic acid, AA and  $\omega$ -3 eicosapentaenoic acid, EPA) fatty acid concentrations in plasma;  $n=6$  per group. (C) A heatmap demonstrating the relative levels of all lipid metabolites measured in each liver sample. (D) Total hepatic cholesterol;  $n=6$  per group. (E) Total hepatic triglycerides;  $n=6$  per group. (F) Low-density lipoprotein (LDL) cholesterol levels after 16 weeks of diet and ASO treatment;  $n=4$  per group. (G) High-density lipoprotein (HDL) cholesterol levels after 16 weeks of diet and ASO treatment;  $n=4$  per group. (H) Quantification of aortic root lesion area;  $n=7-10$  per group. Graphs display mean  $\pm$  SEM. Statistical significance is determined by 2-way ANOVA, datasets with different letter identifiers are significantly ( $p<0.05$ ) different.

more dependent on *Fads1* expression. These divergent effects of *Fads1* knockdown are possibly due to downstream changes in  $\omega$ -3 PUFA derived pro-resolving lipid mediator profiles, which differ based on dietary inputs.

In summary, this work demonstrates that ASO-mediated knockdown of the  $\Delta$ -5 desaturase FADS1 impacts many of the cardiometabolic phenotypes that were originally genetically linked to the *FADS1-2-3* locus in a highly diet-specific manner. These findings highlight *Fads1* as a regulator of inflammation initiation and resolution, and highlight the interplay between endogenous and exogenous (dietary) fatty acids in diseases characterized by unresolved inflammation.

**CHAPTER 3**

**FADS1 OPPOSES HEPATOCELLULAR CARCINOMA PROGRESSION BY  
BALANCING PRO-INFLAMMATORY AND PRO-RESOLVING LIPID  
MEDIATORS**

**3.1 Introduction**

Obesity rates continue to climb in developed societies around the globe,<sup>107,108</sup> which is increasing overall mortality by causing deleterious health consequences ranging from metabolic syndrome all the way to cancer.<sup>109-115</sup> Adiposity contributes to oncogenesis through various mechanisms at play both locally and systemically in obese individuals. For example, peripheral insulin resistance resulting from obesity causes the pancreas to produce more insulin in order to compensate, which promotes chronic hyperinsulinemia. Insulin is a potent growth factor that, when present at inappropriately high concentrations for too long, can drive tumor formation and progression.<sup>116,117</sup> However, many insulin-independent mechanisms can also have injurious and pathogenic effects in the setting of obesity that drive adipose tissue remodeling.<sup>113</sup> Superfluous lipid accumulation in tissue can promote local inflammatory signaling and immune cell recruitment to aid in clearance of excess lipid.<sup>118,119</sup> In the chronically hyperlipidemic setting of obesity, homeostatic clearance mechanisms cannot efficiently remedy the tissue lipid burden, which leads to sustained inflammatory signaling and a microenvironment fitting for oncogenesis. A combination of these factors likely underlies the observation that obese individuals run a higher risk of death from malignancies relative to their leaner counterparts.<sup>113,120,121</sup> When

further dissected, clinical data also reveal that the increase in relative risk ranges considerably depending on the type of cancer and its tissue of origin.

Particularly, the relative risk of death from liver cancer is strikingly enhanced by adiposity, as measured by body-mass index (BMI).<sup>122</sup> Specifically, men with a BMI  $\geq 35$  are roughly 4.5 times more likely to die from liver cancer than men with BMI 18.5-24.9.<sup>122</sup>

Excess lipid retention in the liver, which is clinically recognized as steatosis or non-alcoholic fatty liver (NAFLD), is the most prevalent liver disorder in developed societies (excluding diseases of excess alcohol consumption).<sup>123-125</sup> Steatosis can prompt inflammatory and fibrotic responses, which push the liver into a pathological state known as non-alcoholic steatohepatitis (NASH).<sup>126</sup> Chronic NASH is the most severe form of NAFLD and is a major cause of cirrhosis and hepatocellular carcinoma (HCC), which are irreversible and fatal end-stage liver diseases requiring organ transplant.<sup>127</sup> HCC, which develops and progresses in the setting of chronic hepatic inflammation, is the most common primary liver malignancy in adults and is the most common cause of death in people suffering from cirrhosis.<sup>127,128</sup>

While NASH is known to be a strong determinant of HCC risk, the specific insults and pathological mechanisms that drive the development of end-stage liver disease remain elusive. Recent studies have utilized genetic, proteomic, and lipidomic approaches to profile NAFLD, NASH, and NASH-associated HCC specimens in order to better understand molecular changes occurring in the liver during disease progression. Lipidomic profiling reveals decreased levels of EPA

and DHA in murine models of NASH-associated cancer relative to healthy controls,<sup>129</sup> which agree with other studies which suggest that consumption of  $\omega$ -3 PUFA (by way of a diet rich in fish) reduces HCC risk.<sup>130</sup> Lipidomic data also demonstrate positive correlations between the  $\omega$ -6/ $\omega$ -3 PUFA ratio in circulation and NASH-associated cirrhosis in humans, implying that changes in relative PUFA abundances in tissue influence mammalian liver pathophysiology.<sup>131</sup> Furthermore, studies have started to shed light on changes that occur as livers transition from simple steatosis (SS) to NASH in order to better understand early disease mechanisms. Liver and red blood cell lipid profiling demonstrates lower relative quantities of AA, EPA, and DHA in NASH versus SS patients, which further corroborates other findings.<sup>131</sup> However, the same study demonstrated that *FADS1* and *FADS2* were actually up-regulated in NASH versus SS and healthy controls.<sup>131</sup> This contradictory finding raises questions about *FADS1/2* catalytic activity, protein expression, genetic variation in the *FADS1-2-3* gene cluster, and PUFA feedback signaling. Taken together, recent studies suggest that the dysregulation of PUFA metabolism impacts NASH development, and highlight significant gaps in knowledge surrounding how these correlative changes contribute to disease.

Considering the trends observed between PUFA levels and liver disease revealed by lipidomic and genetic profiling studies, we hypothesized that *Fads1* knockdown would dysregulate PUFA metabolism and dramatically alter pro-inflammatory and pro-resolving lipid mediator balance to impact hepatic inflammation in the context of obesity-driven HCC. While the majority of global

HCC cases result from viral infection (hepatitis B and/or C),<sup>132</sup> non-virally driven HCC are on the rise, particularly in developed countries home to Westernized high-fat diets (HFD) and high rates of obesity.<sup>133-137</sup> Here, we have adapted a murine model of carcinogen-induced, HFD-driven HCC in order to recapitulate obesity-related HCC pathology.<sup>138</sup> This model is unique because it requires two “hits” in order to promote carcinogenesis: postnatal 7,12-Dimethylbenz[a]anthracene (DMBA) carcinogen exposure, and obesity caused by chronic high fat feeding.<sup>138</sup> Because *Fads1*<sup>-/-</sup> mice can only survive for approximately 8-12 weeks without dietary provision of AA/EPA,<sup>28,29</sup> we treated wild-type male mice (females are almost completely protected in this HCC model, and excluded from this study) with ASOs to selectively knock down *Fads1* and circumvent the issue of postnatal lethality. Based on evidence from other studies, we hypothesized that *Fads1* knockdown could alter local inflammatory signaling and promote tumorigenesis even in the absence of the high-fat nutritional stress. To test this, we included chow-fed experimental cohorts to evaluate both diet-dependent and diet-independent changes in liver pathophysiology brought on by reduced *Fads1* expression. Studies have suggested that altered FADS1 expression and function (based on substrate/product levels) may play a role in liver disease progression,<sup>129,131</sup> yet the mechanisms underlying these observations remain unknown. These work here aim to clarify our understanding of how changes in FADS1-dependent PUFA metabolism influence various disease mechanisms contributing to HCC development and progression.

## **3.2 Materials and Methods**

### **Animal Studies**

To study the specific role of the *Fads1* in obesity-driven liver disease without the associated postnatal lethality of genetic *Fads1* deletion,<sup>28,29</sup> we employed an *in vivo* ASO-mediated knockdown approach in wild-type male mice on a C57BL/6J background. To induce tumorigenesis, 50  $\mu$ L of 0.5% DMBA (in acetone) was painted onto the dorsal skin of pups at day 3 post-birth. Upon weaning at approximately 3 weeks of age, mice were fed chow or high-fat (D12492, Research Diets, Inc.) diets and injected intraperitoneally with ASOs (50mg/kg BW per week) for the duration of the 30-week study period. *Fads1* knockdown was studied under both dietary contexts to test the consequences of altered PUFA metabolism in the presence and absence of the HFD nutritional insult. From a caloric standpoint, HFD fed to mice was 60% fat, 20% protein, and 20% carbohydrate. All mice studies were approved by the Institutional Animal Care and Use Committee of the Cleveland Clinic.

### **Analysis of Liver Tumor Burden**

Whole livers were harvested from experimental mice and photographed for visual evidence of overall tumor burden. Livers were subsequently separated into left, median, right, and caudal lobes. Both the ventral and dorsal sides of the separated liver lobes were photographed for purposes of tumor counting and measurement. Tumor area was quantified using ImageJ software by measuring the surface area of clearly visible tumors relative to overall visible liver surface

area.

### **Quantification of Pro-Inflammatory and Pro-Resolving Lipid Mediators by LC-MS/MS**

Livers collected from wild-type mice exposed to control or *Fads1* ASO treatment and diets for 30 weeks were minced in ice-cold methanol containing internal deuterium-labeled standards and stored at -80°C. These standards, which included d<sub>5</sub>-RvD2, d<sub>4</sub>-LTB<sub>4</sub>, d<sub>8</sub>-5-HETE, d<sub>4</sub>-PGE<sub>2</sub> and d<sub>5</sub>-LXA<sub>4</sub>, were used to assess extraction recovery. The tissue samples were then centrifuged (3,000 rpm) and the supernatants were subjected to solid phase extraction and LC-MS/MS analysis, essentially as described by English et al.<sup>70</sup> Briefly, lipid mediators were extracted by C18 column chromatography and were eluted in methyl formate fractions. The solvent was then evaporated under N<sub>2</sub> gas and lipid mediators were resuspended in methanol:water (50:50). For analysis, a high performance liquid chromatograph (HPLC, Shimadzu) coupled to a QTrap5500 mass spectrometer (AB Sciex) was used and operated in negative ionization mode. Identification and quantification of lipid mediators was achieved using multiple reaction monitoring transitions, information-dependent acquisition and enhanced product ion scanning.<sup>70</sup> The levels of individual lipid mediators were normalized to extraction recovery of internal deuterium-labeled standards and quantified based on calibration curves using external standards for each mediator. The levels of each compound were then imported into MetaboAnalyst where further statistical analyses could be performed. For this, missing value

imputation was performed in which half the minimum positive value was used for compounds that were not detected in all samples. Next, the data were subjected to a log transformation and autoscaling so that all metabolites carried equal importance. We then conducted partial least squares-discriminant analysis and volcano plot analysis.

### **Real-Time PCR Analysis of Gene Expression**

Cells or tissue RNA extraction was performed as previously described for all mRNA analyses.<sup>62,64,65,77</sup> Quantitative real time PCR (qPCR) analyses were conducted as previously described.<sup>62,64,65,77</sup> mRNA expression levels were calculated based on the  $\Delta\Delta$ -CT method. qPCR was conducted using the Applied Biosystems 7500 Real-Time PCR System. Primers used for qPCR are available on request.

### **Glucose Tolerance Testing**

Glucose tolerance tests were performed after a 4-6 hour fast by injecting 1 g/kg body weight of glucose into the peritoneal cavity. Tail vein plasma glucose levels were measured using a commercial glucometer (ACCU-CHEK Performa, Roche). Glucose tolerance tests were performed on mice that had been treated with diet and ASO for 15 weeks.

## **Liver Histological Analysis**

Hematoxylin and eosin staining of paraffin-embedded liver sections was performed as previously described.<sup>62</sup> Histopathologic evaluations were scored in a blinded fashion by a board certified pathologist (Daniela S. Allende – Cleveland Clinic).

## **Total Hepatic Triglyceride, Free Cholesterol, and Phosphatidylcholine Analyses**

Extraction of liver lipids and quantification of total hepatic triglyceride, free cholesterol, and phosphatidylcholine was conducted using enzymatic assays as described previously.<sup>64,65</sup>

## **Statistical Analysis**

All data were analyzed using either one-way or two-way analysis of variance (ANOVA) where appropriate, followed by Tukey-HSD post hoc analysis. Differences were considered significant at  $p < 0.05$ . Statistical analyses were performed using JMP Pro 10 (SAS Institute; Cary, NC), Graphpad Prism 6 (La Jolla, CA) and Metaboanalyst 3.0 (<http://www.metaboanalyst.ca/>) software.

## **3.3 Results**

### ***Fads1* Knockdown Prevents Weight Gain and Improves Glucose Tolerance**

The studies here focused on how changes in PUFA metabolism impact pathobiology of obesity-driven HCC. As obesity-related HCC rates continue to

climb around the world, we sought to investigate the interplay of altered lipid metabolism and liver cancer in a murine model of HCC of obesity-driven HCC.<sup>138</sup> Given that *Fads1*<sup>-/-</sup> mice fail to thrive and cannot be used in long-term studies without PUFA supplementation,<sup>28,29</sup> we utilized an ASO-mediated knockdown approach to reduce tissue expression of *Fads1* in carcinogen-exposed wild-type mice maintained on either chow or HFD to investigate how changes in dietary lipid and endogenously-derived PUFA impact metabolic health and disease severity. Consistent with observations from previous studies using ASO-mediated *Fads1* knockdown, mice treated with *Fads1* ASO gained significantly less weight over the course of the planned 30-week study period (Figure 20A). This effect was independent of diet, causing *Fads1* ASO treated mice to weigh nearly 50% less than their control ASO treated counterparts in the setting of chow diet (Figure 20B). When fed HFD, *Fads1* ASO-treated mice weighed approximately 60% less than their control ASO-treated counterparts (Figure 20A). Consistent with reduced body weights, *Fads1* ASO-treated mice had significantly less epididymal white adipose tissue (WAT) relative to their respective total body weights compared to controls (Figure 20C). To our surprise, chow-fed control animals had more WAT than HFD controls (Figure 20C). Since chow-fed animals appeared much leaner than HFD-fed counterparts overall, this observation is likely a consequence of differences in fat storage depots. Specifically, HFD-fed animals had much more subcutaneous and visceral WAT than chow-fed animals, but only the more readily-accessible epididymal fat pads were harvested for analysis. Differences in body weight and

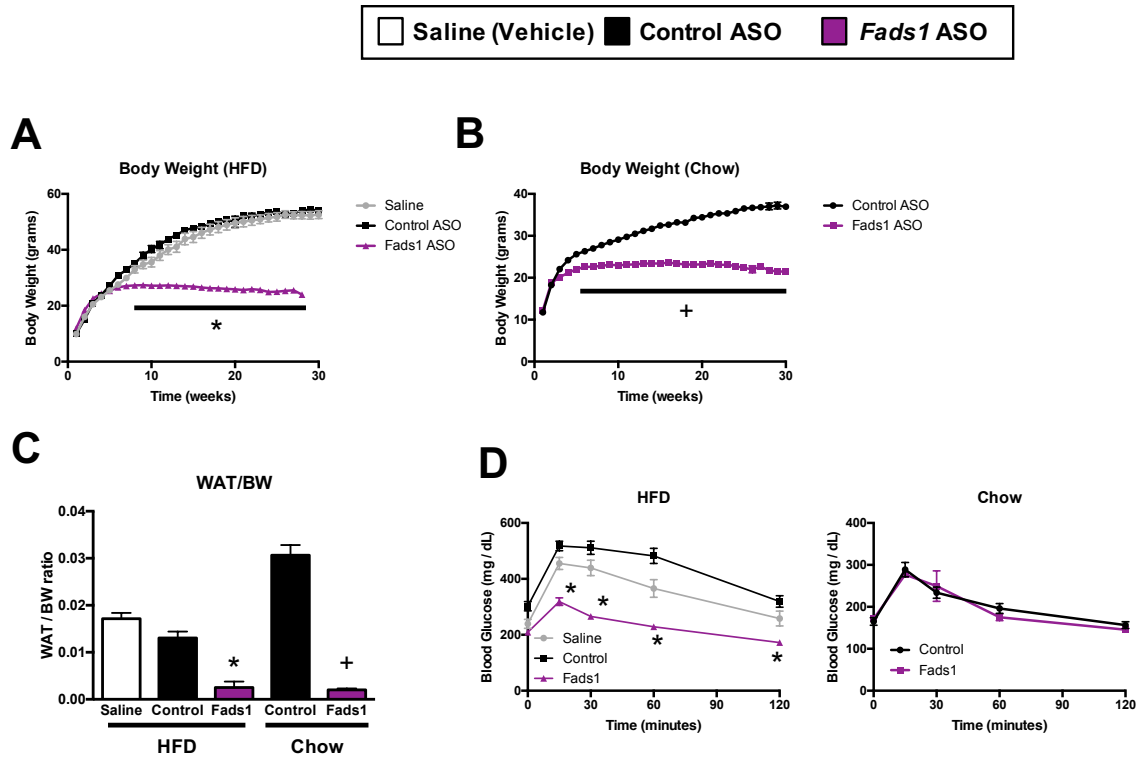


**Figure 20. *Fads1* Knockdown Prevents Weight Gain and Improves Glucose Tolerance. (A)** Body weight of mice fed HFD and treated with ASOs over the course of the 30-week study period. *n*=10-14 per group. **(B)** Body weight of mice fed chow and treated with ASOs over the course of the 30-week study period. *n*=10-14 per group. **(C)** Ratio of epididymal fat pad weight to total body weight. *n*=10-14 per group. **(D)** Glucose tolerance tests in mice fed diets and treated with ASOs for 15 weeks; *n*=8 per group. Graphs display mean  $\pm$  SEM. Statistical significance is determined by 2-way ANOVA, \* = significantly different from the control ASO – HFD group (\**p*<0.05, \*\**p*<0.01); + = significantly different from control ASO group within the chow diet group (\**p*<0.05, \*\**p*<0.01, \*\*\**p*<0.001).

apparent adiposity brought on by *Fads1* ASO treatment translated to improved glucose tolerance in HFD-fed animals (Figure 20D). No differences in glucose tolerance were observed between saline (vehicle) and control (non-targeting) ASO treated mice, suggesting that *Fads1* knockdown improves regulation of blood glucose (Figure 20D). Peripheral insulin resistance and impaired glucose tolerance are common consequences of obesity, and resulting chronic hyperinsulinemia (and/or diabetes) can drive tumorigenesis.<sup>139</sup> These data imply that *Fads1* plays a role in weight gain and blood glucose regulation, which is consistent with genome-wide association studies that have linked *FADS1-2-3* variants to circulating blood glucose levels and diabetes risk.<sup>49</sup>

### ***Fads1* Knockdown Dramatically Increases Tumor Burden in HFD-Fed Animals, Independent of Adiposity**

Despite being leaner and having improved glucose tolerance, *Fads1* ASO-treatment significantly reduced survival (Figure 21A, 21B) and caused far more severe liver cancer than vehicle and control ASO treatment over the course of the 30-week study period (Figure 21C). In fact, *Fads1* ASO-treated animals were succumbing to disease at such high rates that the remaining mice in these treatment cohorts had to be sacrificed at 28 weeks rather than 30 weeks in order to preserve study sample size. Gross inspection of livers from study animals demonstrates that *Fads1* ASO treatment dramatically increases tumor burden compared to controls in the setting of HFD (Figure 21C), and quantification confirms that both tumor number and surface area were increased (Figure 21D,

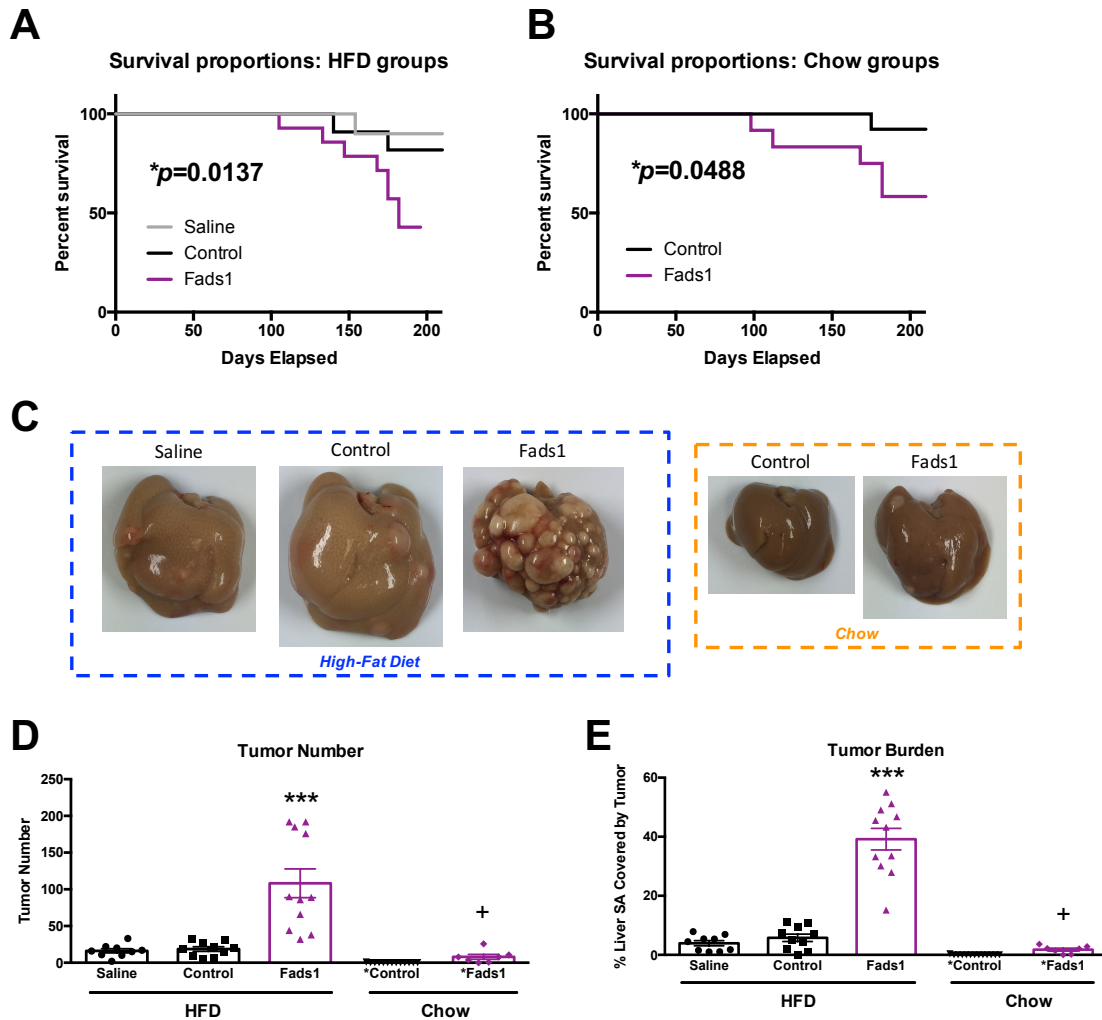


**Figure 21. *Fads1* Knockdown Increases Liver Tumor Burden, Independent of Diet and Adiposity.** (A) Kaplan–Meier plot of mice fed HFD and treated with ASOs over the course of the 30-week study period.  $n=10-14$  per group. (B) Kaplan–Meier plot of mice fed chow and treated with ASOs over the course of the 30-week study period.  $n=10-14$  per group. (C) Whole liver specimens from mice fed diets and treated with ASOs. (D) Quantification of tumor number in liver specimens from mice fed diets and treated with ASOs.  $n=10-14$  per group. (E) Quantification of tumor surface area (SA) in liver specimens from mice fed diets and treated with ASOs.  $n=10-14$  per group. Graphs display mean  $\pm$  SEM. Statistical significance is determined by 2-way ANOVA, \* = significantly different from the control ASO – HFD group ( $*p<0.05$ ,  $**p<0.01$ ); + = significantly different from control ASO group within the chow diet group ( $^{\dagger}p<0.05$ ,  $^{++}p<0.01$ ,  $^{+++}p<0.001$ ).

21E). Histopathological evaluation of hematoxylin and eosin (H&E)-stained liver tissue sections verified the tumors to be bona fide HCC. These data demonstrate an interesting scenario where adiposity is negatively correlated with HCC severity, which contradicts typical liver cancer pathology and implies that *Fads1* plays diverse roles in metabolism and HCC progression.

### ***Fads1* Knockdown is Sufficient to Drive Tumor Growth and Decrease Survival in Chow-Fed Animals**

In the absence of ASO administration, mice only develop HCC in this “two hit” model when fed a HFD for the duration of the 30-week study period following DMBA exposure.<sup>138</sup> Interestingly, *Fads1* ASO treatment reduced survival and was sufficient to drive tumorigenesis in chow-fed mice (Figure 21C), suggesting that *Fads1* may play a diet-independent tumor suppressive role in liver pathophysiology.

### ***Fads1* Regulates Hepatic Inflammation**

Liver gene expression analysis by reveals that *Fads1* ASO treatment reduced hepatic *Fads1* transcript levels by over 95%, independent of diet (Figure 22A). Detailed histopathological scoring of liver pathology demonstrates diet-independent increases in lobular inflammation and immune cell aggregation in the context of *Fads1* knockdown (Figure 22B). Hepatic gene expression analyses corroborate these observations by showing that *Fads1* knockdown increases expression of transcripts encoding proteins involved in inflammatory

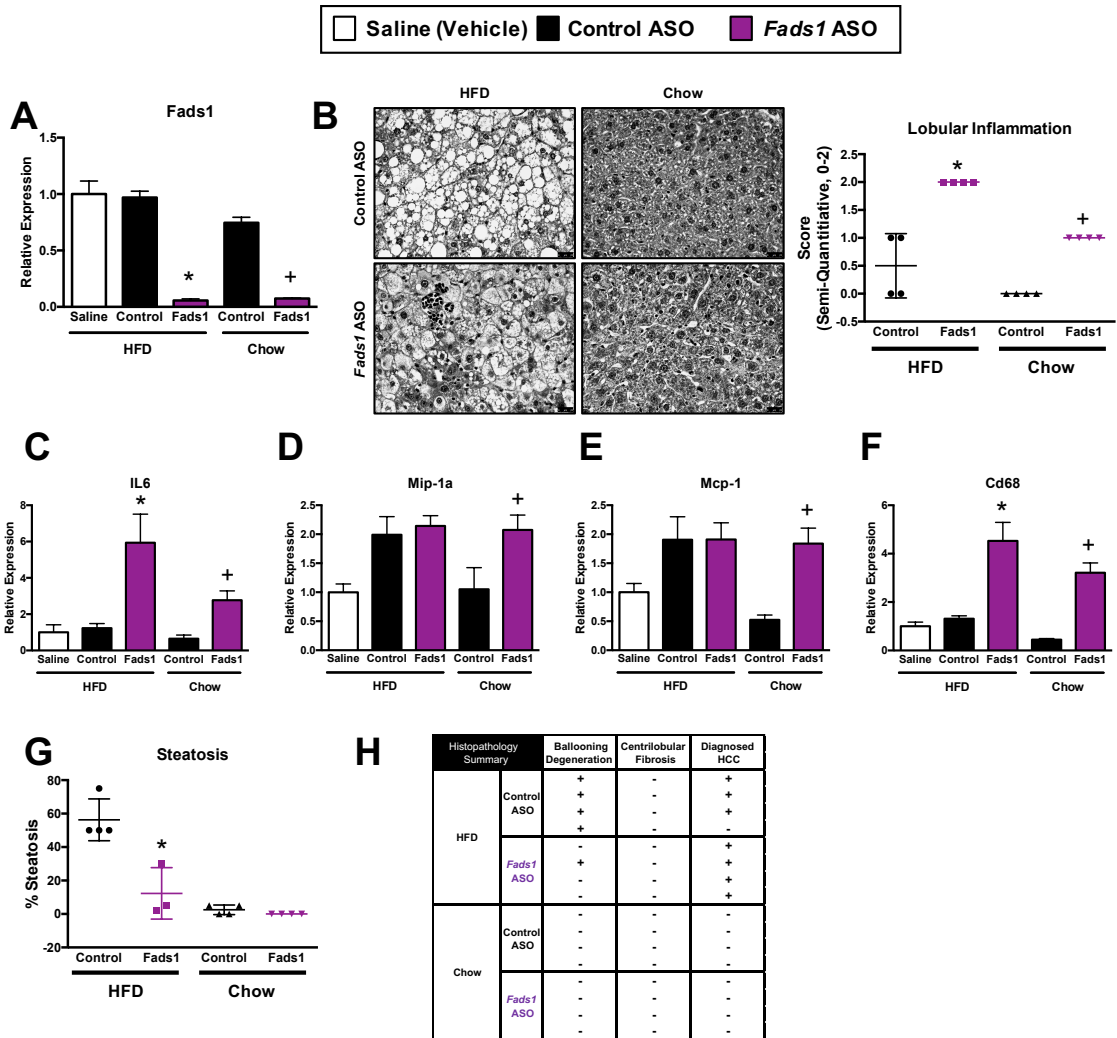


**Figure 22. *Fads1* Regulates Hepatic Inflammation.** (A) Hepatic *Fads1* expression; *n*=6 per group. (B) Liver H&E histology and scoring of lobular inflammation; *n*=4 per group. (C-F) Hepatic expression of inflammatory and immune cell marker genes; *n*=6 per group. (G) Histopathological scoring of liver steatosis; *n*=4 per group. (H) Summary of histopathological parameters and diagnoses; *n*=4 per group. Graphs display mean ± SEM. Statistical significance is determined by 2-way ANOVA, \* = significantly different from the control ASO – HFD group (\**p*<0.05, \*\**p*<0.01); + = significantly different from control ASO group within the chow diet group (+*p*<0.05, \*\**p*<0.01, \*\*\**p*<0.001).

responses (*Il6*) (Figure 22C) and immune cell chemotaxis (*Mip1a*, *Mcp1*) (Figure 22D, 22E). In agreement with this, *Fads1* knockdown also increases expression of leukocyte-specific genes such as *Cd68* (Figure 22F). Liver histology also reveals that steatosis and ballooning degeneration (swollen hepatocytes undergoing apoptosis) are increased by HFD, and these effects are diminished by *Fads1* knockdown (Figure 22G, 22H). These were surprising findings to us, considering the notion that steatosis is a primary driver of disease early in HCC development. Additionally, Masson's Trichrome staining demonstrates that *Fads1* knockdown does not significantly alter hepatic fibrosis, another strong driver of end-stage liver disease (data not shown). Taken together, these data suggest that *Fads1* knockdown increases HCC burden primarily by increasing hepatic inflammation without altering steatotic or fibrotic mechanisms.

### ***Fads1* is a Key Determinant of Pro-Inflammatory Versus Pro-Resolving Lipid Mediator Balance in the Liver**

Altered balance of pro-inflammatory and pro-resolving lipid mediators in the liver may partially explain the increased inflammation and HCC burden observed in the setting of *Fads1* knockdown. Metabololipidomic quantification and principle component analysis revealed that overall lipid mediator profiles were clearly distinct for dietary and pharmacological (ASO) interventions (Figure 23A). *Fads1* knockdown decreased total hepatic SPM in mice fed chow and HFD (Figure 23B), and increased total leukotriene concentrations in HFD-fed mice (Figure 23C). This causes a striking increase in the leukotriene:SPM ratio, which



indicates an imbalance between pro-inflammatory and pro-resolving lipid mediators that would presumptively impair proper inflammation resolution (Figure 23D). Collectively, these results suggest that *Fads1* plays a fundamental role in balancing concentrations of lipid mediators in tissue, and that *Fads1* knockdown skews the liver towards a more pro-inflammatory and less pro-resolving local microenvironment that is favorable for HCC development and progression.

### ***Fads1* Knockdown Reorganizes Hepatic Lipid Metabolism**

*Fads1* knockdown causes profound changes in the hepatic gene expression and lipid composition, independent of diet. As seen in our previously discussed models utilizing *Fads1* ASO-mediated knockdown, *Fads1* knockdown significantly reduced expression of transcripts encoding enzymes that are required for lipid biosynthesis. *Fads1* knockdown significantly reduced hepatic expression of the master lipogenic transcription factor *Srebp1c* (Figure 24A), and its downstream target genes including *Acc1* and *Fas* (Figure 24B, 24C), which encode enzymes that are particularly important for *de novo* FA synthesis.

Biochemical analysis of liver tissue revealed that reduced expression of lipogenic enzymes translated to changes in overall hepatic lipid composition. *Fads1* knockdown significantly decreased hepatic TG content (Figure 24D), while increasing cholesterol levels (Figure 24E). These findings agree with the observed reduction in expression of enzymes necessary for FA production, since FA are stored primarily in the form of TG. Taken together, these findings

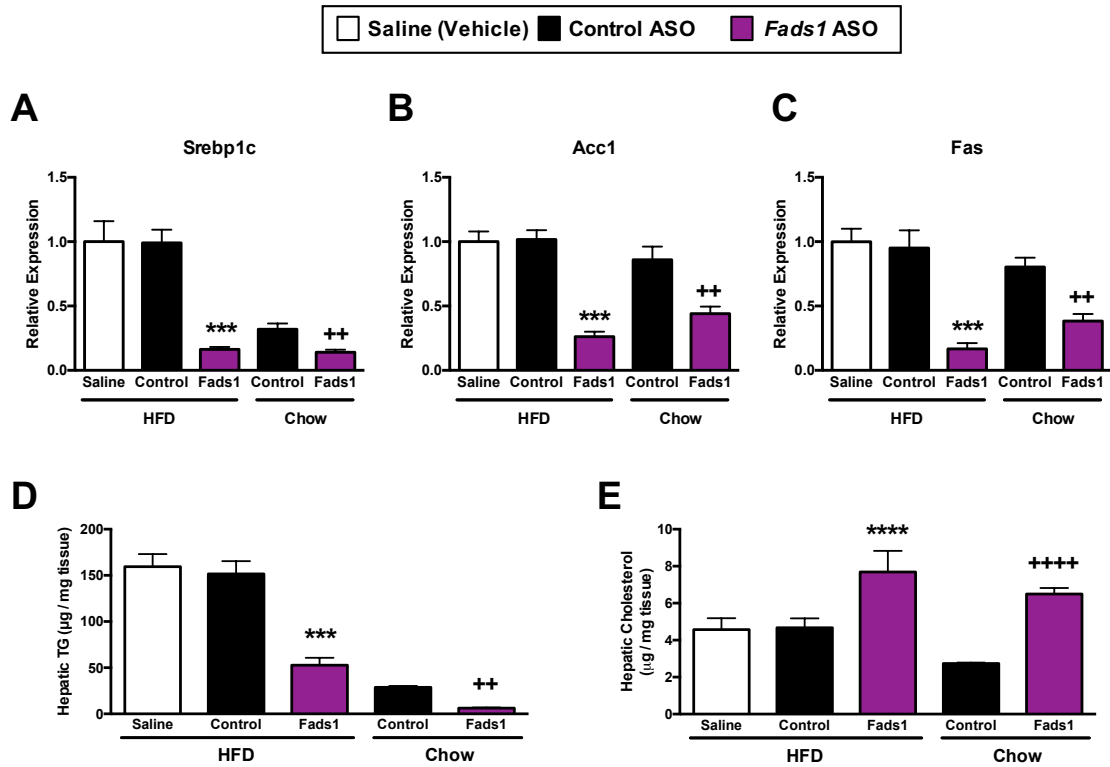


**Figure 24. *Fads1* Knockdown Reorganizes Hepatic Lipid Metabolism.** (A-C) Hepatic expression of lipogenic genes in mice fed diets and treated with ASOs for 30 weeks;  $n=6$  per group. (D) Hepatic triglyceride levels in mice fed diets and treated with ASOs for 30 weeks;  $n=6$  per group. (E) Hepatic cholesterol levels in mice fed diets and treated with ASOs for 30 weeks;  $n=6$  per group. Graphs display mean  $\pm$  SEM. Statistical significance is determined by 2-way ANOVA, \* = significantly different from the control ASO – HFD group (\* $p<0.05$ , \*\* $p<0.01$ ); + = significantly different from control ASO group within the chow diet group (+ $p<0.05$ , \*\* $p<0.01$ , \*\*\* $p<0.001$ ).

demonstrate that *Fads1* expression is important to the regulation of lipid metabolism and composition in the liver.

### **3.4 Discussion**

Chronic unresolved inflammation is a central driver of NALFD-NASH progression and eventual development of end-stage liver diseases, but mechanisms governing the transition from NASH to more advanced liver disease remain poorly understood. While total dietary fat intake is recognized as a strong determinant of NAFLD/NASH risk, the importance of the specific structural identity of ingested lipids is often underappreciated. The studies here provide novel evidence that *Fads1*-driven PUFA biosynthesis plays a role in inflammation resolution and liver disease progression. The main findings of the current study are: (1) *Fads1* knockdown prevents diet-induced obesity and improves glucose tolerance; (2) *Fads1* loss of function results in dramatically enhanced HCC growth in the setting of HFD; (3) *Fads1* knockdown promotes tumorigenesis in the absence of HFD-induced obesity; (4) *Fads1* knockdown reduces survival in a murine model of HCC, independent of diet and adiposity; (5) *Fads1* knockdown promotes hepatic inflammation in a diet-specific manner; (6) *Fads1* knockdown causes an imbalance of pro-inflammatory versus pro-resolving lipid mediators, impairing proper resolution of tissue inflammation; (7) *Fads1* knockdown results in the suppression of hepatic *de novo* lipogenesis and alters liver lipid composition. Collectively, these data support a model in which *Fads1*-dependent PUFA synthesis impacts the balance of pro-inflammatory and pro-resolving lipid

mediators in the liver and the temporally coordinated initiation and resolution of inflammation in hepatic disease.

Recent studies have highlighted inconsistencies in the data with regard to changes in desaturase expression and associated lipid profiles in liver disease and cancers in general, demonstrating clear gaps in knowledge related to how FADS1 contributes to overall metabolic health. Studies measuring mRNA transcript expression find that *FADS1* expression increases with liver disease severity, specifically demonstrating that expression is increased in simple steatosis relative to healthy controls, and further increased in NASH relative to steatosis.<sup>129,131</sup> In agreement with transcript expression data, proteomic studies of liver disease specimens show that increased FADS1 and FADS2 protein counts trend with disease progression.<sup>129</sup> However, lipidomic studies raise questions about enzyme function because data related to PUFA metabolites directly oppose gene and protein expression findings. Lipidomics demonstrate lower hepatic levels of both  $\omega$ -6 and  $\omega$ -3 PUFA – especially AA, EPA, and DHA – in NASH patients compared to SS patients.<sup>131</sup> These data show that FADS1 product PUFA levels are negatively correlated with disease, despite increased desaturase and lipogenic enzyme expression levels. These inconsistent findings could be at least partially explained by genetic variation in the *FADS1-2-3* gene locus. Genetic studies have reported that *FADS* SNPs are associated with altered gene transcription<sup>140</sup> and lower indices of FADS1/2 catalytic activity.<sup>141</sup> This is further complicated by the fact that transcription can also be influenced indirectly by reduced catalytic activity resulting from genetic variation. Cells may

respond to reduced long-chain PUFA abundances by up-regulating transcription of genes (i.e. *FADS1* and *FADS2*) needed to remedy the perceived PUFA deficiency, but increased expression may not be sufficient to restore balance if the product enzymes have impaired catalytic capacity. Additionally, The Human Protein Atlas reports a consistent loss of *FADS1* expression in HCC relative to normal liver, which contradicts proteomic data from mouse models of disease.<sup>142,143</sup> It is also worth noting that *FADS1* expression changes are not consistent across different types of cancer, exemplified by recent reports that *FADS1* expression is lost during lung cancer progression.<sup>144</sup> While each study has drawn its own conclusions related to *FADS* expression and function, the unifying theme is that dysregulation of PUFA desaturation may influence liver disease progression, which accentuates the need for more effective models.

This body of work provides novel evidence that ASO-mediated *Fads1* knockdown augments hepatic inflammation, thus supporting HCC progression. These findings also highlight *Fads1* as a broad regulator of hepatic lipogenesis and a key determinant of the lipid mediator profile within tissue. In summary, these studies highlight the distinct effects diet and *FADS1*-dependent metabolism on unresolved hepatic inflammation and its contribution to liver disease progression.

## CHAPTER 4

### GENERAL DISCUSSION AND FUTURE DIRECTIONS

The studies here provide new insight on the interplay of FADS1-dependent PUFA metabolism and inflammatory signaling in the context of cardiometabolic and hepatic disease. Previous studies have highlighted the potentially pathogenic role(s) of altered PUFA metabolism in various disease states,<sup>145</sup> but FADS1-dependent effects on inflammatory disease development and progression have not been explored in the context of distinct dietary regimens and consequently altered lipid mediator profiles.

A common theme across these studies is the observed effects that *Fads1* knockdown has on tissue inflammation. In the liver, reduced *Fads1* expression resulted in visible (by H&E) increases in immune cell aggregation. Diagnosed as foamy macrophage clusters, the presence of these aggregates suggests that *Fads1* may be required for regulating local recruitment and subsequent retention of leukocytes during the progressive phases of tissue inflammation. Consistent reductions in tissue levels of SPM may partially underlie the pathological aggregation of macrophages observed with *Fads1* knockdown. SPM are produced to actively resolve inflammation and promote tissue healing processes.<sup>41,42</sup> Clearance of recruited immune cells is a key component of resolution, and SPM-mediated signaling aids in this process to restore tissue homeostasis. Our studies demonstrate that FADS1 may partially regulate the accumulation and removal of immune cell populations in different tissues throughout the body during the development and progression of distinct diseases

afflicting different organ systems. These results suggest that FADS1 could play a broad role in leukocyte signaling and function, and warrant more scrupulous investigation in singular immune cell subpopulation to clarify observed changes in tissue inflammation.

Macrophages play central roles in both the initiation and resolution of local inflammation. Classically activated pro-inflammatory macrophages predominate the early phases of inflammation and generally function to initiate and potentiate inflammatory signals.<sup>82</sup> In contrast, alternatively activated pro-resolving macrophages are more abundant during the later phases of inflammation, where they actively resolve inflammation and facilitate tissue repair. These studies provide novel evidence that FADS1-dependent PUFA metabolism is somehow involved in the differential macrophage polarization programs. Specifically, *Fads1* knockdown promotes skewing towards classic (pro-inflammatory) and away from alternative (pro-resolving) polarization. Compromised alternative activation impairs the local attenuation of inflammatory signaling, which can result in disproportionate and persistent tissue inflammation. Because macrophages are responsible for coordinating the temporal progression of local inflammatory responses, changes in relative polarization patterns can dramatically impact homeostatic and reparative mechanisms in tissues throughout the body.<sup>82</sup> Impaired pro-resolving polarization could underlie the uncontrolled inflammation and advanced disease pathologies observed in the context of *Fads1* knockdown. However, our findings cannot assign changes in inflammation and disease solely to changes in macrophage expression of FADS1

because ASO-mediated knockdown was significant in multiple tissue/organ systems, and incomplete in macrophages. Moving forward, leukocyte-specific genetic deletion of *Fads1* would most accurately model the changes in macrophage biology prompted by *Fads1* knockdown.

Although ASO-mediated knockdown of *Fads1* effectively reduced transcript levels and the FADS1 product/substrate ratio in multiple tissues in experimental animals, we do not claim that it accurately reproduces the effects of *FADS1* variants that have been identified in GWA studies. Tissue-specific studies utilizing genetic models of *FADS1* loss-of-function are needed to more appropriately test the cell-autonomous role(s) of FADS1 in the management of inflammatory disease. Since ASOs only achieve significant knockdown in the liver, adipose, kidney, and certain cells of the reticuloendothelial cell system, this approach does not reflect the fact that the human *FADS1* variants likely impacts expression across all tissues. Additionally, global genetic models of each specific *FADS* SNP are needed to characterize the downstream consequences of particular disease-associated gene variants. Since *FADS1* and *FADS2* share a promoter,<sup>25</sup> SNPs in this region can impact the regulation of both enzymes, which cannot be effectively modeled in our ASO knockdown model. It is also important to note that ASOs may have non-specific effects. ASOs can imprecisely form duplexes with mRNA transcripts that have sequences similar to those in the intended target transcript, causing knockdown of off-target transcripts. It can also not be ruled out that ASOs may cause some degree of inflammation as tissues work to metabolize and clear them from the body. We

have evidence that some indicators of hepatic inflammation are increased with ASO treatment relative to vehicle (saline) controls, suggesting that the liver may be stressed by chronic ASO exposure. Genetic models would clarify our observations by relieving the dependence on pharmacological intervention and eliminating off-target effects.

Even without a tissue-specific genetic knockout model, the present studies utilizing diet and ASO interventions to investigate *Fads1*-governed PUFA metabolism and inflammatory signaling could be strengthened by the PUFA add-back experiments. To achieve this, ASO-treated mice could be fed diets enriched in specific PUFAs to shed light on which phenotypes are most closely associated with surpluses or deficiencies in various PUFA species. In separate experimental models of distinct disease states, our data consistently link targeted changes in PUFA and associated lipid mediator metabolism to impaired inflammation resolution, but fall short of providing mechanistic rationale for the observed effects. PUFA add-back studies could improve the current body of work by showing that restoration of specific PUFAs may rescue observed phenotypes, which would be informative for future studies focusing on the metabolome(s) of individual PUFAs in disease pathophysiology.

The studies here provide the first evidence of PUFA biosynthetic capacity dictating lipid metabolism and influencing diverse inflammatory responses during the development of chronic disease. We investigated *FADS1* biology under diverse dietary conditions in order to better understand how differential lipid intake and metabolism uniquely impact the development of diseases

characterized by disproportionate inflammatory signaling. Relevant to human health, these studies contribute to the overall body of knowledge surrounding the physiological consequences of altering the  $\omega$ -6/ $\omega$ -3 PUFA ratio in tissues throughout the body, either by way of dietary or genetic influence. Studies have suggested that the relative abundances of  $\omega$ -6 and  $\omega$ -3 PUFA in the human diet have changed drastically over time.<sup>146</sup> The human diet has changed appreciably as people have transitioned from historically hunter-gatherer eating habits to modern dietary regimens that are sustained by large-scale agriculture.<sup>146</sup> Dietary shifts resulting from societal progression have particularly impacted the average quantity and composition of fats humans procure from the modern diet. Increased saturated fat and *trans* fat intake are well-defined changes in the modern diet that likely contribute to ever-increasing rates of obesity in the public.<sup>9,147</sup> However, the altered  $\omega$ -6/ $\omega$ -3 PUFA ratio in the diet may predispose individuals to adverse health outcomes independent of total fat intake by changing the balance in local mediators of inflammatory signaling.<sup>31,41,42,146,148</sup> Diets rich in  $\omega$ -3 PUFA and characterized by a resultant low  $\omega$ -6/ $\omega$ -3 PUFA ratio have been linked to reduced biomarkers of inflammation<sup>149</sup> and CVD risk,<sup>150-152</sup> yet the mechanisms underlying these associations are poorly defined. The present work supports existing evidence that prioritizing dietary  $\omega$ -3 PUFA over  $\omega$ -6 PUFA, thereby reducing the  $\omega$ -6/ $\omega$ -3 PUFA ratio, alleviates severity of diseases characterized by dysregulated and chronically unresolved inflammation.<sup>153-155</sup> This work investigates how these dietary alterations effect health in the setting of variable *Fads1* expression, and provides novel evidence

that FADS1 may be a central regulator of the PUFA metabolome and critical determinant of disease progression in the context of CVD and HCC, ultimately suggesting that impaired lipid mediator balance may partially underlie the metabolic phenotypes linked to genetic variability in the *FADS1-2-3* locus.

## REFERENCES

1. Mu H, Porsgaard T. The metabolism of structured triacylglycerols. *Prog Lipid Res.* 2005;**44**(6):430-448. doi: 10.1016/j.plipres.2005.09.002.
2. Wang CS, Hartsuck J, McConathy WJ. Structure and functional properties of lipoprotein lipase. *Biochim Biophys Acta.* 1992;**1123**(1):1–17. doi:10.1016/0005-2728(92)90119-M.
3. Mead JR, Irvine SA, Ramji DP. Lipoprotein lipase: structure, function, regulation, and role in disease. *J Mol Med.* 2002;**80**(12): 753–69. doi:10.1007/s00109-002-0384-9.
4. USDA National Nutrient Database for Standard Reference. Nutrient Data Laboratory, Agricultural Research Service, United States Department of Agriculture.
5. Sacks FM, Lichtenstein AH, Wu JHY, Appel LJ, Creager MA, Kris-Etherton PM, Miller M, Rimm EB, Rudel LL, Robinson JG, Stone NJ, Van Horn LV (15 June 2017). Dietary fats and cardiovascular disease: a presidential advisory from the american heart association. *Circulation.* 2017;**135**:00–00. doi: 10.1161/CIR.0000000000000510.
6. Institute of Medicine. Dietary reference intakes for energy, carbohydrate, fiber, fat, fatty acids, cholesterol, protein, and amino acids. The National Academies Press. 2005. <https://doi.org/10.17226/10490>.
7. Joint WHO/FAO Expert Consultation on Diet, Nutrition and the Prevention of Chronic Diseases (WHO technical report series 916). World Health Organization. 2003;**916**:81–94. ISBN 92-4-120916-X.

8. Schwab U, Lauritzen L, Tholstrup T, Haldorssoni T, Riserus U, Uusitupa M, Becker W. Effect of the amount and type of dietary fat on cardiometabolic risk factors and risk of developing type 2 diabetes, cardiovascular diseases, and cancer: a systematic review. *Food & Nutrition Research*. 2014;**58**:25145. doi:10.3402/fnr.v58.25145.
9. Hooper L, Martin N, Abdelhamid A, Davey Smith G. Reduction in saturated fat intake for cardiovascular disease. *Cochrane Database Syst Rev*. 2015;**6**:CD011737. doi:10.1002/14651858.CD011737.
10. Jakobsen MU, O'Reilly EJ, Heitmann BL, Pereira MA, Bälter K, Fraser GE, Goldbourt U, Hallmans G, Knekt P, Liu S, Pietinen P, Spiegelman D, Stevens J, Virtamo J, Willett WC, Ascherio A. Major types of dietary fat and risk of coronary heart disease: a pooled analysis of 11 cohort studies. *Am J Clin Nutr*. 2009;**89**(5): 1425–32. doi:10.3945/ajcn.2008.27124.
11. Rajaram S, Haddad EH, Mejia A, Sabaté J. Walnuts and fatty fish influence different serum lipid fractions in normal to mildly hyperlipidemic individuals: a randomized controlled study. *Am J Clin Nutr*. 2009;**89**(5):1657S-1663S. doi: 10.3945/ajcn.2009.26736S.
12. Simopoulos AP. Omega-3 fatty acids in health and disease and in growth and development. *Am J Clin Nutr*. 1991;**54**(3):438-63.
13. Gregory MK, Gibson RA, Cook-Johnson RJ, Cleland LG, James MJ. Elongase Reactions as Control Points in Long-Chain Polyunsaturated Fatty Acid Synthesis. *PLoS ONE*. 2011;**6**(12):e29662. doi: <https://doi.org/10.1371/journal.pone.0029662>

14. Brenner, R.R. The desaturation step in the animal biosynthesis of polyunsaturated fatty acids. *Lipids*. 1971;**6**(8):567-575. doi: <https://doi.org/10.1007/BF02531137>.
15. Spector AA. Essentiality of fatty acids. *Lipids*. 1999;**34**(S1):S1–S3. <https://doi.org/10.1007/BF02562220>.
16. Jump DB. The biochemistry of n-3 polyunsaturated fatty acids. *J Biol Chem*. 2002;**277**(11):8755-8758. doi: 10.1074/jbc.R100062200.
17. Kotronen A, Seppänen-Laakso T, Westerbacka J, Kiviluoto T, Arola J, Ruskeepää AL, Yki-Järvinen H, Orešič M. Comparison of lipid and fatty acid composition of the liver, subcutaneous and intra-abdominal adipose tissue, and serum. *Obesity*. 2010;**18**:937–944. doi:10.1038/oby.2009.326.
18. Calder PC, Harvey DJ, Pond CM, Newsholme EA. Site-specific differences in the fatty acid composition of human adipose tissue. *Lipids*. 1992;**27**(9):716-20.
19. Martinez M, Mougan I. Fatty acid composition of human brain phospholipids during normal development. *J Neurochem*. 1998;**71**:2528—2533.
20. Salem N, Litman B, Kim HY, Gawrisch K. Mechanisms of action of docosahexaenoic acid in the nervous system. *Lipids*. 2001;**36**(9):945-959. doi: <https://doi.org/10.1007/s11745-001-0805-6>.
21. Moriguchi T, Greiner R S, Salem N. Behavioral deficits associated with dietary induction of decreased brain docosahexaenoic acid concentration.

- Journal of Neurochemistry. 2000;**75**:2563–2573. doi:10.1046/j.1471-4159.2000.0752563.x.
22. Salem N, Moriguchi T, Greiner RS, McBride K, Ahmad A, Catalan JN, Slotnick B. Alterations in brain function after loss of docosahexaenoate due to dietary restriction of n-3 fatty acids. *J Mol Neurosci.* 2001;**16**(2-3):299-307. <https://doi.org/10.1385/JMN:16:2-3:299>.
  23. Cho H.P., Nakamura M.T., Clarke S.D. Cloning, expression, and nutritional regulation of the mammalian Delta-6 desaturase. *J Biol Chem*, 274 (1999), pp. 471-477.
  24. Cho H.P., Nakamura M., Clarke S.D. Cloning, expression, and fatty acid regulation of the human delta-5 desaturase. *J Biol Chem*, 274 (1999), pp. 37335-37339.
  25. Marquardt A, Stöhr H, White K, Weber BH. cDNA cloning, genomic structure, and chromosomal localization of three members of the human fatty acid desaturase family. *Genomics.* 2000;**66**(2):175-83. doi: 10.1006/geno.2000.6196.
  26. Uhlén M, Fagerberg L, Hallström BM, Lindskog C, Oksvold P, Mardinoglu A, Sivertsson Å, Kampf C, Sjöstedt E, Asplund A, Olsson I, Edlund K, Lundberg E, Navani S, Szigartyo CA, Odeberg J, Djureinovic D, Takanen JO, Hober S, Alm T, Edqvist PH, Berling H, Tegel H, Mulder J, Rockberg J, Nilsson P, Schwenk JM, Hamsten M, von Feilitzen K, Forsberg M, Persson L, Johansson F, Zwahlen M, von Heijne G, Nielsen J, Pontén F.

- Tissue-based map of the human proteome. *Science*. 2015;**347**(6220):1260419. doi: 10.1126/science.1260419.
27. Human Protein Atlas. available from [www.proteinatlas.org](http://www.proteinatlas.org).  
<https://www.proteinatlas.org/ENSG00000149485-FADS1/tissue>.
  28. Fan YY, Monk JM, Hou TY, Callway E, Vincent L, Weeks B, Yang P, Chapkin RS. Characterization of an arachidonic acid-deficient (fads1 knockout) mouse model. *J Lipid Res*. 2012;**53**:1287-1295. doi: 10.1194/jlr.M024216.
  29. Fan YY, Callaway E, J MM, J SG, Yang P, Vincent L, R SC. A new model to study the role of arachidonic acid in colon cancer pathophysiology. *Cancer Prev Res*. 2016;**9**:750-757. doi: 10.1158/1940-6207.CAPR-16-0060.
  30. Fumagalli M, Moltke I, Grarup N, Racimo F, Bjerregaard P, Jørgensen ME, Korneliussen TS, Gerbault P, Skotte L, Linneberg A, Christensen C, Brandslund I, Jørgensen T, Huerta-Sánchez E, Schmidt EB, Pedersen O, Hansen T, Albrechtsen A, Nielsen R. Greenlandic Inuit show genetic signatures of diet and climate adaptation. *Science*. 2015;**349**(6254):1343-1347. doi: 10.1126/science.aab2319.
  31. James MJ, Gibson RA, Cleland LG. Dietary polyunsaturated fatty acids and inflammatory mediator production. *Am J Clin Nutr*. 2000;**71**(S1):343S-348S.

32. Bergström S, Danielsson H, Samuelsson B. The enzymatic formation of prostaglandin E2 from arachidonic acid. *Biochim Biophys Acta*. 1964;**90**(207):207–10. doi:10.1016/0304-4165(64)90145-x.
33. Funk CD. Prostaglandins and leukotrienes: advances in eicosanoid biology. *Science*. 2001;**294**(5548):1871–1875. doi:10.1126/science.294.5548.1871.
34. Soberman RJ, Christmas P. The organization and consequences of eicosanoid signaling. *J Clin Invest*. 2003;**111**(8):1107–1113. doi:10.1172/JCI18338.
35. Dennis EA. Diversity of group types, regulation, and function of phospholipase A2. *J Biol Chem*. 1994;**269**(18):13057–60.
36. Dennis EA, Cao J, Hsu YH, Magrioti V, Kokotos G. Phospholipase a2 enzymes: Physical structure, biological function, disease implication, chemical inhibition, and therapeutic intervention. *Chem Rev*. 2011;**111**:6130-6185. doi: 10.1021/cr200085w.
37. Smith WL, Garavito RM, DeWitt DL. Prostaglandin endoperoxide H synthases (cyclooxygenases)-1 and -2. *J Biol Chem*. 1996;**271**(52):33157-33160.
38. Vick BA, Zimmerman DC. Oxidative systems for the modification of fatty acids: the lipoxygenase pathway. 1987;**9**:53–90. doi:10.1016/b978-0-12-675409-4.50009-5.

39. Capdevila JH, Falck JR, Harris RC. Cytochrome P450 and arachidonic acid bioactivation. Molecular and functional properties of the arachidonate monooxygenase. *J Lipid Res.* 2000;**41**(2):163-181.
40. Dennis EA, Norris PC. Eicosanoid storm in infection and inflammation. *Nat Rev Immunol.* 2015;**15**:511-523. doi: 10.1038/nri3859.
41. Serhan CN. Pro-resolving lipid mediators are leads for resolution physiology. *Nature.* 2014;**510**:92-101. doi: 10.1038/nature13479.
42. Serhan CN, Chiang N, Dalli J. The resolution code of acute inflammation: Novel pro-resolving lipid mediators in resolution. *Semin Immunol.* 2015;**27**:200-215. doi: 10.1016/j.smim.2015.03.004.
43. Dobrian AD, Lieb DC, Cole BK, Taylor-Fishwick DA, Chakrabarti SK, Nadler JL. Functional and pathological roles of the 12- and 15-lipoxygenases. *Prog Lipid Res.* 2011;**50**(1):115–31. doi:10.1016/j.plipres.2010.10.005.
44. Capra V, Rovati GE, Mangano P, Buccellati C, Murphy RC, Sala A. Transcellular biosynthesis of eicosanoid lipid mediators. *Biochim Biophys Acta.* 2015;**1851**(4):377-82. doi: 10.1016/j.bbalip.2014.09.002.
45. Everett BM, Smith RJ, Hiatt WR. Reducing ldl with pcsk9 inhibitors – the clinical benefit of lipid drugs. *N Engl J Med.* 2015;**373**:1588-1591. doi: 10.1056/NEJMc1509961.
46. Teslovich TM, Musunuru K, Smith AV, et al. Biological, clinical and population relevance of 95 loci for blood lipids. *Nature.* 2010;**466**:707-713. doi: 10.1038/nature09270.

47. Lettre G, Palmer CD, Young T, et al. Genome-wide association study of coronary heart disease and its risk factors in 8,090 african americans: The nhlbi care project. *PLoS Genet.* 2011;**7**:e1001300. doi: 10.1371/journal.pgen.1001300.
48. Sabatti C, Service SK, Hartikainen AL, et al. Genome-wide association analysis of metabolic traits in a birth cohort from a founder population. *Nat Genet.* 2009;**41**:35-46. doi: 10.1038/ng.271.
49. Dupuis J, Langenberg C, Prokopenko I, et al. New genetic loci implicated in fasting glucose homeostasis and their impact on type 2 diabetes risk. *Nat Genet.* 2010;**42**:105-116. doi: 10.1038/ng.520.
50. Ingelsson E, Langenberg C, Hivert MF, et al. Detailed physiologic characterization reveals diverse mechanisms for novel genetic loci regulating glucose and insulin metabolism in humans. *Diabetes.* 2010;**59**:1266-1275. doi: 10.2337/db09-1568.
51. Martinelli N, Girelli D, Malerba G, Guarini P, Illig T, Trabetti E, Sandri M, Friso S, Pizzolo F, Schaeffer L, Heinrich J, Pignatti PF, Corrocher R, Olivieri O. Fads genotypes and desaturase activity estimated by the ratio of arachidonic acid to linoleic acid are associated with inflammation and coronary artery disease. *Am J Clin Nutr.* 2008;**88**:941-949.
52. Ameer A, Enroth S, Johansson A, et al. Genetic adaptation of fatty-acid metabolism: A human-specific haplotype increasing the biosynthesis of long-chain omega-3 and omega-6 fatty acids. *Am J Hum Genet.* 2012;**90**:809-820. doi: 10.1016/j.ajhg.2012.03.014.

53. Chambers JC, Zhang W, Sehmi J, et al. Genome-wide association study identifies loci influencing concentrations of liver enzymes in plasma. *Nat Genet.* 2011;**43**:1131-1138. doi: 10.1038/ng.970.
54. Wang L, Athinarayanan S, Jiang G, Chalasani N, Zhang M, Liu W. Fatty acid desaturase 1 gene polymorphisms control human hepatic lipid composition. *Hepatology.* 2015;**61**:119-128. doi: 10.1002/hep.27373.
55. Demirkan A, van Duijn CM, Ugocsai P, et al. Genome-wide association study identifies novel loci associated with circulating phospho- and sphingolipid concentrations. *PLoS Genet.* 2012;**8**:e1002490. doi: 10.1371/journal.pgen.1002490.
56. Eijgelsheim M, Newton-Cheh C, Sotoodehnia N, et al. Genome-wide association analysis identifies multiple loci related to resting heart rate. *Hum Mol Genet.* 2010;**19**:3885-3894. doi: 10.1093/hmg/ddq303.
57. Zhang JY, Kothapalli KS, Brenna JT. Desaturase and elongase-limiting endogenous long-chain polyunsaturated fatty acid biosynthesis. *Curr Opin Clin Nutr Metab Care.* 2016;**19**:103-110. doi: 10.1097/MCO.0000000000000254.
58. Tosi F, Sartori F, Guarini P, Olivieri O, Martinelli N. Delta-5 and delta-6 desaturases: Crucial enzymes in polyunsaturated fatty acid-related pathways with pleiotropic influences in health and disease. *Adv Exp Med Biol.* 2014;**824**:61-81. doi: 10.1007/978-3-319-07320-0\_7.
59. Crooke ST. Progress in antisense technology. *Annu Rev Med.* 2004;**55**:61-95. doi: 10.1146/annurev.med.55.091902.104408.

60. Shewale SV, Boudyguina E, Zhu X, Shen L, Hutchins PM, Barkley RM, Murphy RC, Parks JS. Botanical oils enriched in n-6 and n-3 fads2 products are equally effective in preventing atherosclerosis and fatty liver. *J Lipid Res.* 2015;**56**:1191-1205. doi: 10.1194/jlr.M059170.
61. Shewale SV, Brown AL, Bi X, Boudyguina E, Sawyer JK, Alexander-Miller MA, Parks JS. In vivo activation of leukocyte gpr120/ffar4 by pufas has minimal impact on atherosclerosis in ldl receptor knockout mice. *J Lipid Res.* 2017;**58**:236-246. doi: 10.1194/jlr.M072769.
62. Brown JM, Betters JL, Lord C, Ma Y, Han X, Yang K, Alger HM, Melchior J, Sawyer J, Shah R, Wilson MD, Liu X, Graham MJ, Lee R, Crooke R, Shulman GI, Xue B, Shi H, Yu L. Cgi-58 knockdown in mice causes hepatic steatosis but prevents diet-induced obesity and glucose intolerance. *J Lipid Res.* 2010;**51**:3306-3315. doi: 10.1194/jlr.M010256.
63. Izem L, Morton RE. Molecular cloning of hamster lipid transfer inhibitor protein (apolipoprotein F) and regulation of its expression by hyperlipidemia. *J Lipid Res.* 2009;**50**:676-684. doi: 10.1194/jlr.M800429-JLR200.
64. Brown JM, Bell TA, 3rd, Alger HM, Sawyer JK, Smith TL, Kelley K, Shah R, Wilson MD, Davis MA, Lee RG, Graham MJ, Crooke RM, Rudel LL. Targeted depletion of hepatic acat2-driven cholesterol esterification reveals a non-biliary route for fecal neutral sterol loss. *J Biol Chem.* 2008;**283**:10522-10534. doi: 10.1074/jbc.M707659200.

65. Brown JM, Chung S, Sawyer JK, Degirolamo C, Alger HM, Nguyen T, Zhu X, Duong MN, Wibley AL, Shah R, Davis MA, Kelley K, Wilson MD, Kent C, Parks JS, Rudel LL. Inhibition of stearoyl-coenzyme a desaturase 1 dissociates insulin resistance and obesity from atherosclerosis. *Circulation*. 2008;118:1467-1475. doi: 10.1161/CIRCULATIONAHA.108.793182.
66. Feldstein AE, Lopez R, Tamimi TA, Yerian L, Chung YM, Berk M, Zhang R, McIntyre TM, Hazen SL. Mass spectrometric profiling of oxidized lipid products in human nonalcoholic fatty liver disease and nonalcoholic steatohepatitis. *J Lipid Res*. 2010;51:3046-3054. doi: 10.1194/jlr.M007096.
67. Folch J, Lees M, Sloane Stanley GH. A simple method for the isolation and purification of total lipids from animal tissues. *J Biol Chem*. 1957;226:497-509.
68. Simons B, Kauhanen D, Sylvanne T, Tarasov K, Duchoslav E, Ekroos K. Shotgun lipidomics by sequential precursor ion fragmentation on a hybrid quadrupole time-of-flight mass spectrometer. *Metabolites*. 2012;2:195-213. doi:10.3390/metabo2010195.
69. Bligh EG, Dyer WJ. A rapid method of total lipid extraction and purification. *Can J Biochem Physiol*. 1959;37:911-917. doi: 10.1139/o59-099.
70. English JT, Norris PC, Hodges RR, Dartt DA, Serhan CN. Identification and profiling of specialized pro-resolving mediators in human tears by lipid

mediator metabolomics. Prostaglandins Leukot Essent Fatty Acids. 2017;**117**:17-27. doi: 10.1016/j.plefa.2017.01.004.

71. Koeth RA, Wang Z, Levison BS, Buffa JA, Org E, Sheehy BT, Britt EB, Fu X, Wu Y, Li L, Smith JD, DiDonato JA, Chen J, Li H, Wu GD, Lewis JD, Warrier M, Brown JM, Krauss RM, Tang WH, Bushman FD, Lusis AJ, Hazen SL. Intestinal microbiota metabolism of L-carnitine, a nutrient in red meat, promotes atherosclerosis. Nat Med. 2013;**19**:576-585. doi: 10.1038/nm.3145.
72. Willner EL, Tow B, Buhman KK, Wilson M, Sanan DA, Rudel LL, Farese RV Jr. Deficiency of acyl-CoA:cholesterol acyltransferase 2 prevents atherosclerosis in apolipoprotein E-deficient mice. Proc Natl Acad Sci USA. 2003;**100**:1262-1267. doi: 10.1073/pnas.0336398100.
73. Lee RG, Kelley KK, Sawyer JK, Farese RV Jr, Parks JS, Rudel LL. Plasma cholesterol esters provided by lecithin:cholesterol acyltransferase and acyl-CoA:cholesterol acyltransferase have opposite atherosclerotic potential. Circ. Res. 2004;**95**:998-1004. doi: 10.1161/01.RES.0000147558.15554.67.
74. Bell TA III, Kelley K, Wilson MD, Sawyer JK, Rudel LL. Dietary fat-induced alterations in atherosclerosis are abolished by ACAT2-deficiency in ApoB100 only, LDLr<sup>-/-</sup> mice. Arterioscler Thromb Vasc Biol. 2007;**27**:1396-1402. doi: 10.1161/ATVBAHA.107.142802.

75. Fredman G, Hellmann J, Proto JD, Kuriakose G, Colas RA, Dorweiler B, Connolly ES, Solomon R, Jones DM, Heyer EJ, Spite M, Tabas I. An imbalance between specialized pro-resolving lipid mediators and pro-inflammatory leukotrienes promotes instability of atherosclerotic plaques. *Nat Commun.* 2016;**7**:12859. doi: 10.1038/ncomms12859.
76. Zhu X, Lee JY, Timmins JM, Brown JM, Boudyguina E, Mulya A, Gebre AK, Willingham MC, Hiltbold EM, Mishra N, Maeda N, Parks JS. Increased cellular free cholesterol in macrophage-specific *Abca1* knock-out mice enhances pro-inflammatory response of macrophages. *J Biol Chem.* 2008;**283**:22930-2294. doi: 10.1074/jbc.M801408200.
77. Lee MW, Odegaard JI, Mukundan L, Qiu Y, Molofsky AB, Nussbaum JC, Yun K, Locksley RM, Chawla A. Activated type 2 innate lymphoid cells regulate beige fat biogenesis. *Cell.* 2015;**160**:74-87. doi: 10.1016/j.cell.2014.12.011.
78. Lord CC, Betters JL, Ivanova PT, Milne SB, Myers DS, Madenspacher J, Thomas G, Chung S, Liu M, Davis MA, Lee RG, Crooke RM, Graham MJ, Parks JS, Brasaemle DL, Fessler MB, Brown HA, Brown JM. *Cgi-58/abhd5*-derived signaling lipids regulate systemic inflammation and insulin action. *Diabetes.* 2012;**61**:355-363. doi: 10.2337/db11-0994.
79. Naik SU, Wang X, Da Silva JS, Jaye M, Macphee CH, Reilly MP, Billheimer JT, Rothblat GH, Rader DJ. Pharmacological activation of liver X receptors promotes reverse cholesterol transport in vivo. *Circulation.* 2006;**113**:90–97. doi: 10.1161/CIRCULATIONAHA.105.560177.

80. Temel RE, Tang W, Ma Y, Rudel LL, Willingham MC, Ioannou YA, Davies JP, Nilsson LM, Yu L. Hepatic Niemann-Pick C1-like 1 regulates biliary cholesterol concentrations and is a target of ezetimibe. *J Clin Invest*. 2007;**117**:1968–1978. doi 10.1172/JCI30060.
81. Tabas I, Bornfeldt KE. Macrophage phenotype and function in different stages of atherosclerosis. *Circ Res*. 2016;**118**:653-667. doi: 10.1161/CIRCRESAHA.115.306256.
82. Peled M, Fisher EA. Dynamic aspects of macrophage polarization during atherosclerosis progression and regression. *Front Immunol*. 2014;**5**:579. doi: 10.3389/fimmu.2014.00579.
83. Joseph SB, Castrillo A, Laffitte BA, Mangelsdorf DJ, Tontonoz P. Reciprocal regulation of inflammation and lipid metabolism by liver X receptors. *Nat. Med*. 2003;**9**:213-219. doi: 10.1038/nm820.
84. Peet DJ, Turley SD, Ma W, Janowski BA, Lobaccaro JM, Hammer RE, Mangelsdorf DJ. Cholesterol and bile acid metabolism are impaired in mice lacking the nuclear oxysterol receptor LXR alpha. *Cell* 1998;**93**:693-704. PMID: 9630215.
85. Joseph SB, McKilligin E, Pei L, Watson MA, Collins AR, Laffitte BA, Chen M, Noh G, Goodman J, Hagger GN, Tran J, Tippin TK, Wang X, Lusis AJ, Hsueh WA, Law RE, Collins JL, Wilson TM, Tontonoz P. Synthetic LXR ligand inhibits the development of atherosclerosis in mice. *Proc Natl Acad Sci USA*. 2002;**99**:7604-7609. doi: 10.1073/pnas.112059299.

86. Venkateswaran A, Laffitte BA, Joseph SB, Mak PA, Wilpitz DC, Edwards PA, Tontonoz P. Control of cellular cholesterol efflux by the nuclear oxysterol receptor LXR alpha. *Proc Natl Acad Sci USA*. 2000;**97**:12097-12102. doi: 10.1073/pnas.200367697.
87. Schultz JR, Luk A, Repa JJ, Medina JC, Li L, Schwendner S, Wang S, Thoolen M, Mangelsdorf DJ, Lustig KD, Shan B. Role of LXRs in control of lipogenesis. *Genes Dev*. 2000;**14**:2831-2838. PMID: PMC317060.
88. Rong X, Albert CJ, Hong C, Duerr MA, Chamberlain BT, Tarling EJ, Ito A, Gao J, Wang B, Edwards PA, Jung ME, Ford DA, Tontonoz P. LXRs regulate ER stress and inflammation through dynamic modulation of membrane phospholipid composition. *Cell Metab*. 2013;**18**:685-697. doi: 10.1016/j.cmet.2013.10.002.
89. Fredman G, Hellmann J, Proto JD, Kuriakose G, Colas RA, Dorweiler B, Connolly ES, Solomon R, Jones DM, Heyer EJ, Spite M, Tabas I. An imbalance between specialized pro-resolving lipid mediators and pro-inflammatory leukotrienes promotes instability of atherosclerotic plaques. *Nat Commun*. 2016;**7**:12859. doi: 10.1038/ncomms12859.
90. Viola J, Soehnlein O. Atherosclerosis - a matter of unresolved inflammation. *Semin Immunol*. 2015;**27**:184-193. doi: 10.1016/j.smim.2015.03.013.
91. Rius B, Lopez-Vicario C, Gonzalez-Periz A, Moran-Salvador E, Garcia-Alonso V, Claria J, Titos E. Resolution of inflammation in obesity-induced

- liver disease. *Front Immunol.* 2012;**3**:257. doi: 10.3389/fimmu.2012.00257.
92. Spite M, Claria J, Serhan CN. Resolvins, specialized proresolving lipid mediators, and their potential roles in metabolic diseases. *Cell Metab.* 2014;**19**:21-36. doi: 10.1016/j.cmet.2013.10.006.
93. Baum SJ, Kris-Etherton PM, Willett WC, Lichtenstein AH, Rudel LL, Maki KC, Whelan J, Ramsden CE, Block RC. Fatty acids in cardiovascular health and disease: A comprehensive update. *J Clin Lipidol.* 2012;**6**:216-234. doi: 10.1016/j.jacl.2012.04.077.
94. Scorletti E, Byrne CD. Omega-3 fatty acids, hepatic lipid metabolism, and nonalcoholic fatty liver disease. *Annu. Rev. Nutr.* 2013;**33**: 231-248.
95. Flachs P, Rossmeisl M, Kopecky J. The effect of n-3 fatty acids on glucose homeostasis and insulin sensitivity. *Physiol. Res.* 2014;**63**(Suppl 1):S93-S118
96. Powell DR, Gay JP, Smith M, Wilganowski N, Harris A, Holland A, Reyes M, Kirkham L, Kirkpatrick LL, Zambrowicz B, Hansen G, Platt KA, van Sligtenhorst I, Ding ZM, Desai U. Fatty acid desaturase 1 knockout mice are lean with improved glycemic control and decreased development of atheromatous plaque. *Diabetes Metab Syndr Obes.* 2016;**9**:185-199. doi: 10.2147/DMSO.S106653.
97. Elajami TK, Colas RA, Dalli J, Chiang N, Serhan CN, Welty FK. Specialized proresolving lipid mediators in patients with coronary artery

- disease and their potential for clot remodeling. *FASEB J.* 2016;**30**:2792-2801. doi: 10.1096/fj.201500155R.
98. Borgeson E, McGillicuddy FC, Harford KA, Corrigan N, Higgins DF, Maderna P, Roche HM, Godson C. Lipoxin a4 attenuates adipose inflammation. *FASEB J.* 2012;**26**:4287-4294. doi: 10.1096/fj.12-208249.
99. Borgeson E, Johnson AM, Lee YS, Till A, Syed GH, Ali-Shah ST, Guiry PJ, Dalli J, Colas RA, Serhan CN, Sharma K, Godson C. Lipoxin a4 attenuates obesity-induced adipose inflammation and associated liver and kidney disease. *Cell Metab.* 2015;**22**:125-137. doi: 10.1016/j.cmet.2015.05.003.
100. Elias I, Ferre T, Vila L, Munoz S, Casellas A, Garcia M, Molas M, Aquido J, Roca C, Ruberte J, Bosch F, Franckhauser S. Alox5ap overexpression in adipose tissue leads to lxa4 production and protection against diet-induced obesity and insulin resistance. *Diabetes.* 2016;**65**:2139-2150. doi: 10.2337/db16-0040/-/DC1.
101. Demetz E, Schroll A, Heim C, et al. The arachidonic acid metabolome serves as a conserved regulator of cholesterol metabolism. *Cell Metab.* 2014;**20**:787-798. doi: 10.1016/j.cmet.2014.09.004.
102. Yoshikawa T, Shimano H, Yahagi N, Ide T, Amemiya-Kudo M, Matsuzaka T, Nakakuki M, Tomita S, Okazaki H, Tamura Y, Iizuka Y, Ohashi K, Takahashi A, Sone H, Osuga JI J, Gotoda T, Ishibashi S, Yamada N. Polyunsaturated fatty acids suppress sterol regulatory element-binding protein 1c promoter activity by inhibition of liver X receptor (LXR) binding

- to LXR response elements. *J Biol Chem.* 2002;**277**:1705-1711. doi: 10.1074/jbc.M105711200.
103. Alberti S, Schuster G, Parini P, Feltkamp D, Diczfalusy U, Rudling M, Angelin B, Björkhem I. Hepatic cholesterol metabolism and resistance to dietary cholesterol in LXRbeta-deficient mice. *J Clin Invest.* 2001;**107**:565-573. doi: 10.1172/jci9794.
104. Janowski BA, Willy PJ, Devi TR, Falck JR, Mangelsdorf DJ. An oxysterol signaling pathway mediated by the nuclear receptor LXR alpha. *Nature.* 1996;**383**:728-731. doi: 10.1038/383728a0.
105. Levental KR, Lorent JH, Lin X, Skinkle AD, Surma MA, Stockenbojer EA, Gorfe AA, Levental I. Polyunsaturated lipid regulate membrane domain stability by tuning membrane order. *Biophys J.* 2016;**110**:1800-1810. doi: 10.1016/bpj.2016.03.012.
106. Shaikh SR, Kinnun JJ, Leng X, Williams JA, Wassall SR. How polyunsaturated fatty acids modify molecular organization in membranes: insight from NMR studies of model systems. *Biochim Biophys Acta.* 2015;**1848**:211-219. doi: 10.1016/j.bbamem.2014.04.020.
107. Ogden CL, Carroll MD, Fryar CD, Flegal KM. Prevalence of obesity among adults and youth: United States, 2011–2014. NCHS data brief, no 219. Hyattsville, MD: National Center for Health Statistics. 2015.
108. Obesity and overweight Fact sheet. WHO. June 2016. Retrieved 2 October 2017.

109. Manson JE, Willett WC, Stampfer MJ, et al. Body weight and mortality among women. *N Engl J Med*. 1995;**333**:677-685.
110. Willett WC, Manson JE, Stampfer MJ, et al. Weight, weight change, and coronary heart disease in women: risk within the 'normal' weight range. *JAMA*. 1995;**273**:461-465.
111. Stevens J, Plankey MW, Williamson DF, et al. The body mass index-mortality relationship in white and African American women. *Obes Res*. 1998;**6**:268-277.
112. Lindsted KD, Singh PN. Body mass and 26 y risk of mortality among men who never smoked: a re-analysis of men from the Adventist Mortality Study. *Int J Obes Relat Metab Disord*. 1998;**22**:544-548.
113. Calle EE, Thun MJ, Petrelli JM, Rodriguez C, Heath CW Jr. Body-mass index and mortality in a prospective cohort of U.S. adults. *N Engl J Med* 1999;**341**:1097-1105.
114. Kopelman P. Obesity as a medical problem. *Nature*. 2000;**404**:635-643.
115. Lew EA, Garfinkel L. Variations in mortality by weight among 750,000 men and women. *J Chronic Dis*. 1979;**32**:563-576.
116. Wang Y, Hua S, Tian W, Zhang L, Zhao J, Zhang H, Zhang W, Xue F. Mitogenic and anti-apoptotic effects of insulin in endometrial cancer are phosphatidylinositol 3-kinase/Akt dependent. *Gynecol Oncol*. 2012;**125**(3):734-741.

117. Djiogue S, Nwabo Kamdje AH, Vecchio L, Kipanyula MJ, Farahna M, Aldebasi Y, Seke Etet PF. Insulin resistance and cancer: the role of insulin and IGFs. *Endocr Relat Cancer*. 2013;**20**(1):R1-R17.
118. Nishimura S, Manabe I, Nagasaki M, Eto K, Yamashita H, Ohsugi M, et al. CD8<sup>+</sup> effector T cells contribute to macrophage recruitment and adipose tissue inflammation in obesity. *Nat Med*. 2009;**15**:914–2010.1038.
119. Nishimura S, Manabe I, Nagasaki M, Hosoya Y, Yamashita H, Fujita H, et al. Adipogenesis in obesity requires close interplay between differentiating adipocytes, stromal cells, and blood vessels. *Diabetes*. 2007;**56**:1517–2610.2337/db06-1749.
120. Louie SM, Roberts LS, Nomura DK. Mechanisms linking obesity and cancer. *Biochim Biophys Acta*. 2013;**1831**(10):1499-508.
121. Calle EE, Kaaks R. Overweight, obesity and cancer: epidemiological evidence and proposed mechanisms. *Nat Rev Cancer*. 2004;**4**:579-591. doi:10.1038/nrc1408.
122. Pérez-Hernández AI, Catalán V, Gómez-Ambrosi J, Rodríguez A, Frühbeck G. Mechanisms linking excess adiposity and carcinogenesis promotion. *Front Endocrinol*. 2014;**5**:65. doi:10.3389/fendo.2014.00065.
123. Shaker M; et al. Liver transplantation for nonalcoholic fatty liver disease: New challenges and new opportunities. *World journal of gastroenterology: WJG*. 2014;**20**(18):5320. doi:10.3748/wjg.v20.i18.5320.
124. Rinella ME. Nonalcoholic fatty liver disease: a systematic review. *JAMA*. 2015;**313**(22): 2263–73.

125. Fatty Liver Disease (Nonalcoholic Steatohepatitis). NIDDK. November 2016. Retrieved 2 October 2017.
126. Clark JM, Diehl AM. Nonalcoholic fatty liver disease: an underrecognized cause of cryptogenic cirrhosis. *JAMA*. 2003;**289**(22):3000–3004. doi:10.1001/jama.289.22.3000.
127. Forner A, Llovet JM, Bruix J. Hepatocellular carcinoma. *The Lancet*. 2012;**379**(9822):1245–1255. doi:10.1016/S0140-6736(11)61347-0.
128. W Alazawi, M Cunningham, J Dearden, GR Foster. Systematic review: outcome of compensated cirrhosis due to chronic hepatitis C infection. *Aliment Pharmacol Ther*. 2010;**32**:344-355.
129. Muir K, Hazim A, He Y, Peyressatre M, Kim D, Song X, Beretta L. Proteomic and lipidomic signatures of lipid metabolism in NASH-associated hepatocellular carcinoma. *Cancer Res*. 2013;**73**(15). doi: 10.1158/0008-5472.CAN-12-3797.
130. Sawada N, Inoue M, Iwasaki M, Sasazuki S, Shimazu T, Yamaji T, Takachi R, Tanaka Y, Mizokami M, Tsugane S. Consumption of n-3 fatty acids and fish reduces risk of hepatocellular carcinoma. *Gastroenterology*. 2012;**142**:1468-1475.
131. Arendt B M, Comelli EM, Ma DWL, Lou W, Teterina A, Kim T, Fung SK, Wong DKH, McGilvray I, Fischer SE, and Allard JP. Altered hepatic gene expression in nonalcoholic fatty liver disease is associated with lower hepatic n-3 and n-6 polyunsaturated fatty acids. *Hepatology*. 2015;**61**:1565–1578. doi:10.1002/hep.27695.

132. Ferlay J, Shin HR, Bray F, Forman D, Mathers C, Parkin DM. Estimates of worldwide burden of cancer in 2008: GLOBOCAN 2008. *Int J Cancer*. 2010;**127**:2893-2917
133. Sherman M. Hepatocellular carcinoma: epidemiology, surveillance, and diagnosis. *Semin Liver Dis*. 2010;**30**:3-16.
134. C Bosetti, F Levi, P Boffetta, F Lucchini, E Negri, C La Vecchia. Trends in mortality from hepatocellular carcinoma in Europe, 1980–2004. *Hepatology*. 2008;**48**:137-145.
135. Qiu D, Katanoda K, Marugame T, Sobue T. A Joinpoint regression analysis of long-term trends in cancer mortality in Japan (1958–2004). *Int J Cancer*. 2009;**124**:443-448.
136. Tanaka Y, Kurbanov F, Mano S, et al. Molecular tracing of the global hepatitis C virus epidemic predicts regional patterns of hepatocellular carcinoma mortality. *Gastroenterology*. 2006;**130**:703-714.
137. Davis GL, Alter MJ, El-Serag H, Poynard T, Jennings LW. Aging of hepatitis C virus (HCV)-infected persons in the United States: a multiple cohort model of HCV prevalence and disease progression. *Gastroenterology*. 2010;**138**:513-521.
138. Yoshimoto S, Tze Mun Loo TM, Atarashi K, Kanda H, Sato S, Oyadomari S, Iwakura Y, Oshima K, Morita H, Hattori M, Honda K, Ishikawa Y, Hara E, Ohtani N. Obesity-induced gut microbial metabolite promotes liver cancer through senescence secretome. *Nature*. 2013;**499**:97–101. doi:10.1038/nature12347.

139. El-Serag HB, Tran T, Everhart JE. Diabetes increases the risk of chronic liver disease and hepatocellular carcinoma. *Gastroenterology*. 2004;**126**:460-468.
140. Lattka E, Eggers S, Moeller G, Heim K, Weber M, Mehta D, et al. A common FADS2 promoter polymorphism increases promoter activity and facilitates binding of transcription factor ELK1. *J Lipid Res* 2010;**51**:182-191.38.
141. Merino DM, Johnston H, Clarke S, Roke K, Nielsen D, Badawi A, et al. Polymorphisms in FADS1 and FADS2 alter desaturase activity in young Caucasian and Asian adults. *Mol Genet Metab* 2011;**103**:171-178.
142. Uhlen M, Zhang C, Lee S, Sjöstedt E, Fagerberg L, Bidkhori G, Benfeitas R, Arif M, Liu Z, Edfors F, Sanli K, von Feilitzen K, Oksvold P, Lundberg E, Hober S, Nilsson P, Mattsson J, Schwenk JM, Brunnström H, Glimelius B, Sjöblom T, Edqvist PH, Djureinovic D, Micke P, Lindskog C, Mardinoglu A, Ponten F. A pathology atlas of the human cancer transcriptome. *Science*. 2017;**357**(6352). doi: 10.1126/science.aan2507.
143. Human Protein Atlas. available from [www.proteinatlas.org](http://www.proteinatlas.org).  
<https://www.proteinatlas.org/ENSG00000149485-FADS1/pathology>.
144. Wang D, Lin Y, Gao B, et al. Reduced Expression of FADS1 Predicts Worse Prognosis in Non-Small-Cell Lung Cancer. *Journal of Cancer*. 2016;**7**(10):1226-1232. doi:10.7150/jca.15403.
145. Gil A. Polyunsaturated fatty acids and inflammatory diseases. *Biomed Pharmacother*. 2002;**56**(8):388-96.

146. DeFilippis AP, Sperling LS. Understanding omega-3's. *Am Heart J*. 2006;**151**(3):564-70.
147. Mozaffarian D, Katan MB, Ascherio A, Stampfer MJ, Willett WC. Trans fatty acids and cardiovascular disease. *N Engl J Med*. 2006;**354**(15):1601-13.
148. Calder PC. Polyunsaturated fatty acids, inflammation, and immunity. *Lipids*. 2001;**36**(9):1007-1024.
149. Lopez-Garcia E, Schulze MB, Manson JE, Meigs JB, Albert CM, Rifai N, Willett WC, Hu FB. Consumption of (n-3) fatty acids is related to plasma biomarkers of inflammation and endothelial activation in women. *J Nutr*. 2004;**134**(7):1806-1811.
150. Daviglius ML, Stamler J, Orenca AJ, Dyer AR, Liu K, Greenland P, Walsh MK, Morris D, Shekelle RB. Fish consumption and the 30-year risk of fatal myocardial infarction. *N Engl J Med*. 1997;**336**(15):1046-1053.
151. Kinsella JE, Lokesh B, Stone RA. Dietary n-3 polyunsaturated fatty acids and amelioration of cardiovascular disease: possible mechanisms. *Am J Clin Nutr*. 1990;**52**(1):1-28.
152. Kris-Etherton PM, Harris WS, Appel LJ; American Heart Association. Nutrition Committee. Fish consumption, fish oil, omega-3 fatty acids, and cardiovascular disease. *Circulation*. 2002;**106**(21):2747-2757.
153. Araya J, Rodrigo R, Videla LA, Thielemann L, Orellana M, Pettinelli P, Poniachik J. Increase in long-chain polyunsaturated fatty acid n-6/n-3 ratio

in relation to hepatic steatosis in patients with non-alcoholic fatty liver disease. *Clin Sci*. 2004;**106**(6):635-643.

154. Simopoulos AP. Essential fatty acids in health and chronic disease. *Hepatology*. 2015;61:119-128. doi: 10.1002/hep.27373. *Am J Clin Nutr*. 1999;**70**(3 Suppl):560S-569S.
155. Simopoulos AP. The importance of the omega-6/omega-3 fatty acid ratio in cardiovascular disease and other chronic diseases. *Exp Biol Med*. 2008;**233**(6):674-88. doi: 10.3181/0711-MR-311.